Bill Davis

# NATIONAL ACADEMY OF SCIENCES

# NATIONAL RESEARCH COUNCIL

## of the

# UNITED STATES OF AMERICA

# UNITED STATES NATIONAL COMMITTEE

## International Union of Radio Science


1974 Annual Meeting
October 14-17

Sponsored by USNC/URSI
in cooperation with
Institute of Electrical and Electronics Engineers

University of Colorado
Boulder, Colorado

**Price $3.00**

1974 Meeting
Condensed Program

| | | | |
|---|---|---|---|
| **Sunday October 13** | | | |
| 8PM- - - - - | USNC Meeting | | Sheraton |
| **Monday October 14** | | | |
| 9AM-noon | General Session | | NBS Audit. |
| 1:30PM-5PM | II-1 | Propagation in the Atmosphere | Forum Room |
| | III-1 | Ionospheric Modeling | 156 |
| | IV-1 | VLF Hiss and Planetary Radiation | 159 |
| | V-1 | Radio and Radar Observations from Spacecraft | 157 |
| | VI-1 | High Frequency Methods | West B'room |
| | VIII-1 | Man-made Radio Noise | 305 |
| 5:15PM | Business Meetings I(Forum Rm), IV(159), VI(W.B'rm) | | |
| 8PM | Marconi Lecture | | Macky Audit. |
| **Tuesday October 15** | | | |
| 8:30AM-noon | I-1/V | Measurement Standards in Radio Astronomy | 159 |
| | II-2 | Radio Oceanography - I | Forum Room |
| | II-3 | Selected Topics in Propagation | 157 |
| | III-2 | Winds, Waves, and Disturbances | 156 |
| | IV-2 | Energetic Electrons, Plasma, Magnetosphere | 305 |
| | VI-2 | Numerical Methods - I | West B'room |
| | VI-3 | Communication Channels--Satellites | East B'room |
| 1:30PM-5PM | I-2 | Laser Parameter Measurements | 159 |
| | II-4 | Radio Oceanography - II | Forum Room |
| | III-3/IV | VLF and ELF | 156 |
| | V-2 | Observational Results | 157 |
| | VI-4 | Numerical Methods - II | West B'room |
| | VI-5 | Adaptive Arrays and Signal Processing Systems | East B'room |
| | VIII-2 | Atmospheric Radio Noise | 305 |
| 5:15PM | Business Meetings II(156), V(157), VIII(159) | | |
| 6:30PM | Cocktail Hour and Banquet | | Sheraton |
| **Wednesday October 16** | | | |
| 8:30AM-noon | I-3 | Time and Frequency Technology and Navigation | 159 |
| | II-5 | Radio Oceanography - III | Forum Room |
| | III-4 | Ionospheric Heating - I | 156 |
| | V-3 | VLBI Instrumentation and Techniques | 157 |
| | VI-6 | Antennas and Arrays | West B'room |
| | VI-7 | Interaction of EM Waves--Bio. Material, etc. | East B'room |
| | VIII-3/VI | Noise and Radio System Performance Models | 305 |
| 1:30PM-5PM | I-4/VI | Antenna Measurements | 159 |
| | II-6 | Future of Radio Oceanography--Open Forum | Forum Room |
| | III-5 | Ionospheric Heating - II | 156 |
| | V-4 | Techniques, Receivers, Antennas | 157 |
| | VI-8/II | | West B'room |
| 5:15PM | Business Meeting Commission III(156) | | |
| 8:00PM | USNC Meeting | | Sheraton |
| **Thursday October 17** | | | |
| 8:30AM-noon | I-5 | Microwave Techniques, Bio. Res.--Workshop | 159 |
| | II-7 | Remote Sensing of Land Surfaces | Forum Room |
| | III-6 | Propagation at HF and Higher Frequencies | 156 |
| | V-5 | Solar System | 157 |
| | VI-9 | Transients | West B'room |
| 1:30PM-5PM | I-6 | Selected Topics | 159 |
| | II-8 | Precipitation | Forum Room |
| | III-7 | Scintillation and Irregularities | 156 |
| | VI-10 | Wave Guide and Transmission Systems | West B'room |

United States National Committee

INTERNATIONAL UNION OF RADIO SCIENCE

# PROGRAM AND ABSTRACTS

1974 Annual Meeting
October 14-17

Sponsored by USNC-URSI in cooperation with IEEE Societies and Groups on

Antennas and Propagation
Circuit Theory
Geoscience Electronics
Information Theory
Instrumentation and Measurement
Microwave Theory and Techniques

Hosted by

Environmental Research Laboratories, NOAA
Institute for Basic Standards, NBS
Institute for Telecommunication Sciences, ITS

Boulder, Colorado

NOTE

Programs and Abstracts of the USNC-URSI Meetings are available from:

USNC/URSI
National Academy of Sciences
2101 Constitution Avenue, N.W.
Washington, D. C. 20418

at $2.00 for meetings prior to 1970 and $3.00 for subsequent meetings. The full papers are not published in any collected format, and requests for them should be addressed to the authors who may have them published on their own initiative. Please note that these meetings are national and are not organized by international URSI, nor are these programs available from the international Secretariat.

## MEMBERSHIP

United States National Committee

INTERNATIONAL UNION OF RADIO SCIENCE

| | |
|---|---|
| Chairman | F.S. Johnson, University of Texas, Dallas |
| Vice Chairman | J.V. Evans, Lincoln Laboratory, MIT |
| Secretary | C.G. Little, Environmental Res. Labs, NOAA |
| Editor | T.B.A. Senior, University of Michigan |
| Immediate Past Chairman | A. T. Waterman, Jr., Stanford University |

Commission Chairmen

Commission I: Radio Measurement Methods and Standards
George Birnbaum
Science Center of Rockwell International
1049 Camino dos Rios
Thousand Oaks, CA 91360

Commission II: Radio and Non-ionized Media
Isadore Katz
Applied Physics Laboratory
The Johns Hopkins University
8621 Georgia Avenue
Silver Spring, MD 20910

Commission III: On the Ionosphere
John M. Kelso
ITT Electro-physics Laboratories, Inc.
9140 Old Annapolis Road
Columbia, MD 21043

Commission IV: On the Magnetosphere
Andrew F. Nagy
Dept. of Electrical Ingineering
University of Michigan
Ann Arbor, MI 48104

Commission V: Radio and Radar Astronomy
Alan H. Barrett
Research Laboratory of Electronics (26-457)
Massachusetts Institute of Technology
Cambridge, MA 02139

Commission VI: Radio Waves and Transmission Information

Aharon A. Ksienski
ElectroScience Laboratory
Ohio State University
1320 Kinnear Road
Columbus, OH 43212

Commission VII: Radio Electronics

Peter L. Bender
Joint Institute for Laboratory Astrophysics
University of Colorado
Boulder, CO 80302

**Members at Large**

| | |
|---|---|
| P.M. Banks | G.H. Hagn |
| C.I. Beard | A. Ishimaru |
| W.C. Erickson | H.C. Ko |
| L.B. Felsen | M.G. Morgan |
| J.W. Findlay | J.S. Nisbet |
| E.E. Gossard | W.F. Utlaut |

Officers of URSI resident in the United States

| | |
|---|---|
| Honorary President | S. Silver |
| Vice President | H.G. Booker |
| Chairman, Commission III | S.A. Bowhill |
| Chairman, Commission IV | F.L. Scarf |
| Chairman, Commission VI | K.M. Siegel |
| Vice Chairman, Commission I | H.M. Altschuler |
| Vice Chairman, Commission V | G. Westerhout |
| American Geophysical Union | A.J. Dessler |
| IEEE | E. Weber |
| United States Government | |
| Department of Commerce | A.H. Shapley |
| Department of Defense | E. Paroulek |
| Air Force | C.J. Sletten |
| Army | A.R. Rasmussen |
| Navy | A.H. Schooler |
| FCC | H. Fine |
| NASA | E.R. Schmerling |
| NSF | R. Fleischer |
| OTP | W. Dean, Jr. |
| Foreign Secretary, NAS | G.S. Hammond |
| Chairman, NRC Division of Physical Sciences | R. Smoluchowski |
| Honorary Members | H.H. Beverage |
| | A.H. Waynick |

## DESCRIPTION OF

## INTERNATIONAL UNION OF RADIO SCIENCE

The International Union of Radio Science is one of 14 world scientific unions organized under the International Council of Scientific Unions (ICSU). It is commonly designated as URSI (from its French name, Union Radio Scientifique Internationale). Its aims are (1) to promote the scientific study of radio communications; (2) to aid and organize radio research requiring cooperation on an international scale and to encourage the discussion and publication of the results; and, (3) to facilitate agreement upon common methods of measurement and the standardization of measuring instruments. The International Union itself is an organizational framework to aid in promoting these objectives. The actual technical work is largely done by the National Committees in the various countries.

The officers of the International Union are:

| | |
|---|---|
| President | W.J.G. Beynon (UK) |
| Immediate Past President: | W. Dieminger (West Germany) |
| Vice Presidents: | H.G. Booker (USA)<br>W.N. Christiansen (Australia)<br>V.V. Migulin (USSR)<br>J. Voge (France) |
| Secretary General: | C.M. Minnis (Belgium) |
| Honorary Presidents: | B. Decaux (France)<br>C. Manneback (Belgium)<br>J.A. Ratcliffe (UK)<br>S. Silver (USA)<br>R.L. Smith-Rose (UK) |

The Secretary's office and the headquarters of the organization are located at 7, Place Emile Danco, 1180 Brussels, Belgium. The Union is supported by contributions (dues) from 37 member countries. Additional funds for symposia and other scientific activities of the Union are provided by ICSU from contributions received for this purpose from UNESCO.

The International Union has seven permanent bodies called Commissions for centralizing studies in the principal technical fields. In addition, Commission VIII has been established on a provisional basis. The names of the Commissions and the chairmen are as follows:

I Radio Standards and Measurements
P. O. Lundbom (Sweden)

II. Radio and Non-ionized Media
P. Misme (France)

III. On the Ionosphere
S. A. Bowhill (USA)

IV. On the Magnetosphere
F. L. Scarf (USA)

V. Radio Astronomy
J. L. Locke (Canada)

VI. Radio Waves and Circuits
K. M. Siegel (USA)

VII. Radio Electronics
A. L. Cullen (UK)

VIII. On Radio Noise of Terrestrial Origin
N. C. Clarence (South Africa)

Every three years, the International Union holds a meeting called the General Assembly. The next General Assembly, the XVIII, will be held in Lima, Peru, in August 1975. The Secretariat prepares and distributes the Proceedings of these General Assemblies. The International Union arranges international symposia on specific subjects pertaining to the work of one Commission or to several Commissions. The International Union also cooperates with other Unions in international symposia on subjects of joint interest.

Radio is unique among the fields of scientific work in having a specific adaptability to large-scale international research programs, for many of the phenomena that must be studied are world-wide in extent and yet are in a measure subject to control by experimenters. Exploration of space and the extension of scientific observations to the space environment is dependent on radio for its communication link and at the same time expands the scope of radio research. One of its branches, radio astronomy, involves cosmos-wide phenomena. URSI has in all this a distinct field of usefulness in furnishing a meeting ground for the numerous workers in the manifold aspects of radio research; its meetings and committee activities furnish valuable means of promoting research through exchange of ideas.

## SPECIAL MEETINGS

Sunday Evening, October 13

Meeting of U.S. National Committee for URSI
Sheraton-Boulder Inn 8:00 pm

Monday Evening, October 14

Marconi Lecture: Macky Auditorium 8:00 pm

Lecturer: Mr. George Millington, Ministry of Posts and Telecommunications, London, England.

Tuesday Evening, October 15

Cocktail Hour and Banquet
Sheraton-Boulder Inn 6:30 pm
Banquet Speaker: To be announced.

Wednesday Evening, October 16

Meeting of U.S. National Committee for URSI
Sheraton-Boulder Inn 8:00 pm

Schedule of Commission Business Meetings:

| | |
|---|---|
| Commissions I, IV and VI | 5:15 pm, Monday, October 14 |
| Commissions II, V and VIII | 5:15 pm, Tuesday, October 15 |
| Commission III | 5:15 pm, Wednesday, October 16 |

## GENERAL SESSION

Monday, October 14 9:00 am - 12:00 noon
CHAIRMAN: F. S. Johnson, The University of Texas

G-1 THREE-DIMENSIONAL WIND FIELDS FROM DUAL DOPPLER RADAR OBSERVATIONS: Richard G. Strauch, National Oceanic and Atmospheric Administration, Boulder, Colorado.

The wind fields in precipitation systems can be inferred from radial velocity measurements taken with two Doppler radars that view the hydrometer scatterers from different directions. Together, the two radars can measure a two-dimensional particle velocity field, and, when the contribution of the fall velocity of the particles is removed, a two-dimensional wind field is obtained. The three-dimensional wind field can be inferred by applying the continuity equation for an incompressible fluid to a series of two-dimensional wind fields observed in tilted planes throughout the precipitation system. This analysis procedure has been used at the NOAA Wave Propagation Laboratory to deduce wind fields in snow, stratiform rain, and convective storms. The method has also been applied to studies of the air motion in the convective boundary layer using chaff as the air motion tracer. This presentation briefly outlines the experimental procedure, gives an error analysis for the data reduction method, and presents three-dimensional wind fields observed within severe storms and in a variety of other meteorological events.

G-2 A SYNOPSIS OF RADIO AND PHOTOMETRIC EFFECTS OBSERVED WHEN THE IONOSPHERE IS MODIFIED BY A HIGH-POWER GROUND-BASED TRANSMITTER: William F. Utlaut, Institute for Telecommunication Sciences, Boulder, Colorado.

High-power, HF ground-based radio transmitters have been used to intentionally modify the electron temperature and density in the ionosphere since 1970. A number of new, and, in many cases, unexpected ionospheric effects have been observed by a number of investigators participating in a coordinated program utilizing the Platteville, Colorado, 2 MW facility to induce the modification. Modification studies have also been carried out using the Arecibo, Puerto Rico, facility. This paper will provide a synoptic view of some of the salient effects observed during modification. The phenomena to be discussed include: 1) large-scale F-region irregularities, aligned with the geomagnetic field, that produce artificial spread F conditions; multiple, spatially distributed returns on high-resolution sky-maps; and enhanced scintillation of VHF and UHF satellite signals which have passed through the disturbed region, 2) modification of ambient airglow at 6300 Å, and 5577 Å, 3) small-scale, field-aligned F- and E-region irregularities that produce

a large radar scattering cross section (~$10^5$ to $10^8$ $m^2$) which permits aspect-sensitive scattering of HF through UHF signals so that communications at those frequencies is possible over very long paths, 4) VHF and UHF signal scatter for which the received signal frequency is shifted upward and downward from that transmitted and which is believed to be caused by electron plasma waves and ion-acoustic waves generated by the HF modifier, and 5) D region modification.

G-3 THE EARTH AS A RADIO SOURCE: Donald A. Gurnett, University of Iowa, Iowa City, Iowa.

Satellite-borne radio wave experiments have shown that the earth emits non-thermal radio emissions over a very broad range of frequencies, extending from as low as 1 kHz to several MHz. Two main components can be identified in the spectrum. The first component is a very weak quasi-static continuum which usually extends from the local plasma frequency (sometimes as low as 1 kHz) with decreasing intensity up to the limit of detectability which is usually several hundred kHz. A distinct enhancement is evident in the spectrum at frequencies below the solar wind plasma frequency where the radiation is permanently trapped within the low density regions of the magnetospheric cavity. The second component in the spectrum consists of a very intense sporadic emission with peak intensity in the range from about 100 kHz to 300 kHz and significant intensities extending over the range from 50 kHz to 500 kHz. At peak intensity the total power emitted in this frequency range is about $10^9$ watts, which is more than the total decametric radio emission from Jupiter. The earth is, therefore, a very powerful planetary radio source. This radio emission is referred to as terrestrial kilometric radiation. Direction finding observations with spinning spacecrafts show that the kilometric radiation appears to originate from low altitudes in the auroral zones. At large radial distances the radiation is primarily observed on the poleward side of two cone-shaped surfaces which are centered on the earth and symmetrically located with respect to the northern and sourthern auroral zones. Comparisons with auroral photographs obtained from the low altitude, polar orbiting, DAPP satellite show that the terrestrial kilometric radiation is closely correlated with the occurrence of discrete auroral arcs. This association indicates that the kilometric radiation is probably generated by the intense "inverted V" electron precipitation bands which cause the discrete auroral arcs.

## GENERAL SESSION

G-4 NEW FACILITIES AT THE ARECIBO OBSERVATORY: E. K. Conklin and M. M. Davis, National Astronomy and Ionosphere Center, Arecibo, Puerto Rico.

A major upgrading of the facilities at Arecibo is nearly completed. Alignment of the 38,000 new aluminum surface panels is proceeding towards a goal of 3 mm rms across the 1000-foot diameter, using both conventional survey techniques and a laser distance measuring system developed at NAIC. The alignment is monitored by aperture efficiency measurements at 1420, 2380, 2695 and 4830 MHz. Useful operation is expected up to about 7.2 GHz. The stability of the suspended feed structure has been improved to allow pointing accuracies of about 10 arc-sec rms, and a new on-line computer will provide both telescope control and data analysis. Major new radio astronomy systems include low-noise 1420 and 1667 MHz receivers for H and OH spectral lines, and a 1008 channel autocorrelator. The antenna beamwidth and sensitivity at these frequencies is 3.2 arc-min and 8K per Jy. Operation is also planned at 2380 and 4830 MHz; at these frequencies we expect continuum observations to reach the confusion limit at about $5 \times 10^4$ sources/steradian. A new radar system, operating at 2380 MHz, has been installed. It includes a 450 KW CW transmitter and low-noise maser receivers. A 100-foot parabolic reflector is under construction 10 km north of the 1000-foot reflector, to be used as a radar interferometer. This system will provide about 3 km resolution on Venus during the 1975 conjunction, 30 km resolution on Mercury, and should be able to detect the Galilean satellites of Jupiter and the rings of Saturn. A new 100 KW 50 MHz transmitter will be used for lunar radar and ionospheric backscatter experiments.

G-5 MICROWAVE METHODS FOR ACOUSTIC SURFACE WAVES WITH APPLICATION TO WAVEGUIDES: Arthur A. Oliner, Polytechnic Institute of New York, Brooklyn, New York.

The recent enormous interest in acoustic surface waves is based on the recognition that VHF and UHF devices using these waves offer superior performance, combined with very small size and weight, and with increased reliability and ruggedness. The talk will first briefly review the nature of acoustic surface waves and will in the process illustrate their potential for superior device performance.

Acoustic wave behavior is more complicated than that for electromagnetic waves because two bulk wave types exist instead of one and because the boundary conditions for acoustic waves in solids are much more involved. As a result, acoustic wave

behavior in complicated geometries is difficult to describe analytically, and only relatively few such solutions exist. The author and his colleagues have developed a rigorous and systematic analytical procedure for acoustic wave problems based on the adaptation to acoustics of certain established methods in electromagnetic microwaves. As a result, rigorous equivalent networks can be (and have been) derived for various purely acoustical situations. These networks and the microwave approach offer both a systematic analytical procedure and substantial physical insight for those trained in electromagnetics. These methods have been applied with striking success to various waveguiding structures for acoustic surface waves (some of which resemble certain waveguides for integrated optics). The analytical results compare very well with available measured data and with purely numerical results; illustrative examples will be presented.

## COMMISSION II, Session 1

Monday, October 14 1:30 pm - 5:00 pm
PROPAGATION IN THE ATMOSPHERE
CHAIRMAN: C. I. Beard, Naval Research Laboratory

1-1 LABORATORY INVESTIGATION OF REFRACTIVE INDEX STRUCTURE IN THE MARITIME BOUNDARY LAYER: R. Bolgiano, Jr., Cornell University, Ithaca, New York; Z. Warhaft, Appleton Laboratory, Slough, Bucks, England; M. Coantic, Institut de Mécanique Statistique de la Turbulence, Marseille, France.

Conditions of temperature inversion, moisture lapse, and wind shear similar to those occurring in the atmosphere have been produced, under laboratory control, in the I.M.S.T. Air-Sea Interaction Facility. A refractometer has been employed, together with resistance thermometers and hot-wire anemometers, to study the structure of refractive index and its relation to dynamic stability. Clear evidence has been observed of the evaporation duct and of the intense gradients of its profile. Also, at critical Richardson number, brief periods of intense refractivity irregularities have been seen in otherwise quiet flow. This "bursting" phenomenon resembles closely intermittency observed in the free atmosphere. By detailed study of the fluid dynamical conditions underwhich these bursts occur, and of the structure within bursts as compared to that outside, considerable illumination of the cause and character of fine-scale refractive index fluctuations in the maritime atmosphere is achieved.

1-2 REMOTE PROBING OF THE VERTICAL AIR MOTIONS IN CLEAR AIR CONVECTIVE STRUCTURES: J. R. Rowland and A. Arnold, Johns Hopkins University, Silver Spring, Maryland.

During the Fall of 1973, an experiment was conducted in which an FM-CW radar, a high power pulsed radar, and an acoustic sounder were used to probe the convective layer. In this experiment the geometry of individual convective elements was observed with the three remote probes. In addition, fine-scale measurements of the vertical velocity structure throughout the convective layer were obtained from the doppler return of the acoustic sounder. Comparisons of these doppler measurements with estimates of vertical air motions obtained from insect trajectories indicated on the FM-CW radar records show close agreement. In this paper a detailed analysis is made relating the geometrical patterns observed by all three remote probes to the vertical velocity structure observed with the acoustic sounder and FM-CW radar.

1-3 A RADIO ACOUSTIC SOUNDING SYSTEM FOR MEASUREMENT OF ATMOSPHERIC TEMPERATURE: E. M. North, Jr., and A. M. Peterson, Radio Science Laboratory, Stanford University.

A technique for remote measurement of temperature profiles in the atmosphere to heights of about 2.5 kilometers has been developed and successfully tested at Stanford University. The equipment used is called a Radio Acoustic Sounding System (RASS) because a burst of sound energy propagating vertically upward is tracked by a C-W doppler radar. Air temperature at each height is determined from the instantaneous speed of the sound pulse and a complete profile can be obtained in only a few seconds. In order to improve accuracy, the measurements are normally averaged for several minutes, but even so, the sampling rate is high enough to continuously monitor the temperature profile.

An analysis shows that the RMS error in temperature measurement due to noise is less than $0.2^{o}K$ for 20 dB SNR and increased to $0.9^{o}K$ when SNR is only 6 dB. Vertical motion of only one meter per second causes an error nearly twice this large, but such motion is generally short lived so its effect can be reduced by averaging.

Radiosonde and captive balloon profileometer measurements have confirmed the predicted accuracy of the Radio-acoustic technique.

1-4 SUNSET RADAR FACILITY: J. L. Green, T. E. VanZandt, J. W. Warnock, R. W. Winkler, L. Thomas, F. J. Eggert, National Oceanic and Atmospheric Administration, Boulder, Colorado.

The Aeronomy Laboratory of the National Oceanic and Atmospheric Administration (NOAA) has constructed a large VHF radar facility in a deep canyon near Boulder, Colorado. This radar will be used to study winds, waves and turbulence in the troposphere and stratosphere. The antenna has an area of 7200 $m^2$, and an east-west beam width of 2.3 degrees. The radar wave length is 7.41 m, the transmitter power is 250 Kw, and the range resolution is 150 m. This radar facility is sited under a region of prominent mountain lee wave activity. Preliminary results will be shown.

1-5 EFFECTS OF FREQUENCY AGILITY AND LINEAR FM ON TRACKING ERRORS DUE TO GLINT: R. J. Polge, B. K. Bhagavan and L. Callas, University of Alabama, Huntsville, Alabama.

A computer program was developed for the simulation of an experimental array radar tracking a scintillating target. The target is modeled as an N-scatterer configuration, and the return signal takes into account difference in range, masking coefficient, and phase delay of the scatterers. The program was validated and exercised for various target trajectories and types of modulation. The study shows that much of the tracking errors at short and medium range are due to glint, and that linear FM reduces significantly the range error due to glint while frequency agility reduces angle error by a factor of three

to five. A combination of linear FM and frequency agility reduces both types of error. Eight distinct frequencies are recommended for the implementation of frequency agility.

1-6 A SPATIAL FILTER REMOTE PROBE: R. W. Lee, Stanford Electronics Laboratories, Stanford, California.

The use of spatial filters on both the transmitting and receiving apertures on a line-of-sight path makes possible the determination of the velocity, turbulence, and turbulence spectrum profile along the path with high spatial resolution. This resolution is achieved directly, with no data processing required other than the measurement of frequency and amplitude. No assumptions are made regarding the stationarity of the medium, or the spectrum of refractivity. The limitations of the technique arise from signal-to-noise considerations, imperfect spatial filters, and multiple scattering. Results from a simple 61 m optical path suggest that the theoretical resolution of 0.7 m was achieved. A more sophisticated system is under construction, for operation over a 220 m vertical path, with up to 200 resolution elements.

1-7 REMOTE ATMOSPHERIC PROBING, USING SPATIAL AND TEMPORAL FILTERING IN A MM-WAVE PROPAGATION EXPERIMENT: K. Leuenberger, Stanford University, Stanford, California.

New methods have been developed to use amplitude--as well as phase--data on a line-of-sight mm-wave receiver array. As a consequence, the resolution along the propagation path has been improved, such as to prevent the "ill-conditioning" properties of the procedures used to probe both wind velocity $v_\perp$ and the turbulence coefficient $C_n^2$ in the past, under all common conditions. In basically two ways which we call coherent or incoherent, a weighted sum is performed with the signals of an 8-element array to obtain a spatial filter. The coherent-type (complex) filtering yields two-sided, generally asymmetrical fluctuation spectra. A special feature of this method is the fact that the point of sensitivity on path can be shifted over essentially its whole range without any loss of resolution. Results of spectra as well as remotely probed data will be shown.

## COMMISSION III, Session 1

Monday, October 14 1:30 pm - 5:00 pm
IONOSPHERIC MODELING
CHAIRMAN: John M. Kelso, ITT Electrophysics Laboratories, Inc., Columbia, Maryland

1-1 SENSITIVITY OF HF PROPAGATION CHARACTERISTICS TO ELECTRON DENSITY PARAMETERS: C. M. Rush and W. Edwards, Air Force Cambridge Research Laboratories, Bedford, Massachusetts.

Using ray-tracing techniques to numerically simulate HF communication circuit parameters, the sensitivity of the final results to the form of the assumed electron density profile is investigated. Various electron density models that have been reported in the literature and used in HF propagation prediction schemes have been normalized and the dependence of such propagation characterisitics as the MUF, D and E region absorption, F region absorption and group delay, on profile shape has been determined. In addition, the change in propagation characteristics resulting from uncertainties in the critical frequencies and the heights of the different ionospheric levels, has been studied. These uncertainties can arise as the result of the normal daily ionospheric variability about its median value or from the inability to accurately predict the magnitude of certain ionospheric parameters. It will be seen that the differences in HF propagation circuit performance associated with different ionospheric models are much smaller compared to those differences in propagation characteristics arising as the result of errors in the prediction of certain ionospheric parameters such as the critical frequency and height of the F2 region.

1-2 ANALYSIS OF SWEEP-FREQUENCY SKY-WAVE BACKSCATTER IONOGRAM DATA FOR IONOSPHERIC LAYER PARAMETERS: N. Narayana Rao, University of Illinois, Urbana, Illinois.

Methods are presented for the derivation of earth-concentric quasi-parabolic ionospheric layer parameters from data obtained by sweep-frequency sky-wave backscatter technique. Two types of data are considered: (a) the leading edge, i.e., the minimum time-delay trace of the backscatter ionogram and (b) discrete oblique ionogram traces in high-resolution backscatter. For case (a), the method employs three data points on the leading edge. For case (b), three data points on the oblique ionogram trace with one of the data points being the point of coincidence of the ionogram trace with the leading edge are used. The methods are illustrated by using both synthetic and experimental data. The validity of the results obtained from the analysis of the experimental data is discussed.

1-3 PREDICTION OF DIFFERENTIAL TIME DELAY ERRORS IN HF HYPERBOLIC POSITION-FIXING SYSTEMS: N. Narayana Rao, R. I. Beckwith and E. W. Ernst, University of Illinois, Urbana, Illinois.

Differential time delay errors in HF hyperbolic position-fixing systems arising from ionospheric propagation time delays are estimated by using a propagation prediction model for several path-pairs employed in a time-of-arrival experiment. The reduction in the differential time delay errors afforded by the prediction model is discussed by a comparison of the prediction model results with experimental observations. The paper is concluded with a brief description of a possible method of application of the differential time delay error prediction in practice to correct for the ionospheric effect.

1-4 REAL TIME CORRECTION OF IONOSPHERIC INDUCED ERRORS IN REMOTE SENSING RADAR DATA: D. E. Patton, D. B. Odom and C. E. Riley, Raytheon Company, Sudbury, Massachusetts.

One difficulty in analyzing ionospherically propagated data is identifying the propagation mode and correcting for time dispersion introduced by the ionosphere. Approaches usually used assume specular reflection at a virtual height which is either held constant or varied in a simple manner. Due to increased accuracy requirements placed on sensing radar sites and the speed and versatility of mini-computers it is now feasible to consider using a ray-tracing approach to calculate propagation parameters either on site, or via time sharing terminals. This paper presents the results of a study of the accuracies obtained using both one and three dimensional ray-tracing programs suitable for real time data analysis and frequency selection. The approach relies on backscatter ionogram data for real time updating of the ionospheric model. In this study, predictions were made of the mode structure on two paths and then were compared to oblique ionograms to determine the accuracy in the delay time and the Maximum Useful Frequencies (MUF) obtained for each mode. The results showed that the differences in the predicted and measured delay times were less than 100 microseconds. In addition, significant improvement in the mode MUF over that obtained using median ionospheric predictions were obtained. The errors introduced by ionospheric tilts were analyzed and the results compared with the three-dimensional ray-tracing program. It is concluded that it is feasible to use a ray-tracing approach to aid in the real time analysis and operation of a high frequency remote sensing site. This approach will yield improved accuracy in selection of operating frequencies, calculating the true ground range, and in minimizing the effects of multimode propagation.

## COMMISSION III, Session 1

1-5 HF PROPAGATION PREDICTIONS: PROGRAM PROLIFERATION IN THE REAL WORLD: David B. Sailors, Naval Electronics Laboratory Center, San Diego, California.

Of the more than 20 odd HF frequency prediction programs developed over the last 15 years, four were selected to compare predicted MUF and observed oblique sounder data. Measurements of 25 paths were collected to form a data base of over 3000 observed MOF's. This data base was compared against the predicted values from the ITSA-1, the ITS-78 (red deck), the ITS-78 (blue deck) Shimazaki, and the ITS-78 (blue deck) Ostrow programs. The predicted and observed data were screened into 15 subsets of data to see the effect of path length, geomagnetic latitude, sunspot number, and season. The dependence with season showed that the ITS-78 (red deck) predicts high on average; the ITS-78 (blue deck) Ostrow predicts low; the ITS-78 (blue deck) Shimazaki predicts between the red deck and the MOF's; and the ITSA-1 more nearly follows the observed MOF's. The r.m.s residual and the standard error of the estimate of regression were calculated to determine the minimum overall residual, to determine if the observed and predicted data were linearly related, and to see if regression could improve the results. The ITS-78 (blue deck) Shimazaki had the lowest r.m.s residual (4.5 MHz). Both the ITS-78 (blue deck) Shimazaki and the ITSA-1 appear to vary linearly with the observed MOF's. With regression the error of the ITS-78 (blue deck) Shimazaki was reduced to 1.5 MHz and the error of the ITSA-1 to 1.8 MHz. None of the programs adequately represented the polar region; in these regions the mean MOF seemed to be more usuable.

1-6 THE APPLICATION OF IONOSPHERIC MODELS TO THE "STARTING PROBLEM" IN DERIVATION OF IONOSPHERIC VERTICAL IONIZATION DENSITY PROFILES FROM IONOGRAMS: S. M. Ostrow, National Oceanic and Atmospheric Administration, Boulder, Colorado.

Arbitrary assumptions about the ionization of the lower ionosphere can introduce serious errors in ionospheric vertical ionization density profiles derived from ionograms, particularly when conditions depart significantly from the average. It is shown that simple ionospheric models with parameters derived only from ionogram measurements, can be used to improve the accuracy of vertical ionization profiles deduced from ionograms. Profiles obtained by use of these models are compared with those obtained by use of other "starting" techniques. The relative merits of different approaches to the "starting problem" are discussed.

1-7 A MODEL OF IONIZATION IN THE MESOSPHERE: L. C. Hale and E. T. Chesworth, The Pennsylvania State University, University Park, Pennsylvania.

Experimental evidence is presented that attachment of light positive ions and electrons to particulates, probably ice crystals nucleated on meteoritic dust, plays a major role in ionization processes in the mesosphere. A simple model incorporating this attachment plus solar controlled detachment of electrons can explain a variety of observations of mesospheric ionization under both quiet and disturbed conditions. The model suggests reasons for observed correlations among ionization parameters at different altitudes determined by direct probe measurements and radio wave absorption. The model is consistent with larger values of nitric oxide at the mesopause level than current gas-phase theories.

1-8 SEASONAL AND SOLAR FLUX DEPENDENCE OF MID-LATITUDE SLAB THICKNESS: J. A. Klobuchar, Air Force Cambridge Laboratories, Bedford, Massachusetts; H. Hajeb Hosseinieh, Emmanuel College, Boston, Massachusetts.

Over six and one half years of monthly mean slab thickness values obtained from Total Electron Content data taken at Hamilton, Massachusetts and f0F2 data from the Wallops Island, Virginia ionosonde have been studied for their seasonal and solar flux dependence. Nighttime monthly mean slab thickness values, averaged over 23 to 03 hours local time exhibit no consistent seasonal or solar cycle variation. However, mean daytime slab thickness, averaged over the 10 to 16 hour local time period, has a strong seasonal dependence, in phase with solar declination, and a 10.7 cm. solar flux dependence which is large in summer, but which is zero during the months December through April. The contribution of the E and the F1 regions was subtracted from monthly mean slab thickness values for the 10-16 hour local time period for the solar maximum years of 1969 and 1970, and the resultant F2 region slab thickness was used to infer values of neutral temperature using a theoretical expression relating slab thickness to neutral temperature derived by Titheridge (1973). Comparisons of these derived Tn values with those obtained from the Salah and Evans (1972) empirical model obtained from actual observations of $T_n$ from the Millstone Hill Thomson scatter facility showed an annual variation twice as large for the $T_n$ values derived from slab thickness. A numerical model of mid-latitude slab thickness behavior as a function of time of day, day of year, and 10.7 cm. solar flux has been derived. The overall model accuracy is approximately ten percent with smaller errors in the daytime period.

## COMMISSION IV, Session 1

Monday, October 14 1:30 pm - 5:00 pm
VLF HISS AND PLANETARY RADIATION
CHAIRMAN: T. V. Evans, Massachusetts Institute for Technology
Lexington, Massachusetts

1-1 THE LOCATION OF THE TERRESTRIAL KILOMETRIC RADIATION SOURCE REGION: William S. Kurth, Mark M. Baumback, and Donald A. Gurnett, University of Iowa, Iowa City, Iowa.

Radio wave experiments on board the HAWKEYE-1 and IMP-8 satellites are used in direction finding studies to locate the source region of terrestrial kilometric radiation. This radiation has peak intensity between 100 kHz and 300 kHz and is emitted in intense, sporadic bursts lasting from several minutes to several hours. The total power emitted from more intense events is about $10^9$ watts. HAWKEYE-1 is in polar orbit and IMP-8 is in an orbit near the ecliptic plane and each spacecraft spins such that the earth often lies near the plane perpendicular to the spin axes. Both experiments sample the intensity of radiation in a narrow pass band near 200 kHz using long dipole antennas which are perpendicular to the spin axis. The resulting spin-modulated signal is decoded to find the angle of arrival of the radiation. The source region has a small angular size and appears to be located at low altitudes in the auroral zones. Other information is available which supports this conclusion. The radiation pattern observed at large radial distances appears as two solid cones centered on the earth and symmetric with the auroral zones. Close correlation between kilometric radiation bursts and discrete auroral arcs indicate that the radiation may be generated by "inverted V" electron precipitation bands which also cause the discrete arcs. Also, the energy required to produce such intense bursts of radiation is available in the auroral oval.

1-2 OBSERVATIONS OF THE EARTH AT LOW FREQUENCIES: M. L. Kaiser and R. G. Stone, Goddard Space Flight Center, Greenbelt, Maryland.

We have studied the spatial distribution of low-frequency ($25\ \text{kHz} \leq f < 1\ \text{MHz}$) terrestrial radio noise as observed by Radio Astronomy Explorer-2 from lunar orbit. Through the use of the lunar occultation technique, we are able to do some source location mapping and can get an estimate of the size of the source regions. We discuss here the characteristics of three types of noise we have categorized: 1) broad-band intense noise with a time scale of hours, 2) narrow-band intense noise with a time scale of minutes, and 3) low-level continuum observed when the first two sources are inactive. Type 1 noise seems to occur over a very broad region, perhaps extending well back into the magnetotail, whereas the second type of noise is sharply localized and occurs in the near vicinity of the Earth.

The low-level continuum appears to emanate from a region several Earth radii across centered on the Earth and is conceivably synchrotron emission from trapped particles in the Van Allen zones. Correlation of these noise types with particle precipitation and magnetospheric indices will be discussed along with a comparison with the low-frequency portion of Jupiter's radio spectrum.

1-3 SPECTRAL BEHAVIOR OF JUPITER NEAR 1 MHz: Larry W. Brown, Goddard Space Flight Center, Greenbelt, Maryland.

Emission from Jupiter was observed by the IMP-6 spacecraft at 24 frequencies between 425 and 9990 kHz. The Jovian bursts were identified through the phase of the observed modulated signal detected from the spinning dipole antenna. Five-hundred days of data have been scanned with a positive detection of 320 events. The spectral behavior can be divided into three types. At the upper satellite frequencies the emission follows the same spectral behavior as Earth-based observations. These bursts are usually the weakest in intensity and the shortest-lived of the satellite observed bursts. They are seldom detected much below a frequency of 1 MHz, and show a high correlation with Earth-based instruments. A second type occurs below 1 MHz and shows a low- and high-frequency cutoff similar to low-frequency Earth noise (L. W. Brown Ap. J. 180, 1973). The emission peak occurs near 870 kHz with a bandwidth of approximately 300 kHz. Stronger bursts have emission peaks nearer 737 kHz, whereas weaker bursts peak near 1100 kHz. A third type occurs for bursts with very large intensities lasting over long periods of time. This emission is a combination of the first two types, and contains a complex and variable spectral behavior resulting from variations in the low-frequency emission peak and bandwidth. Power spectral analysis shows that a periodicity one-half the Jovian rotational period exists. Such a period could result if emission sources existed near Jupiter's poles, as for Earth noise. Histograms of occurrence probability versus Jovian longitude support this supposition. The traditional decameter sources are less important at lower frequencies with an increasing dominance of the emission when the polar regions are observable. This increased polar emission fits well with the observed spectral behavior at low frequencies and its similarity to Earth noise.

1-4 PROPERTIES OF ELF ELECTROMAGNETIC HISS ABOVE THE EARTH'S IONOSPHERE DEDUCED FROM PLASMA WAVE EXPERIMENTS ON THE OV1-17 AND OGO-6 SATELLITES: M. C. Kelley, University of California, Berkeley, California; B. T. Tsurutani, Jet Propulsion Laboratory, Pasadena, California.

Naturally occurring ELF (10-1000 Hz) emissions known as plasmaspheric hiss are thought to be generated near the magnetic equator just inside the plasmapause. The emissions, after leaving the

source region essentially have access to all parts of the plasmaphere and propagate downward into the upper ionosphere. The large scale features of hiss at these heights have been studied using two simultaneous low altitude polar orbiting satellite experiments: the a.c. electric field experiment on board OV1-17 (altitude: 450 km) and the magnetic search coil experiment on board OGO-6 (altitude: 400-1100 km). The peak OGO-6 signal strength is found at latitudes poleward of the plasmapause. The peak of the OV1-17 signal at lower altitudes occurs several degrees poleward of the OGO-6 maximum. The peak wave intensity correlates well with geomagnetic activity, as indicated by Kp and $D_{ST}$. The high altitude boundary of the signal is statistically found to move equatorward with increasing geomagnetic activity. Strong global asymmetries of the hiss intensity exist. In winter, the hiss is about a factor of three less intense than in summer or during equinoctial months. An explanation of many of these features will be presented.

1-5 INNER ZONE MAGNETOSPHERIC HISS: B. T. Tsurutani and E. J. Smith, Jet Propulsion Laboratory, Pasadena, California; R. M. Thorne, University of California, Los Angeles, California.

Extremely low frequency (200-1000 Hz) electromagnetic hiss has been detected in the inner zone magnetosphere ($L < 2$) by the search coil magnetometer aboard the polar orbiting OGO-6 satellite. These naturally occurring emissions were primarily dectected during intervals of strong magnetic activity, such as storms and substorms. The approximate spectrum, intensity, L-value and local time distributions of the hiss are described. Cyclotron resonance between these emissions and relativistic inner zone electrons can cause pitch angle scattering and loss of the electrons. Calculations are presented which show that the hiss resonates with electrons with parallel resonant energies of >0.4 to >3.0 Mev from $L = 2.0$ to $L = 1.1$ respectively. Using an average, observed hiss intensity of $4 \times 10^{-7}$ $\gamma^2$/Hz and an average observed signal bandwidth, typical turbulent lifetimes for electrons between $L = 2.0$ and 1.1 are computed to be 10 to 60 days respectively. This result agrees with the observations of enhanced electron precipitation during magnetic storms and establishes that cyclotron resonance scattering is an important loss mechanism in the inner zone. Possible origins of the inner zone hiss are discussed, and a model for the source of the waves is presented.

1-6 NEW RESULTS FROM THE SIPLE STATION VLF WAVE INJECTION EXPERIMENT: R. A. Helliwell, J. Katsufrakis, T. F. Bell and R. Raghuram, Stanford University, Stanford, California.

VLF waves in the 1.5-16 kHz range are injected into the magnetosphere from a VLF transmitter located at Siple Station, Antarctica. The injected waves are often amplified up to 30 dB and may cause either stimulation or suppression of VLF emissions which are observed at Roberval, Quebec, Canada. Specific new results not previously reported are: 1) An attenuation band, about 100 Hz wide, may be created in the spectrum just below the frequency of the Siple signal. This band shows no change immediately after the signal is turned off, but gradually disappears over a period of 10-15 seconds. Power line radiation into the magnetosphere may also produce the same kind of attenuation band. 2) Signal growth and associated triggering are inhibited by whistler-mode echoes of preceding signals; injected signals may also quench the natural emission activity. 3) Large variations in the growth rates and emission activity are observed as a function of frequency; activity appears to maximize near one-half the minimum electron gyrofrequency on the path of propagation. Possible applications of these new results include VLF communications through the magnetosphere, diagnostics of the energetic trapped particle population and controlled electron precipitation into the ionosphere.

1-7 EAST-WEST EXTENT OF INDIVIDUAL WHISTLER DUCTS: M. G. Morgan, Dartmouth College, Hanover, New Hampshire.

Whistler ducts seen by ground stations during relatively quiet periods are plotted as tracks in L-LMT (local magnetic time) polar coordinate space, showing the persistence of the ducts and their L variation. Such maps obtained simultaneously at two $L \simeq 4$ stations separated 1.6 hr in LMT are found to be essentially identical. Individual whistlers from the same causative sferic occur simultaneously at the two stations but with duct L-values at the western station seen 1.6 hr previously in LMT by the eastern station. Whistler activity tends to begin and end not simultaneously at the two stations but at the same LMT. The conclusion is that the individual ducts, though thin in the cross-L direction, are extensive in the east-west direction, standing in an L-LMT pattern fixed in magnetospheric coordinates and unchanging in UT. Density studies should reveal whether or not these shells are plasma flow contours. However, even if they are flow contours, the equatorial radial component of the velocity of the flow will not be equal to dL/dt of a duct seen at a ground station unless the flow is exactly co-rotational. Whereas no UT variations of the duct patterns have been seen, they are anticipated during disturbances. The results suggest that the creation of a duct pattern in some LMT sector is a requirement for whistlers to occur and, given a supply of sferics in its broadly conjugate area, a station will see them only as it turns through the standing pattern.

COMMISSION V, Session 1

Monday, October 14 1:30 pm - 5:00 pm
RADIO AND RADAR OBSERVATIONS FROM SPACECRAFT
CHAIRMAN: T. W. Thompson, Jet Propulsion Laboratory

1-1 A SURVEY OF PLANETOLOGY STUDIES BY SPACECRAFT RADAR: W. E. Brown, Jr., Jet Propulsion Laboratory, Pasadena, California.

There have been two spacecraft radar systems that have been used to deduce surface parameters of the Moon and other systems are in various stages of planning and development for Venus and Mars. The Surveyor landing radar was the first such system to be used for science purposes and the echo characteristics were successfully used to measure lunar surface dielectric constant as 3.4 and infer that the surface was basic (basalt-like) material. Also, the Surveyor radar was the first to identify the modification in radar backscatter cross-section caused by fresh new craters about 50-100 meters in diameter.

The second spacecraft radar system was specifically designed for science observations and was flown on Apollo 17 (1972). The Apollo Lunar Sounder Experiment (ALSE) was a 3 frequency coherent imaging radar capable of imaging subsurface features at depths as great as 2000 meters below the surface. It also produced new data on the lunar profile. Subsurface imagery is currently being studied by geologists and data on near surface layering (within 100 meters of the surface) are being produced. The continuous profile data show small elevation changes (50 to 100 meters) over the concentric rings in the major basins and are proving very useful in identifying and classifying surface features on the front side as well as the backside of the Moon.

The future systems include an altimeter for the Pioneer Venus Orbiter (1979), an imaging system called Venus Orbiting Imaging Radar (VOIR) (1984), and a sounding radar for a Mars Orbiter. Other studies are concerned with spacecraft radar systems for observing comets, outer planets and their satellites. The scientific interest in radar systems as measurement devices centers about their versatility in observing surface features (through clouds or in darkness), surface roughness (on a 2 to 20 cm scale), the intrinsic range (profile) information and the electrical properties (mineral and free water content inferences). It is recognized that the radar, as a remote sensor, complements the visible, IR, UV wavelength imaging systems. The longer wavelengths used by radars provide a means of studying a unique class of planetary surface and subsurface properties.

1-2 LOCAL LUNAR TOPOGRAPHY FROM THE APOLLO 17 RADAR IMAGERY: C. Elachi, W. E. Brown, Jr., L. Roth, T. W. Thompson and M. Tiernan, Jet Propulsion Laboratory, Pasadena, California

During the flight of Apollo 17, an on-board multifrequency radar sounding experiment was conducted to detect lunar subsurface layers. However the VHF data provided radar surface imagery and profiling over two complete lunar orbits. We are using this data as a direct technique to measure crater profiles and depths. We measured the depth and depth/diameter for the main craters on the Apollo 17 track (Maraldi, Hevelius and others) and compared the direct radar measurement to previous measurements derived from optical observations. We will report and discuss these measurements and the potentials of radar systems in future orbiting missions (Venus-Pioneer, Mars Orbiter, VOIR).

1-3 WAVE REFLECTION AND TRANSMISSION AT INTERFACES INVOLVING GRADED DIELECTRICS: R. A. Simpson, Center for Radar Astronomy, Stanford, California.

Mathematical techniques for obtaining reflection and transmission coefficients at a dielectric boundary for both horizontal and vertical polarizations are outlined. The assumed geometry includes two half-spaces between which a layer of linearly increasing permittivity is sandwiched. Results are discussed in terms of active and passive remote sensing of planetary bodies.

1-4 VENUS EXPLORATION WITH ORBITAL IMAGING RADAR: R. S. Saunders and Charles Elachi, Jet Propulsion Laboratory, Pasadena, California.

The surface of Venus is the last major unknown in our exploration of the terrestrial planets. By 1980 it is anticipated that much of the planet will be imaged from Arecibo at resolutions of one to ten km. These images should reveal regional differences in the surface morphology and allow initial determination of geologic provinces. For a continuing program of Venus exploration, it is desirable to obtain complete coverage of the surface from an orbital imaging radar. The Mariner experience with Mars demonstrates the necessity to obtain complete high resolution coverage. A misleading conception of Mars evolved following Mariners 4, 6, and 7. Only Mariner 9, with complete areal coverage allowed geologic interpretation. The 100 m resolution B frames were essential to this effort. Venus has a dense atmosphere, and like the Earth and Mars is likely to have surface modifying processes related to the atmosphere. If these processes result in deposition-erosion at the surface of Venus as they do on the Earth and Mars, then, as with these two planets, much may be revealed about the past

climatic and tectonic history of the planet. Only erosion can reveal the details of depositional and tectonic events. Unlike the Moon, where the major processes are revealed at one km resolution, planets with abundant volatiles must be imaged at resolutions of at least 100 m to reveal the process that has operated and thus reconstruct the geologic history. Experience gained from the Apollo Lunar Sounder Experiment has provided the experience in radar data processing to justify confidence that an orbiting imaging radar is a realistic goal for the future exploration of Venus.

1-5 THE RINGS OF SATURN; A FUTURE BISTATIC-RADAR TARGET: Essam A. Marouf and G. Leonard Tyler, Stanford University, Stanford, California.

In a few years, a spacecraft will fly-by the massive planet Saturn occulting its system of rings as viewed from Earth. A coherently transmitted signal when received after encountering the rings will help in unfolding many secrets of this unique system. This paper presents an analysis of such a radio experiment. The rings are modeled as a circularly symmetric slab of randomly distributed particles moving in Keplerian orbits close to Saturn's equator. The coherently transmitted wave emerges from the rings as a narrow-band stochastic process. The mean, or coherent, signal changes in phase and amplitude. These two effects are best understood in terms of an equivalent uniform slab of a complex refractive index that depends on the physical parameters of the model used. A multiple scattering formulation for this refractive index requires the solution of a modified single particle scattering problem. By replacing the classical boundary value approach by an initial value method (I.V.M.) a solution for the modified single particle scattering is developed. The I.V.M. is validated via a comparison with the classical Mie solution for plane wave scattering on a dielectric sphere. To complete the characterization of the received process, assumed Gaussian, the autocorrelation and power spectral density of the incoherent part of the signal are also derived. The shape, bandwidth, and total power are related to the spacecraft antenna pattern, the experiment geometry, and the bistatic radar cross section per unit ring area. The I.V.M. is invoked here again to compute explicitly the bistatic radar cross section per unit ring area as a function of the rings model parameters.

1-6 FIFTEEN YEARS OF SPACE RADIO ASTRONOMY: Robert G. Stone, Goddard Space Flight Center, Greenbelt, Maryland.

For more than a decade now, radio observations in the frequency range from 10 MHz to 10 kHz have been obtained from space vehicles orbiting above the plasmasphere. This review covers both observations and their interpretations, as well as the

techniques developed to obtain source direction information. The electrically short dipole, easily deployed and calibrated, continues to be used extensively. The Radio Astronomy Explorer (RAE) satellites, each with a pair of 227m-long V antennas, remain the only successful attempt at deploying "large" antennas. The "spinning dipole" method of direction finding has been highly developed. This technique cross-correlates the antenna pattern with the spin-modulated data. The phase, adjusted for maximum correlation, is related to source direction. Occultations are being observed by RAE-2 in its 1100-km lunar orbit. The first occultations to be investigated include those of solar and magnetospheric sources. Future planned techniques will also be discussed. The following observations and their interpretations will be reviewed: (a) the average cosmic noise spectrum to 200 kHz and the general feature of sky maps at 3.93 and 6.55 MHz, (b) properties and trajectories of solar bursts between .05 and 1 AU, (c) the spectrum and properties of Jovian emission, (d) the spectra and location of several magnetospheric sources (a comparison of magnetospheric spectra of the Earth and Jupiter is striking), (e) a brief account of atmospheric and man-made noise, and (f) the possibility of low-frequency emission from Saturn and other sources.

1-7 DECAMETRIC AND HECTOMETRIC OBSERVATIONS OF JUPITER FROM THE RAE-1 SATELLITE: M. D. Desch and T. D. Carr, University of Florida, Gainesville, Florida.

An analysis of data from the Radio Astronomy Explorer 1 (RAE-1) satellite at 8 frequencies between 4700 and 450 kHz, inclusive, revealed the presence of bursts from Jupiter as well as from the sun. There was a strong correlation of occurrence probability of the Jovian bursts with the System III longitude histograms showed little resemblence to those characteristic of the higher decametric frequencies. A pronounced dependence of occurrence probability on the phase of Io was apparent at 4700, 3930, and 2200 kHz, and an equally strong Europa effect was discovered at 1300, 900, and 700 kHz. The active phases of Io were near $90^{\circ}$ and $240^{\circ}$ from superior geocentric conjunction as in the case of the higher frequencies, but the favored Europa phase is $190^{\circ}$, suggestive of initial propagation along field-aligned ducts. The spectrum of Jupiter's peak burst flux densities was extended from 4700 kHz down to 450 kHz, revealing a well-defined maximum at 8 MHz. We suggest that Jupiter's most intense burst emission arises from a region about 1.7 radii from the magnetic dipole center, where the field is about 1/5 that at the planetary surface.

COMMISSION V, Session 1

1-8 JOVIAN DECIMETRIC EMISSION AS DEDUCED FROM PIONEER 10 ELECTRON FLUXES: J. L. Luthey, S. Gulkis, M. Klein, Jet Propulsion Laboratory, Pasadena, California.

Synchrotron radiation from Jupiter has been calculated using Pioneer 10 electron fluxes and magnetic field data. In the region of overlap between ground-based and in-situ measurements (2.96-6$R_J$), the decimetric emission is equaled or exceeded by the computed flux. The radial distribution of emission for L>2.9 is at least 2.5 times observed values at 10.4 cm and 21 cm of earlier epochs; and the shape of the observed radial distribution demands that more emission must come from L<2.9. Straightforward extrapolation of the integral flux from L=2.9 to 1.1 yields radio flux densities that are at least 5 times the observed flux densities with a spectrum that is positive or flat depending primarily on the density of low energy electrons. The computed angle of the electric vector is consistent with ground-based measurements.

1-9 A SURVEY OF THE GALACTIC BACKGROUND RADIATION AT 3.93 AND 6.55 MHz: J. K. Alexander and J. C. Novaco, Goddard Space Flight Center, Greenbelt, Maryland.

A map of the Galactic background at 3.93 and 6.55 MHz is presented for the whole sky between declinations of $\pm 60^{o}$. The data were taken with the V antenna on RAE-1, in orbit around the Earth. The V antenna has an angular resolution of approximately one steradian. The observations are being confirmed by data from RAE-2, currently in operation in lunar orbit. This satellite will also extend the sky mapping to other frequencies in the 1-10 MHz band using two independent receivers. The dominant aspect of the maps at 3.93 and 6.55 MHz is a region of high brightness that encompasses the region toward the Galactic center and a large region of low brightness that extends to high Galactic latitudes from near the Galactic equator at $\ell \sim 215^{o}$. There are several minor lows which are probably due to absorption in discrete complexes of Galactic HII. At $\ell = 80^{o}$, $b = 0^{o}$ there is a low, possibly due to absorption in the Cygnus X complex. At 6.55 MHz there is a weak low at $\ell \sim 195^{o}$, $b \sim 40^{o}$ that may be associated with the filamentary nebulosity found by Meaburn, possibly blended with absorption from the I Orion association. This low and another in the 3.93 MHz map at $\ell \sim 40^{o}$, $b \sim -30^{o}$ appear to be coincident with filamentary nebulosity associated with the Cetus Arc.

1-10 PLANETARY RADIO ASTRONOMY ON THE MARINER MISSIONS JUPITER SATURN 1977: James W. Warwick, University of Colorado, Boulder, Colorado; Joseph K. Alexander, Goddard Space Flight Center, Greenbelt, Maryland.

The missions will provide novel perspectives on energetic particles, plasmas, and fields in Jupiter's environment, and hopefully identify rigorous new constraints on all proposed mechanisms for the decametric radio emissions. MJS77 will carry the first low frequency receiver to fly into Jupiter's vicinity, probably within the orbit of Io. The receiver senses right-hand and left-hand polarization over the frequency range 1.2 kHz to 40.5 MHz, in a series of operating modes covering both fast and slow bursts. These modes are programmed by the MJS77 Flight Data System so as to create a nominal 266-2/3 bits per second data stream shortly after launch and also in the encounter phase of the missions. Depending somewhat on the spacecraft radio frequency interference signature we expect to observe Jupiter and Saturn emissions throughout the four years of flight, and beyond. Furthermore, we expect to observe solar emissions which will be especially intriguing during the many months when the spacecraft lies opposite the Earth with respect to the sun. During encounter phases, the experiment will occasionally operate in a special high-data-rate mode employing the same data channels normally occupied by the television system, which are 115.2kbits per second. These brief, but highly detailed, periods can perhaps identify sferics and subsequent whistlers. At encounter, the system sensitivity in principle exceeds that of the largest ground-based radio telescopes by a power factor of about $10^5$. However, to safeguard the front-end circuitry, the receiver will then operate with no less than 45 dB of attenuation, which reduces this advantage to only a few decibels.

## COMMISSION VI, Session 1

Monday, October 14 1:30 pm - 5:00 pm
HIGH-FREQUENCY METHODS
CHAIRMAN: R. G. Kouyoumjian, Ohio State University

1-1 CHARACTERISTICS OF SLOT ANTENNAS IN PLASMA-CLAD CONES:
K. E. Golden and G. E. Stewart, The Aerospace Corporation, El Segundo, California.

The radiation and admittance characteristics of slot antennas in conical reentry bodies can be approximated in various ways. For bodies which are large in comparison with the signal wavelength, the antenna characteristics are controlled primarily by the curvature of the surface in the vicinity of the slot. Depending on the radiation pattern cut or the relative orientation of slots, different approximations can be employed. Computations based on a tangent cylinder technique are presented which give excellent agreement with laboratory measured data except in cases where scattering from the tip or rear edge of the vehicle are significant. Mutual admittance and radiation characteristics for X-band rectangular slots are presented for both radial and circumferential slot antennas. For radial slots, tip effects are negligible, while for circumferential slots the edge effects must be considered. Radiation patterns and admittance characteristics of slot antennas have been compared with actual reentry vehicle flight data. The on-board antenna measurements (isolation and aperture admittance) are used as a diagnostic tool to obtain the electronic properties of the boundary layer plasma sheath. The equivalent integrated reentry boundary layer conductivity and thickness are determined from the measured change in the S and C-band antenna isolation. The average collision frequency is then derived from changes in the C-band aperture admittance. Computed antenna gain and radiation patterns based on a tangent cylinder model cone are then compared with flight data giving good agreement in both the pre-reentry (free space) and reentry portions of flight.

1-2 A COMBINED MOMENT METHOD - GEOMETRICAL THEORY OF DIFFRACTION TECHNIQUE FOR APPLICATION IN THE TIME DOMAIN:
G. A. Thiele, T. H. Newhouse and G. K. Chan, The Ohio State University, Columbus, Ohio.

In recent years the frequency domain analysis of antennas and antennas on metallic bodies wherein the body is not large in terms of the wavelength has been greatly facilitated by advances in the solution of integral equation formulation via the method of moments. Such techniques may be referred to as low frequency methods. They are limited only by computer storage as to the size of structure that may be analyzed. On the other hand, the geometrical theory of diffraction (GTD) is

best suited to structures that are arbitrarily large in terms of the wavelength. However, determination of the transient response of wire antennas on or near a large finite structure is difficult with either method alone. The combination of the two techniques is accomplished in the frequency domain by representing a wire antenna with the method of moments and using GTD techniques to represent the structure on or near which the wire antenna is located. The representation of the structure appears as an addition term $\Delta Z_{mn}$ to the usual impedance matrix elements $Z_{mn}$ such that $Z'_{mn} = Z_{mn} + \Delta Z_{mn}$. Thus, it is computationally practical to generate sufficient frequency domain data such that an accurate Fourier transform to the time domain may be accomplished. Results will be presented for several problems such as a monopole on a circular disc and a monopole near a conducting step.

1-3 A UNIFORM ASYMPTOTIC THEORY FOR THE DIFFRACTION OF AN ELECTROMAGNETIC FIELD BY A CURVED WEDGE: S. W. Lee and G. Deschamps, University of Illinois, Urbana, Illinois.

The diffraction of a high frequency vector electromagnetic field by a conducting curved wedge formed by two smooth surfaces $\Sigma_1$ and $\Sigma_2$ meeting along a curve $\Gamma$ is considered. The high frequency incident field is of the form $E_i(r) = A(r)e^{ik_0S(r)}$ where $k_0$ is a large parameter and S and A satisfy respectively the eikonal and transport equations. The classical geometrical optics field is the sum $E_g = E_1 + E_2$ of two fields where $E_1$ coincides with $E_i$ over the illuminated region and $E_2$ is the field geometrically reflected on the surfaces $\Sigma_1$ and $\Sigma_2$. Each of these fields is discontinuous along shadow boundaries $SB_1$ and $SB_2$ generated respectively by the rays of fields $E_1$ and $E_2$ that meet $\Gamma$. The diffracted field away from the shadow boundaries is given by Keller's geometrical theory of diffraction (GTD). Its expression may be simplified, in the full vector case, by making use of rotations about the edge. Then a single diffraction function $\chi$ can be used to relate $E_1$ and $E_2$ respectively to diffracted fields $E_I$ and $E_{II}$. On the shadow boundaries the GTD diffracted field becomes infinite. A systematic method to avoid this difficulty is to construct a "uniform" solution which can be done by modifying separately $E_1$ and $E_2$. Such methods are based on assuming a form of solution (ansatz) inspired by that for the Sommerfeld half-plane problem. They have been applied to scalar field incident on plane wedges, and to vector fields incident on plane edges. A different form of solution has also been proposed for the vector field incident on a curved wedge. Here the original form of the ansatz is applied to this problem where F is a Fresnel integral and $\tilde{F}$ its asymptotic form. The argument of F is $k^{\frac{1}{2}}\xi$, with $= S_I - S_1$ the difference between the

eikonal of the primary field $E_1$ and that of diffracted field $E_I$. The root $\xi$ of $\xi^2$ is chosen to be positive on the dark side of SB. It can be shown that $E_I - FE_1$ is continuous and finite at SB where it is composed of two terms: the first one depends on the edge curvature and the second involves spatial derivatives of the incident field at the observation point. For the general vector problem these derivatives must be computed with respect to a frame rotating about the edge. For some particular incident fields the last two terms can be combined into a single diffracted ray field satisfying the transport equation relative to the eikonal of the diffracted field. These extra terms have often been neglected or missed.

1-4 A DYADIC DIFFRACTION COEFFICIENT FOR AN ELECTROMAGNETIC WAVE WHICH IS RAPIDLY-VARYING AT AN EDGE: Y. M. Hwang and R. G. Kouyoumjian, Ohio State University, Columbus, Ohio.

Pathak and Kouyoumjian [1] have given an expression for the edge diffracted electric field which is proportional to the product of the incident electric field at the point of diffraction $Q_E$ and a dyadic diffraction coefficient. In this paper their result is generalized to the case where the incident field is rapidly-varying at $Q_E$ so that the diffracted field is also proportional to the spatial derivatives of the incident field at $Q_E$ thereby introducing a dyadic diffraction coefficient of higher-order, which will be referred to here simply as the dyadic slope diffraction coefficient. The dyadic slope diffraction coefficient is found from a canonical wedge problem where the incident field vanishes at $Q_E$ and only the higher-order (slope) diffracted field is present in the solution. The integral representation of this diffracted field is evaluated asymptotically and a slope diffraction coefficient which is the sum of only two dyads is obtained. Like the edge diffraction coefficient of reference [1], this slope diffraction coefficient is valid in the transition regions adjacent to the shadow and reflection boundaries. The edge diffracted field is then the sum of the ordinary diffracted field of order $k^{-1/2}$ given by [1] and the slope diffracted field of order $k^{-3/2}$. Several examples are presented where the incident field vanishes (or is otherwise rapidly-varying) at the edge to demonstrate the accuracy and utility of the new diffraction coefficient.

[1] P. H. Pathak and R. G. Kouyoumjian, "The Dyadic Diffraction Coefficient for a Perfectly-Conducting Wedge", Report 2183-4, Ohio State University, 1970.

1-5 EFFECTS OF TORSIONAL SURFACE RAYS ON THE RADIATION FROM APERTURES IN CONVEX CYLINDRICAL SURFACES: P. H. Pathak and R. G. Kouyoumjian, Ohio State University, Columbus, Ohio.

The geometrical theory of diffraction (GTD) is extended to include the effects of torsional surface rays on the radiation from apertures in arbitrary, convex conducting cylinders. As in the GTD solution given previously for torsionless surface rays[1], the radiated electric field vector is decomposed into components along the normal (n) and the binormal (b) directions of the surface diffracted ray. Launching and diffraction coefficients are employed to describe the excitation of the surface ray field, and the field radiated tangentially from the surface ray. In the present GTD solution it is found that the n component of the diffracted electric field is unaffected by torsion to first order; whereas the b component is affected by torsion even to first order. In the transition region adjacent to the shadow boundary the component of the field directly radiated from the aperture is represented by Fock-type functions. In the illuminated region, the field directly radiated by the aperture is treated by geometrical optics. The present GTD result is duduced from an asymptotic analysis of the field radiated by an arbitrarily oriented, infinitesimal magnetic current moment on a circular cylinder. As a result of an extensive numerical study based on the GTD solution for the circular cylinder, certain conclusions are reached concerning the range of parameters for which torsion is important; selected patterns are shown to confirm these observations. The accuracy of this GTD solution is tested by comparison with numerical results based on the eigenfunction solution. The modifications of the GTD solution introduced for the circular cylinder case are readily extended to the arbitrary convex cylinder.

1. P. H. Pathak and R. G. Kouyoumjian: "The Radiation from Apertures in Curved Surfaces," NASA Report CR-2263, Ohio State University, 1973. (Also a paper on this topic was presented at the Sept. 1971 URSI meeting at U.C.L.A.)

1-6 DIFFRACTION FROM AN EDGE SCATTERING CENTER NEAR A SPECULAR POINT: K. M. Mitzner, Northrop Corporation, Hawthorne, California.

For high frequency backscatter from an open convex shell, the edge diffraction will partially cancel the specular reflection when the specular point is sufficiently close to the edge. This paper considers the case in which the edge is of sufficiently

high curvature and is appropriately oriented so that the incident phase varies rapidly along the edge in the vicinity of the specular point. In this case, the cancelling field appears to emanate from a single edge scattering center which, as predicted by Geometrical Theory of Diffraction (GTD), is a point at which the direction of incidence is normal to the edge. The diffraction from this scattering center is the sum of a physical optics term which involves a Fresnel integral plus a fringe wave term of simpler form. As the specular point recedes from the edge, the edge diffraction contribution approaches the value predicted by standard GTD.

## COMMISSION VIII, Session 1

Monday, October 14 1:30 pm - 5:00 pm
MAN-MADE RADIO NOISE
CHAIRMAN: G. Hagn, Stanford Research Institute

1-1 THE ELECTROMAGNETIC PULSE FROM NUCLEAR DETONATIONS: G. H. Price, Stanford Research Institute, Menlo Park, California.

Models of the processes whereby a nuclear detonation emits a coherent electromagnetic pulse are reviewed, and causes of the asymmetry in the current system necessary for the radiation of a signal are discussed. These causes include the earth atmosphere interface, the atmospheric-density gradient, anisotropy of the environment by virtue of the presence of the earth's magnetic field, nonuniform emission of the energetic radiation ($\gamma$ and X rays) by the detonation, and asymmetries of the delivery vehicle and device case. The available experimental data are then examined in the light of the models. These data suffice to establish the models as probably correct in their identification of the principal processes whereby the nuclear electromagnetic pulse is generated, but they are inadequate for a quantitative assessment of the models' accuracy.

1-2 LONG TERM MEASUREMENTS OF RADIO NOISE STATISTICS UTILIZING A LSI MICROPROCESSOR: Mike Gray, Art Cohen, H. Dean McKay, Andy Hish Associate, Chatworth, California.

The availability of low-cost, small, large-scale integration (LSI) microprocessors has made it possible to acquire statistical radio noise data in near real-time. A test program is underway to instrument a 2-MV power distribution line utilizing an array of unattended remote units and a 16-bit minicomputer. The scheme utilizes a microprocessor as a remote-control and signal processor. All elements of the remote collection unit such as the antenna selection, bandwidth selection, calibration, frequency selection are controlled by the microprocessor. Detection is accomplished utilizing a high speed A/D converter. The system will collect and process electromagnetic environmental data on a 24-hour basis for several years. Statistical radio noise data will be generated as a function of distance from the line, time of day, season, atmospheric conditions, and aging. Outputs of the system are serial ASCII and include peak in a sample period, true RMS, quasi-peak (both ANSI and CISPR), average, and log average, converted to field-intensity or other engineering units. In addition, statistical data on zero-crossings, pulse width interval, and pulse repetition frequency are available.

1-3 AN AUTOMATED MEASUREMENT SYSTEM FOR DETERMINING ENVIRONMENTAL RADIOFREQUENCY FIELD INTENSITIES: R. A. Tell, N. N. Hankin, D. E. Janes, Environmental Protection Agency, Silver Spring, Maryland.

The U. S. Environmental Protection Agency supports a field operations group to obtain baseline data on the levels of existing environmental radiation, to determine any change in the radiological quality of the envronment, to provide data for estimating population exposure to ionizing and nonionizing radiation, and to determine if environmental radiation levels are within established guidelines and standards.

This paper describes a system developed for the purpose of measuring radiofrequency exposure levels found in our electromagnetic environment. The system described is configured around a scanning spectrum analyzer, appropriate calibrated antenna systems, and a minicomputer data acquisition system. The principal features of the system are: 1) the capability of responding to bands of interest over a very broad spectrum of frequencies (e.g., 0.5 MHz to 10 GHz), 2) several antenna systems which allow measurement of significant polarization components of incident fields so that the total power density, or field strength, may be determined for signals impinging from any direction, 3) a wide dynamic range in measuring field amplitudes so that measurements in the close vicinity of powerful emitters will also accurately reveal the relatively lower intensities from weaker, more distant sources, 4) the provision for simplified collection and analysis, including statistical treatment, of RF exposure data, and 5) mobility by means of installation in a van so that environmental measurements may be made at various geographic locations throughout the country. The effects of system errors in absolute measurements are discussed and the applicability of the different forms of data which can be collected are related to the problem of specifying potential hazards. Representative data are presented which demonstrate the various acquisition and analysis approaches which can be used, and the initial use in field-operations (starting this fall) of the monitoring van is discussed.

1-4 TIME AND AMPLITUDE STATISTICS FOR ELECTROMAGNETIC NOISE IN MINES: Motohisa Kanda, National Bureau of Standards, Boulder, Colorado.

The time and amplitude statistics illustrated in this paper are those necessary to adequately describe the time-dependent, EM noise in mines. They are 1) Allan Variance Analyses (AVA), 2) Interpulse Spacing Distributions (ISD), 3) Pulse Duration Distributions (PDD), 4) Average Crossing Rates (ACR), and 5) Amplitude Probability Distributions (APD). These statistics are illustrated using a rather large store of raw analog data

recorded in operational mines through computer software techniques. The parameter assessed through this statistical approach is the magnetic field strength. The absolute values of the magnetic field strength analyzed are obtained with calibrated equipments. The frequency ranges of the magnetic field strengths cover from 10 kHz to 32 MHz. The length of time necessary to provide statistical validity was determined from the Allan Variance Analysis to be about 17 minutes for most of the mines measured. The curves generated for the illustrations characterize the noise environment in the mines from which the corresponding data were taken, and should aid in the design of reliable communication systems for such mines.

1-5 MAN-MADE NOISE SIGNATURE STUDY AT 76 AND 200 kHz: Earl C. Bolton, Institute for Telecommunication Sciences, Boulder Colorado.

A study of man-made noise was made at the frequencies of 76 and 200 kHz. The main objective of the study was to see if various areas of man-made noise sources had type signatures that would, in a general way, be descriptive of these sources. The sources analyzed were automobile ignition systems, and industrial sites and residential sites.

1-6 THE EFFECTS OF MAN-MADE RADIO NOISE ON HIGH FREQUENCY COMMUNICATIONS SITES: W. R. Lauber, Communications Research Centre, Ottawa, Canada.

The expected values of man-made noise at a quiet receiving location (EMNQRL) as noted in CCIR Reports 322 and 258 represent minimum levels of daytime noise at a High Frequency communications site. We report noise measurements at a receiving site on the east coast of Canada obtained for four seasons for the two daytime periods 0800-1200 and 1200-1600 hours. The results show no significant differences between the two time periods and they are in good agreement with the EMNQRL. Tests have also been conducted in the time period 0800-1200 hours at a site near Ottawa for three seasons with good agreement with the EMNQRL. Large differences were noted between day and night noise levels at low frequencies (e.g., 2.5 MHz) at both the above sites. Results are also presented from "degraded" sites, i.e., those that show a large rms error when compared to the EMNQRL and smaller differences between day and night noise levels at the low frequencies. Since the main sources of site degradation are powerline noise and vehicle ignition noise, data have been collected which show the extent of site degradation as related to the distance from the powerline and that a "typical" vehicle located 50 feet from an antenna may raise the average noise power by 6-9 dB over the

background in the 20-30 MHz band. Vehicle door buzzers may raise the average noise power by a further 10-19 dB.

1-7 IMPULSIVE IGNITION NOISE AT 1370 MHz: Donald L. Nielson, Stanford Research Institute, Menlo Park, California.

Automobile ignition noise was recorded in a wide bandwidth at 1370 MHz. From a measurement of impulse width at various amplitude thresholds at this frequency, impulse noise appears to be bandlimited in a receiver with impulse bandwidth of 16 MHz. Probability densities of impulse energy and cumulative distribution of inter-pulse delay are given.

1-8 RECENT IMPROVEMENTS IN THE SUPPRESSION OF IGNITION NOISE: Richard A. Shepherd, James C. Gaddie, Stanford Research Institute, Meno Park, California.

The incidental electromagnetic radiation from an automobile that falls logically under the heading of ignition noise is due to high-frequency (impulsive) currents that flow in the vehicle's wiring. The three major sources of these impulses are 1) the breakdown of the gap between the distributor rotor and the distributor posts, 2) the breakdown of the spark plug gap, and 3) the closure of the breaker points. To suppress the ignition noise, each of these sources can be treated individually. Concepts have been developed and prototypes have been built and tested to incorporate simple low-pass filters directly into the spark plug (by appropriate sizing of the plug's shell and inner electrode) and into the distributor. The goal was to start with a selected vehicle that was already suppressed by the techniques used in mass production and to improve this suppression by 10 dB over the frequency band 30 to 500 MHz. The amount of suppression obtained, determined by comparison of scanned peak voltage measurements, ranged from about 13 dB to about 20 dB. Interesting aspects and problems of peak measurements of automobile ignition noise are discussed. Economy in fabrication, installation, and maintenance of the suppression system are considered.

COMMISSION I, Session 1; Joint With COMMISSION V

Tuesday, October 15 8:30 am - 12:00 noon
MEASUREMENTS AND STANDARDS IN RADIO ASTRONOMY
CHAIRMAN: H. M. Altschuler, National Bureau of Standards

1-1 ABSOLUTE MEASUREMENTS IN RADIO ASTRONOMY OF FLUX DENSITY AND SKY BRIGHTNESS: John W. Findlay, National Radio Astronomy Observatory, Green Bank, West Virginia.

It is important to many branches of radio astronomy to know the flux density received at the earth from radio sources. The radio source may be of very small angular size, in which case the flux from it is measured in Janskys (1 Jy = $10^{-26}$ watts per square meter per Hz), or the source may be an area of sky; in this case the unit is Jy per steradian. To measure such power densities requires an antenna with a well-known gain and pattern. At NRAO a standard gain horn, 36 m long with an aperture 5.4 x 4 m is used. It is fixed in position in such a way that one strong radio source (Cassiopeia A--3C 461) passes through the horn beam. The beam also sees parts of the galactic plane and some areas of quite cold sky. Absolute measurements are made by comparing the power received by the antenna with that from a resistor. The resistor temperature can be changed by known amounts. Some of the details of measures taken to minimize measurement errors will be described, and the results of work at 820 Mhz and 1400 MHz will be given.

1-2 CAS A AS A STANDARD NOISE SOURCE FOR ACCURATE G/T MEASUREMENTS: W. C. Daywitt, National Bureau of Standards, Boulder, Colorado.

A significant segment of the radio star literature describing Cassiopeia A (Cas A) was reviewed in an effort to determine whether or not Cas A could be used as a standard noise source in accurate G/T measurements of satellite-communication ground stations. A summary is presented from a precision-measurements point of view of the findings of this literature search, revealing effects on the accuracy that should be known among those making and using star flux measurements; including such effects as atmospheric attenuation, decay rate, size corrections, and so forth. However, some effects due to atmospheric refraction and turbulence, and the correct application of decay rates appear to be often overlooked.

1-3 PRECISION FLUX DENSITY MEASUREMENTS OF SELECTED RADIO SOURCES AT 2295 MHz: M. J. Klein and C. T. Stelzried, Jet Propulsion Laboratory, Pasadena, California.

The flux densities of several extragalactic radio sources have been measured at 2295 MHz (13.1 cm) with the 26-m parabolic antenna at the NASA Venus Station, Goldstone, California. The sources, whose flux densities lie between 3 and 40 Jy, were

selected as potentially useful flux calibration standards. The flux-density ratios relative to Virgo A were measured with an accuracy of ± 0.5%. The following considerations contributed to the high precision: the relatively small antenna greatly reduces the sensitivity to pointing errors and corrections for the spatial resolution of the sources while the low system noise temperature (17K) provides the necessary signal-to-noise ratios; the observations were planned over a 2-year period to minimize errors due to diurnal and seasonal effects; two-dimensional maps centered on the source positions were made to determine the background source confusion level. Virgo A was taken as the flux calibration standard because it is included in a separate program being conducted jointly with NBS to measure absolute flux densities.

1-4 ABSOLUTE CALIBRATION OF MILLIMETER WAVELENGTH SPECTRAL LINES: B. L. Ulich, National Radio Astronomy Observatory, Tucson, Arizona.

Methods of calibrating the absolute intensity of spectral line radiation are discussed with emphasis on millimeter wavelength techniques. The results of special observations made with the NRAO 36-foot radio telescope on Kitt peak and a mixer radiometer with RF bandpass filters and a rotating chopper wheel are presented. Standard sources are calibrated for six strong millimeter wavelength spectral lines. The importance of the antenna error pattern in the interpretation of measured antenna temperatures is also discussed.

1-5 ANTENNA GAIN AND FIGURE OF MERIT MEASUREMENTS UTILIZING RESULTS FROM RADIO ASTRONOMY: David F. Wait and Motohisa Kanda, National Bureau of Standards, Boulder, Colorado.

Published results from radio astronomy measurements are being utilized to evaluate the performance of satellite communication earth terminals. The National Bureau of Standards has been involved in analyzing the errors with which certain measurement parameters can be determined using radio sources to provide a convenient means of regularly assessing performance and degradation of the ground based antenna receiving system. The initial effort has been to measure antenna gain and to measure the ratio of antenna gain to system noise temperature of a communications ground receiving station (referred to as G/T or Figure of Merit). These measurements will be briefly described to point out the metrology difficulties and to indicate what radio astronomers could do to make their results more useful to the satellite communications industry.

## COMMISSION II, Session 2

Tuesday, October 15, 8:30 am - 12:00 noon
RADIO OCEANOGRAPHY I
CHAIRMAN: I. Katz, Johns Hopkins University

2-1 SEASAT: AN INTEGRATED SPACECRAFT OBSERVATORY FOR THE OCEANS: John R. Apel, National Oceanic and Atmospheric Administration, Miami, Florida.

The ocean dynamics satellite, SEASAT-A, has been proposed by NASA for launch in 1978. It has the potential for enlarging the breadth and depth of scientific knowledge in oceanography, maritime meteorology, and geodesy. It is a research-oriented program whose strong suit is an array of active and passive microwave and infrared sensors that give it the capability of observing the ocean on a day/night, near-all-weather basis. The sensors to be incorporated in SEASAT-A have predecessors that have been successfully flown on both aircraft and spacecraft. They form a set of integrated, mutually supporting devices that includes a short pulse radar altimeter, a synthetic aperture imaging radar, a microwave wind scatterometer, a scanning microwave radiometer, and a scanning infrared radiometer. From these instruments will flow quantitative information on waves, surface winds, sea surface temperatures, the geoid, currents, tides, and features on the ocean, land, and in the atmosphere. The paper includes a brief review of some of the outstanding research problems in the interaction of microwave energy with the sea surface.

2-2 RADAR IMAGING OF OCEAN SURFACE PATTERNS: W. E. Brown, Jr., C. Elachi and T. W. Thompson, California Institute of Technology, Pasadena, California.

We will present and discuss data collected during the last year with the JPL L-band imaging radar. The radar imagery shows an amazing number of different surface patterns (swells, current edges, roughness fronts, oil spills and possibly internal waves). The imaging radar seems to add a new dimension to the remote sensing of the ocean surface and will be a major instrument in the field of "Radio-Oceanography". We will also report preliminary analysis of the quantitative relation between the radar image spectrum and the wave energy spectrum. The radar image spectrum was obtained by two-dimensional Fast Fourier Transform and presented in false color to enhance the dynamic range. The wave energy spectrum was obtained using the NOAA laser profilometer. From our preliminary analysis, a $k^2$ transform relates the two spectra leading to the conclusion that the radar image intensity is related indirectly to the slope distribution of the ocean surface.

2-3 SEA SURFACE TOPOGRAPHY FROM SPACE - GSFC GEOID: F. O. Vonbun, J. Marsh, and F. Lerch, National Aeronautics and Space Administration, Greenbelt, Maryland; and J. McGoogan, National Aeronautics and Space Administration, Wallops Island, Virginia.

This paper deals with a major area of radio-oceanography namely with a determination of the sea surface topography. Results of the altimeter experiment on Skylab for tests of the Goddard geoid are discussed. Further outlined are the influence of orbital errors on the sea surface topography and numerical examples are given based upon real tracking data. Theoretical orbital error analysis cannot shine any new light on these problems because the error values involved are small (meter range) and the reliability of theoretical error analysis diminishes at these rather small values of orbital errors. Using a space borne altimeter on Skylab revealed for the first time that topography of the worlds oceans can be "measured" with high accuracy. As a matter of fact the S-193 altimeter experiment (McGoogan, et al) exceeded its expectations and have provided quite unique ocean surface topographic information. Surface variations (geoid) are discussed as they relate to those "computed" from satellite orbital dynamics (and the gravity field of the earth) and ground based gravity data obtained from DOD. The recent Goddard geoid has been constructed from 430,000 satellite tracking data elements (range, range rate, angles) in 20,000 ground gravity observations. One of the last experiments on Skylab was to "measure" and/or test this geoid over one orbit. This was the first time that one was able to perform such a test because never before was an altimeter flown in space. Preliminary results reveal that the "computed water surface" deviates only between 5 to 20 meters from the measured one. Orbital height errors have been computed for geodetic type satellites and are in the order of 0.8 to 2 meters. Such errors are somewhat larger for the Skylab due to its relative lower orbit, large area, venting and the fact that only conventional uniform S-band data are available for orbit computations.

2-4 A CLOSED FORM RELATION FOR THE AVERAGE RETURN WAVEFORM FROM A NEAR-NADIR POINTED, SHORT PULSE, SATELLITE BASED RADAR ALTIMETER: G. S. Brown, Applied Science Associates, Inc., Apex, North Carolina.

Relatively small deviations from nadir pointing can result in a rather serious degradation in the accuracy of surface information to be derived from radar altimetry data unless the pointing angle is known. The pointing angle can be estimated rather accurately by a priori knowledge of its effect on the average backscattered waveform. The conventional approach to computing the average return waveform, including pointing error effects, involves a two-dimensional numerical integration over the

scattering surface appropriately weighted by the system point target response and the antenna pattern. Because of computing complexity and the loss of physical insight, this method is not particularly attractive. An alternate approach involves computing the backscattered waveform for a unit impulse incident upon the surface and convolving this result with the system point target response. If we take advantage of the facts that altimeter antennas are normally designed to have circular symmetry in the main beam and that only a portion of the main beam effectively illuminates the surface, the surface impulse response can be reduced to an infinite sum of Bessel functions of the second kind. Convolution of this result with the system point target response effectively reduces the series to one term and a closed form results.

2-5 ANALYSIS OF RADAR MEASUREMENT OF OCEAN WAVE HEIGHT: Tzay Y. Young, University of Miami, Coral Gables, Florida.

This paper examines various factors that affect the accuracy of radar measurement of ocean wave height from space, with particular emphasis on the effect of pulse width. The problem is formulated as one of estimating a parameter of a Gaussian random signal in Gaussian noise. The CramérRao bound on the mean-square estimation error is evaluated. It is shown that at a given signal-to-noise ratio, large or small, the bound is inversely proportional to the pulse width, provided that the radar pulse is sufficiently short. Hence there is an optimal pulse width and overly short pulses will result in a poor performance of the radar system. The result is valid for both optimal estimation and a suboptimal scheme similar to the signal processing methods in practical use. Both beam-limited and pulse-limited radar systems are considered, and performance curves are presented.

2-6 A SIMULATION OF SYNTHETIC APERTURE RADAR IMAGING OF OCEAN WAVES: C. T. Swift, National Aeronautics and Space Administration, Hampton, Virginia.

A simulation of radar imaging of ocean waves with synthetic aperture techniques is presented. The modelling is simplistic from the oceanographic and electromagnetic viewpoint in order to minimize the computational problems, yet reveal some of the physical problems associated with the imaging of moving ocean waves. The model assumes: (1) The radar illuminates a one-dimensional, one harmonic ocean wave that propagates as $\sin\left(\frac{2\pi x}{L} = \omega t\right)$ where L = ocean wavelength and g = acceleration due to gravity, $\omega = \sqrt{2\pi g/L}$. (2) The scattering is assumed to be governed by geometrical optics. (3) The radar is assumed to

be down-looking, with doppler processing (range processing is suppressed due to the one-dimensional nature of the problem). (4) The beamwidth of the antenna (or integration time) is assumed to be sufficiently narrow to restrict the specular points of the peaks and troughs of the wave.

The results show that conventional processing of the image gives familiar results if the ocean waves are stationary, i.e., if $\omega = o$, the specular points are resolved within the resolution element $\varepsilon = \lambda H/2vT$ where $\lambda$ = electromagnetic wavelength, H = aircraft altitude, v = aircraft velocity and T = integration time for the synthetic aperture. When the ocean wave dispersion relationship $\omega = \sqrt{2\pi g/L}$ is satisfied, the image is "smeared" and reduced in intensity due to the motion of the specular points over the integration time. In effect, the image of the ocean is transferred to the near field of the synthetic aperture.

2-7 CALIBRATION OF THE SKYLAB S-194 RADIOMETER BY THE OBSERVATION OF SEA BRIGHTNESS AT L-BAND: W. H. Peake and J. J. Apinis, Ohio State University, Columbus, Ohio; R. Applegate, R. Plugge and G. Pieper, Martin Marietta Corp., Denver, Colorado.

The Skylab S-194 package is an L-Band (1.4 GHz) microwave radiometer with a one square meter antenna viewing the earth at nadir. The instrument thus measures the brightness temperature of the terrestrial surface, averaged over a circular footprint of about 60 miles in diameter, with a temperature resolution of about 1 to $2^{o}$K. A major objective of the instrument is to monitor the microwave brightness over the ocean, and its variation with water temperature, salinity, wave mean square slope, foam cover, etc. This paper reviews the expected performance of the instrument, the adjustments that must be made to the raw data to account for such instrumental and configurational disturbances as finite beamwidth, reflected solar energy, sea surface roughness, etc., and the use of the inflight cosmic noise calibrations to estimate small changes in instrument performance in the flight environment. Selected targets of known brightness temperature will also provide information on systems performance and data to evaluate calibration and correction constants. Observed brightness temperatures from the three SKYLAB missions SL2, SL3, and SL4 are reviewed. Data on a number of passes of S-194 over the ocean, and over a variety of land surfaces, will be used to illustrate the range of brightness temperatures encountered, the consistency of the data from pass to pass, and the degree to which the observations correspond to the predicted performance of the instrument.

2-8 SPECTRAL VARIATION IN THE MICROWAVE EMISSIVITY OF THE ROUGHENED SEAS: Per Gloersen, William J. Webster, Jr. and Thomas T. Wilheit, National Aeronautic and Space

Administration, Greenbelt, Maryland; Duncan B. Ross, National Oceanic and Atmospheric Administration, Miami, Florida; and T. C. Chang, National Academy of Sciences, Resident Research Associate, Washington, D. C.

Recently acquired microwave data obtained from the NASA CV 990 research aircraft over a wavelength range from 0.8 to 21 cm. for various ocean surface wind conditions have yielded the variation of the sea surface emissivity as functions of the wavelength, polarization, the viewing angle, and the surface wind speed. Data acquired at a wavelength of 1.5 cm., horizontal polarization, agree with the data obtained earlier by Nordberg et al. and Hollinger at nadir and 50° viewing angles respectively; the ratio of brightness temperature change to wind speed change was found to be approximately 1°K per meter per second over a wind speed range of 5 to 26 meters per second. Combining these measurements with the earlier measurements, it is evident that microwave radiometry can be used as a remote-sensing anemometer over all wind speed ranges of interest. Analysis of the data revealed that for nadir-viewing instruments, the ratio of the brightness temperature change to wind speed change was approximately constant for the wavelength range of 0.8 to 2.8 cm., about three quarters of that value at 6 cm., and nearly zero at 21 cm. A model which assumes a thin transition layer with continuously varying dielectric constant between the foam or streak bubbles or actively breaking waves and the sea surface leads to calculated surface emissivities which are consistent with the observations.

## COMMISSION II, Session 3

Tuesday, October 15 8:30 am - 12:00 noon
SELECTED TOPICS IN PROPAGATION
CHAIRMAN: Alfred H. LaGrone, University of Texas

3-1 SINGLE-FREQUENCY MAGNETOTELLURIC IMPEDANCE MEASUREMENTS: Robert Sainati and J. Robert Katan, Naval Underwater Systems Center, New London, Connecticut.

In May and June of 1973, single-frequency tensor impedance measurements were performed by the Naval Underwater Systems Center (NUSC) at various sites in the western region of the upper Michigan peninsula. The purpose was to deduce the conductivity structure of the area in order to determine the suitability of a proposed site for the U.S. Navy Sanguine Extremely Low-Frequency (ELF) transmitting station. Normally, such measurements are conducted using spherics as sources, but the availability of the U.S. Navy Sanguine Wisconsin Test Facility (WFT) made it possible to perform them at specific frequencies. The tensor impedance was measured by means of the magnetotelluric (MT) resistivity method for frequencies of 45 and 76 Hz. Conducting data was also obtained using the wave impedance method. The MT method is superior to the wave impedance method because it provides a means for estimating the earth structure and conductivity of an area. The results of single-frequency tensor impedance measurements indicate good correlation between the measured data and the deduced geological structure of each site. A comparison of conductivity values obtained from the MT and the wave impedance measurements shows reasonable agreement at most sites.

3-2 MEASUREMENTS OF HF GROUND WAVE PROPAGATION LOSS OVER SEA WATER: Peder Hansen, Naval Electronics Laboratory Center, San Diego, California.

Experimental measurements of path loss have been made in the 2-32 MHz frequency range on a 150 mile path entirely over sea water. The test objective was to verify theoretical ground wave path loss calculations, including the effect of varying sea state, in order to provide data for the design and frequency management of communication systems. The two modes of measurement were (1) stepped frequency sounder using ten 20ms pulses at each of 31 frequencies, and (2) a high power CW signal at 5 frequencies for verification, and indication of fading characterisitics. Measurements were taken at morning, noon, and evening during a one month period. Data were also recorded at 1 hour intervals during one 24-hour period. Below 10 MHz the measured path loss was found to be stable and less than that predicted by theoretical calculations. Above 10 MHz the path loss observed was quite variable, and at times well below the theoretical values. An attempt has been made to correlate the observed path loss variations with the sea state along the propagation path.

3-3 SUBSURFACE PROBING BY MEASUREMENT OF HIGH FREQUENCY WAVE TILT*: R. J. Lytle, E. F. Laine, D. L. Lager, Lawrence Livermore Laboratory, Livermore, California.

Determining conditions beneath the ground by performing measurements on the surface has numerous applications (e.g., hydrology, resource location and definition of extent, location of geophysical anomalies). Various applications require information on geologic conditions and also accurate spatial information on the location and extent of subsurface regions. It is demonstrated that swept high frequency wave tilt measurements have this good resolution capability. The method is particularly applicable in low conductivity regions (e.g., desert, permafrost, snow and ice). Results are shown indicating that the wave tilt is more sensitive to local subsurface conditions for a vertical magnetic dipole transmitter than for a vertical electric dipole transmitter. Useful information is contained in both the magnitude and phase of the wave tilt, but the phase data has less severe instrumentation requirements. Calculated results based upon ray optic models clearly show the modulation effects of multiple subsurface regions. The data inversion problem (i.e., given experimental results, determine the subsurface conditions) is addressed by illustrating ways of deconvolving the data to obtain results for the conductivity, permittivity, and thickness of subsurface regions. Results are given indicating the resolution obtainable for both vertical and horizontal anomalies.

*This work was performed under the auspices of the U.S. Atomic Energy Commission.

3-4 EARTH PROXIMITY EFFECTS ON THE IMPEDANCE OF HORIZONTAL LINEAR ANTENNAS: D. C. Chang, S. W. Maley, A. S. Abul-Kassem, University of Colorado, Boulder, Colorado.

An experimental investigation has been conducted of the influence of the earth upon the input impedance of horizontal linear antennas. The study was made in the laboratory using a horizontal monopole mounted on a vertical highly conducting plane. The monopole length was adjustable as was its height above the simulated earth. The earth was simulated by a mixture of dry sand and powdered graphite. The proportion of graphite could be varied to change the conductivity and dielectric constant of the mixture. For various mixtures used, the conductivity ranged from 0.17 to 0.68 and the dielectric constant varied from 3.30 to 6.25. The loss tangent of these mixtures varied from 0.22 to 0.47. The physical properties of the sand and graphite are such that it is difficult to achieve and maintain a uniform mixture. Nevertheless it was used for a series of measurements. The coaxial transmission line exciting the monopole was equipped with a slotted section to facilitate the impedance measurements.

The measurements indicated that the presence of the earth significantly influences the monopole impedance only if the height of the antenna above the earth is less than about one-half wavelength. Very little data on previous measurements of this type appear in the literature but agreement between the results of this investigation and previous work is good in cases in which comparison is possible.

3-5 GROUNDWAVE PROPAGATION IN THE PRESENCE OF A CLIFF: C. Cloonan, California Polytechnic State University, San Luis Obispo, California; S. W. Maley, University of Colorado, Boulder, Colorado.

Reflection and transmission of groundwaves by a cliff has been studied theoretically and experimentally. The configuration studied consisted of a cliff and earth with different electrical parameters on the two sides of the cliff. The path of propagation intersects the cliff at an arbitrary angle. The limiting case of a path of propagation parallel to the cliff was also considered. The theoretical formulation made use of the compensation theorem to obtain a two dimensional integral equation. This was then reduced to a one dimensional integral equation by a stationary phase integration. Approximate solutions of the equation yield results for the reflected and transmitted waves for various angles of incidence, cliff heights, and electrical parameters of the ground. Experimental measurements were made using laboratory models at microwave frequencies. The experimental configuration permitted variation, over a limited range of all the important parameters; and it permitted measurement and automatic recording of the amplitude and phase of the vertical component of the electric field as a function of position along the propagation path. The results of the experimental measurements were in good agreement with the theoretical results. The investigation has provided experimental confirmation of some earlier theoretical work due primarily to J. R. Wait and it has led to refinements of other theoretical results.

3-6 UHF WAVE PROPAGATION BEYOND THE HORIZON IN THE PRESENCE OF AN ELEVATED TROPOSPHERIC DUCT: M. Robert Dresp, Mitre Corporation, Bedford, Massachusetts.

A theoretical model has been developed which calculates the electromagnetic field produced by a transmitter on or above the earth when an elevated tropospheric duct is present in the propagation medium. The model is particularly useful for the situation when the transmitter and receiver are far beyond the horizon of each other.

Particular attention is given in this paper to the propagation modes that contribute to the leakage of energy out of the duct. It is shown that the "leaky" modes are only slightly less

significant compared with the trapped or ducted modes in producing high field strengths at points beyond the horizon. Field strengths that are only 10 dB to 20 dB below the free space value are shown to exist at heights well above the tropospheric duct. Experimental propagation data obtained in the presence of an elevated tropospheric duct are shown to be in good agreement with the model results.

## COMMISSION III, Session 2

Tuesday, October 15 8:30 am - 12:00 noon
WINDS, WAVES, AND DISTURBANCES
CHAIRMAN: E. R. Schmerling, National Aeronautics and Space Administration, Washington D. C.

2-1 F-REGION NEUTRAL WINDS DERIVED FROM INCOHERENT SCATTER DATA: Brenton J. Watkins and Howard F. Bates, University of Alaska, Fairbanks, Alaska.

A technique has been devised to use incoherent scatter data (ion temperature and velocity, and electron temperature and density) to derive the F-region neutral wind velocity during periods of Joule heating by the magnetospheric electric field. To be found are three wind velocity components and the neutral temperature. The ion energy-balance and the ambipolar diffusion equations supply two of the four conditions necessary for a unique solution. For the third condition it is assumed that the difference vector between neutral wind and ion drift velocities is primarily zonal. For the fourth condition it is assumed that because the atmosphere expands at approximately constant pressure, the rate of increase in neutral temperature is directly proportional to the input Joule power; the starting (equilibrium) neutral temperature is computed from the ion energy-balance equation for zero heating. Several applications of this method to the Chatanika incoherent scatter data will be presented.

2-2 ELECTRON RECOMBINATION IN THE DISTURBED D-REGION: W. Swider and J. C. Ulwick, Air Force Cambridge Research Laboratories, Bedford, Massachusetts; W. A. Dean, Bedford Research Laboratories, Aberdeen, Maryland.

Daytime electron recombination coefficients, $\alpha_{EFF}$ for the 2-5 November 1969 solar proton event are derived from four electron concentration profiles obtained over a forty-nine hour time span plus the associated ionization production rates as calculated from satellite proton spectra. The agreement between the four effective electron recombination coefficient profiles is quite good. The results are compared with past work by others. The constancy of $\alpha_{EFF}$ over the stated time span implies that daytime $\alpha_{EFF}$ is a characteristic function of the daytime disturbed D-region for ionization rates from about 10 to $10^4$ $cm^3$ $sec^{-1}$ and more. Five twilight $\alpha_{EFF}$ profiles have been determined and are argued to be generally consistent with the concept that twilight changes reflect the sunrise increase and sunset decrease of atomic oxygen and molecular oxygen in the singlet delta state. The nighttime behavior of $\alpha_{EFF}$ is discussed briefly and shown to support our previous contentions concerning this parameter at night.

2-3 A LARGE-SCALE "HOLE" IN THE IONOSPHERIC F-REGION CAUSED BY THE LAUNCH OF SKYLAB: M. Mendillo, Boston University, Boston, Massachusetts; G. S. Hawkins, Smithsonian Astrophysical Observatory, Cambridge, Massachusetts; J. A. Klobuchar, Air Force Cambridge Research Laboratories, Bedford, Massachusetts.

Routine Faraday rotations observations of the VHF signal from the geostationary satellite ATS-3 made at Sagamore Hill, Massachusetts revealed that an unusually large and rapid decay in the ionospheric total electron content (TEC) occurred near 12:35 EST on 14 May, 1973. The disturbance appeared as a dramatic "biteout" of substantial magnitude ($\geq$ 50%) and duration ($\simeq$ hours) in the expected diurnal TEC curve for that day. Observations from other sites revealed that a "hole" in the ionospheric F-region was created over a region of approximately 1000 km in radius. The onset of the TEC disturbance occurred within minutes of the launch of NASA's SKYLAB Workshop by a Saturn V rocket. As the rocket moved at F-region heights, the burning second stage engines passed within 150 km of the Sagamore Hill ray path to ATS-3. A detailed analysis of the aeronomic reactions initiated by the constituents of the exhaust field revealed that the F2-region plasma experienced a devastating loss process as the plume expanded. The specific mechanism involved was the rapid ion-atom interchange reactions between the ionospheric $O^+$ and the hydrogen and water vapor molecules in the plume. Model calculations of the diffusion of the plume in the ionosphere and its effect upon continuity equation calculation for TEC showed an excellent agreement with the observed onset and magnitude of the effect. The phenomenon has interesting astro and geophysical implications.

2-4 F-REGION WIND-DYNAMO EFFECTS ON THE E-REGION ELECTRIC FIELDS AND CURRENTS: S. Fukao and S. Matsushita, National Center for Atmospheric Research, Boulder, Colorado.

Based on a diurnal wind model in the ionospheric F region and an electric conductivity model in the E and F regions, effects of the large electric fields produced by the F-region wind dynamo on the E-region electric fields and currents during a quiet period have been investigated. Since the major consistent tidal wind in the E region seems to be semidiurnal, the E-region wind dynamo produces either a strong semidiurnal or a weak diurnal (due to a large diurnal conductivity effect) current system. The F-region wind dynamo enhances the diurnal component of the E-region fields and currents. These computed field results including magnetospheric dawn-to-dusk electric field effects are compared with the polarization fields observed at a few incoherent scatter facilities. Daily variations of the ExB drift in the low-latitude F region caused by the F-region wind dynamo are also discussed.

2-5 EXCITATION OF ACOUSTIC GRAVITY WAVES IN A REALISTIC THERMOSPHERE: C. H. Liu, University of Illinois, Urbana, Illinois; J. Klostermeyer, Max-Planck-Institut für Aeronomie, Lindau, F. R. G.

The response of the upper atmosphere due to the excitation of acoustic gravity waves by various types of sources is studied under realistic thermospheric conditions. Losses due to viscosity, thermal conductivity and ion drag; the effects of winds as well as the vertical temperature variations are all taken into account. The general solution is obtained in terms of the eight characteristic wave modes that propagate in the atmosphere. An "atmospheric transfer function" is defined which determines the response of the upper atmosphere due to general sources. Examples of the transfer function are computed for model atmospheres. It is found that the transfer function is peaked in the wave-number space indicating strong filtering effects. The behavior of the transfer function is affected by the background winds. These transfer functions are then applied to obtain some transient responses of the atmosphere due to excitations. Results are found to differ substantially from those obtained for lossless, isothermal atmosphere. Implications of the computed results to the interpretation of observed acoustic gravity wave data will be discussed.

2-6 DIFFERENTIAL-DOPPLER STUDIES OF TRAVELING IONOSPHERIC DISTURBANCES: J. C. Ghiloni, Western Electric Company, North Andover, Massachusetts; J. V. Evans, Massachusetts Institute for Technology, Lexington, Massachusetts.

By observing the 400 and 150 MHz signals transmitted by the Navy Navigation Series satellites, a differential-Doppler study of traveling ionospheric disturbances has been conducted at Millstone Hill, Westford, Massachusetts. Observations were made over the period January 1971 through March 1973, during which over 2000 passes of the satellites were tracked using an 84-ft. steerable antenna. The differential-Doppler records obtained show signatures of TIDs with wavelengths in the range 100 km $< \lambda <$ 1000 km, approximately, permitting the incidence, wavelength, latitude and other characteristics to be investigated.

In the equinox and winter there is a marked diurnal variation in the detection of TIDs; this appears to reflect the diurnal variation of the ambient ionosphere. The majority of TIDs then have wavelengths in the range $200 \leq \lambda \leq 300$ km and were seen between $33^{\circ}$ and $36^{\circ}$ geographic latitude. In summer there seemed little concentration in time, wavelength or latitude. The possible dependences between the time of occurrence, wavelength, latitude, amplitude and $K_p$ have been investigated using scatter plots. Based on these there seem no obvious dependences on

magnetic activity. Despite this it appears that the majority of TIDs observed were generated in the auroral zone and were seen propagating toward the south.

## COMMISSION IV, Session 2

Tuesday, October 15 8:30 am - 12:00 noon
ENERGETIC ELECTRON FLUXES AND PLASMA BEHAVIOR OF THE MAGNETOSPHERE
CHAIRMAN: Donald A. Gurnett, University of Iowa

2-1 PERIODIC ESCAPE OF ENERGETIC ELECTRONS FROM THE JOVIAN MAGNETOSPHERE: A. J. Dessler, T. W. Hill, and J. F. Carbary, Rice University, Houston, Texas.

We propose a model wherein the eccentricity of Jupiter's dipole moment, combined with an open-tail configuration of the Jovian magnetosphere, leads to escape of energetic electrons from Jupiter's radiation belt modulated with the period of planetary rotation. In the open-tail model, cold ionospheric plasma is accelerated by the rapid rotation of the planet and thrown out of the magnetosphere on the night side, thus creating an open-tail configuration (Hill et al., Geophys. Res. Lett., 1, 3, 1974). The sense of Jupiter's dipole moment causes energetic electrons to (gradient and curvature) drift against the spin of the planet. Energetic electrons that drift faster than the co-rotation speed can drift into the open-field region on the night side and then stream out into interplanetary space without any appreciable loss of energy. Since the Jovian dipole moment is offset approximately 1/4 $R_J$ from the spin axis, the rate of escape of radiation belt particles will depend on the position of the dipole relative to the sun-Jupiter line, the rate of escape being a maximum when the dipole is on the night side. Thus the radiation will be released at a time varying rate that corresponds to the rotation period of Jupiter.

2-2 THE ELECTRON FLUX PRECIPITATED BY LOW-AMPLITUDE MONOCHROMATIC WAVES IN THE MAGNETOSPHERE: Bruce Dingle, Stanford University, Stanford, California.

The flux of energetic electrons precipitated into the ionosphere as a result of magnetospheric wave-particle interactions is calculated using a simple model. Only monochromatic waves are considered although the wave frequency and amplitude may be (slowly) time varying. The wave amplitude is assumed to be sufficiently small that energetic particle bunching effects need not be considered. The approximations used in the model are discussed in terms of practical physical situations involving both natural and man-made waves. Comparisons are made with other methods of calculating precipitated fluxes and with experimental flux measurements.

2-3 GEOMAGNETIC STORM RECOVERY PHASE ELECTRON PRECIPITATION AND ITS IONOSPHERIC EFFECTS BELOW 90 KM: Walther N. Spjeldvik and Richard M. Thorne, University of California, Los Angeles, California.

Precipitation of radiation belt electrons can provide the dominant production of ionization in the mesosphere at middle latitudes following geomagnetic storms. Fluxes of outer zone electrons are considerably enhanced during the main phase of geomagnetic storms and during the recovery electrons radially diffuse to lower L and decay slowly to reform the characteristic two-zone structure. Within the plasmasphere precipitation loss results primarily from resonant pitch angle scattering with naturally occurring ELF whistler mode wave turbulence. The angular distribution and energy spectrum of precipitating electrons is obtained by evaluating the overall scattering due to wave turbulence and Coulomb collisions. The precipitation is strongly latitude dependent, giving rise to D-region ion production rates typically 1-10/cm$^3$sec at L-4($\Lambda$=60$^o$) and is significant below L=2($\Lambda$=45$^o$). Enhanced D-region ionization should persist for typically a week following the storm, consistent with electron precipitation lifetimes. A simplified model for the mesospheric ion chemistry is developed with emphasis placed on evaluation of the free electron concentration. The precise distribution amongst the multiple hydrated cluster ions is not studied; rather different recombination rates are taken for primary and clustered ions. The model provides an adequate fit with observed quiet time electron concentration in the D-region. It is shown that the stormtime electron precipitation can account for observed radio communication disturbances, including a lowering of the ionospheric reflection height by ~10 km for VLF-waves and a significant increase in the D-region absorption of HF-waves.

2-4 THEORETICAL AND EXPERIMENTAL STUDIES OF THE IONIZATION EXCHANGE BETWEEN THE IONOSPHERE AND PLASMASPHERE: J. L. Massa, R. J. Cicerone, A. F. Nagy, University of Michigan Ann Arbor, Michigan; J. V. Evans, Massachusetts Institute for Technology, Lexington, Massachusetts.

The coupled $O^+$ -$H^+$ time-dependent continuity and momentum equations have been solved numerically in order to evaluate the diurnal variation of the number densities and particle fluxes in the region from near the F2 peak to the geomagnetic equator. The results of the theoretical calculations, corresponding to quiet days and post storm time conditions, appropriate for the Millstone Hill field tube, are compared with the results of radar incoherent backscatter observations from that site. During quiet conditions, the nighttime downward proton fluxes are found to be of the order of $10^8 cm^{-2} sec^{-1}$; recovery of the protonosphere proceeds for many days after a storm empties the field tube. A new analysis program was used to deduce the percentage $H^+$ concentration, as a function of altitude, from the Millstone Hill incoherent radar backscatter data. The reanalyzed data shows that during the daytime the $H^+$ concentration

was less than a few percent, up to an altitude of 800 km, in agreement with the model calculations. However, the nighttime measured percentages of 10-20% are significantly lower than the calculated values.

2-5 COMPARISON OF JOULE DISSIPATION AND PARTICLE HEATING RATES FROM CHATANIKA RADAR DATA: P. M. Banks, J. C. Siren, J. R. Doupnik, University of California, San Diego, California.

Observation of ionospheric electric fields and simultaneous electron density profiles permits computation of the atmospheric Joule dissipation rate as a function of altitude. During periods when Chatanika is in the vicinity of the auroral oval, total Joule heating rates often exceed 10 ergs/cm$^2$/sec. To estimate the amount of energy deposited in the atmosphere by energetic electrons, electron density profiles have been transformed into electron production rates by assuming an altitude dependent recombination coefficient. Since an average of 35.5 ev is expended to create each electron-ion pair, estimates of the atmospheric heating rate can then be made. Results indicate that particle heating is generally smaller than Joule heating.

COMMISSION V - JOINT WITH COMMISSION I (See Page 31)

Tuesday, October 15 8:30 am - 12:00 noon

MEASUREMENTS AND STANDARDS IN RADIO ASTRONOMY

CHAIRMAN: H. M. Altschuler, National Bureau of Standards, Boulder, Colorado

COMMISSION VI, Session 2

Tuesday, October 15 8:30 am - 12:00 noon
NUMERICAL METHODS I
CHAIRMAN: E. K. Miller, Lawrence Livermore Laboratory

2-1 PRACTICAL EVALUATION OF ANTENNA/INTERFACE EFFECTS BY COUPLING SOMMERFELD INTEGRALS WITH INTEGRAL EQUATIONS: R. J. Lytle, D. L. Lager, E. K. Miller, Lawrence Livermore Laboratory, Livermore, California.

Calculating the current distribution on antennas above, below, and penetrating through the ground-air interface requires accurate and rapidly convergent methods both for evaluating Sommerfeld integrals and solving integral equations. Computer codes satisfying these criteria have been developed and used to deduce physical phenomena for a number of problems of practical interest. Among the results discussed is the rate of current decay for electrically long finite length horizontal wires close to the ground. The dependence of the decay rate upon the height of the antenna, relative dielectric constant, and loss tangent is demonstrated via nomographs. Other results presented include plots of the near-interface power flow (Poynting vector) for antennas closely coupled to the ground. These include solutions for antennas above, below, and penetrating the ground-air interface. Also considered is the interaction of antennas located on opposite sides of the interface. Finally, an overview of the wide utility of Sommerfeld integral based integral equation codes is given and the areas of applicability of certain approximations such as ray-optic techniques are examined by comparison with rigorous Sommerfeld theory.

2-2 NEAR FIELDS: INHERENT COMPUTATIONAL DIFFICULTIES IN MOMENT METHOD FORMULATIONS: R. W. Adams, E. K. Miller, A. J. Poggio, Lawrence Livermore Laboratory, Livermore, California.

It has been recently shown that the choice of particular combinations of integral equation, basis function, and weight function can lead to widely varying convergence rates for the current distributions on wire structures. A previous study uncovered deficiencies in various current representations, and called for an investigation of the effect of different formulations on the behavior of near field quantities. Furthermore, the widespread use of moment method formulations for near field evaluation emphasized the need for this type of investigation.

The present study is limited to several widely used computer programs based on moment methods. Each program pertains to particular choice of integral equation, weight function, and basis function. From the computed currents, the near radial

and tangential electric fields are calculated as a function of the axial variable along a straight wire in both antenna and scattering modes. Similar data is also computed along parallel trajectories at varying distances from the wire surface. Graphical presentations of the data indicate the severe errors which may arise in the near field quantities, and a physical interpretation allows a qualitative relationship to be established between the properties of the current representations and the near field behavior. Recommendations are made regarding approximation of the current distribution when one is interested in computing near fields.

2-3 ANALYSIS OF CROSSED WIRES IN A PLANE-WAVE FIELD: R. W. P. King and T. T. Wu, Harvard University, Cambridge, Massachusetts.

The distributions of current and charge per unit length induced in a pair of electrically thin, mutually perpendicular crossed wires by a normally incident plane electromagnetic wave are derived by analytical methods. The conditions on the currents and charges per unit length at the ends of the wires and at their junction are explained and compared with the insufficient ones frequently given in the literature. New integro-differential equations for the currents in the wires are deived and solved approximately by iteration in terms of trigonometric and integral-trigonometric functions. Depending on the electrical lengths of the crossed elements and the location of their junction in the standing-wave patterns, a variety of quite different distributions of current and charge per unit length are obtained. These determine the scattered near and far fields. A number of special cases that involve typical resonant and antiresonant combinations among the six overlapping circuits are considered. The nature of the coupling at the junction is discussed.

2-4 INDUCED CURRENTS IN SINGLE AND CROSSED WIRES: R. W. Burton, Naval Postgraduate School, Monterey, California; R. W. P. King, Harvard University, Cambridge, Massachusetts.

In order to understand the distributions of current and charge per unit length induced in crossed wires, it is advantageous first to study these quantities in a straight wire without the perpendicular member when it is parallel to the inducing electric field. The currents and charges induced in a crossed element will depend on the location of the junction in the standing-wave patterns of the currents and the charges in the element parallel to the electric field. Junction effects are best separated from end effects by making the crossed wires sufficiently long. A number of different distributions of current and charge per unit length along a single wire parallel

to an incident electric field have been computed from Wu's long antenna theory. Graphs of these and of the corresponding measured values are shown for lengths for which the maxima and minima of the current have a number of different positions relative to the maxima and minima of the charge per unit length. Theoretical and measured distributions of current and charge along crossed antennas are shown when the junction is at a current maximum and charge minimum, a current minimum and charge minimum, a current minimum and charge maximum, and intermediate locations.

2-5 AN APPROACH TO THE THIN-WIRE JUNCTION PROBLEM: R. Mittra and W. L. Ko, University of Illinois, Urbana, Illinois.

In this paper we present a new approach to treating the thin-wire junction geometry which arises in the computer modeling of a great many electromagnetic radiation and scattering problems. The method is based upon a finite-difference type interpretation of the differential operator in the Pocklington form of the integro-differential equation representing the junction problem. An important advantage of the method is that it is capable of producing accurate results even with relatively simple basis and testing functions, e.g., pulse and $\delta$-functions. Furthermore, the method does not require the imposition of additional constraints, such as the Kirchhoff current law or the conservation of charge, at the junction points. The method is versatile in that it applies to L-shaped structures as well as to junctions of thin wires of dissimilar radii. Numerical results based on the present finite difference approach have been computed and good agreement with results derived by other independent methods has been observed. An important conclusion of this work is that the conventional interpretation of the differential operator leads to erroneous results since the sampling interval in the conventional finite difference scheme is different from the correct value of the sampling interval found in this paper.

2-6 NUMERICAL CONSIDERATIONS FOR THE SOLUTION OF THE POCKLINGTON INTEGRAL EQUATION APPLIED TO INTERSECTING WIRE STRUCTURES: F. M. Tesche, Science Applications, Inc., Berkeley, California.

In both the wire mesh and the crossed wire models of physical objects it is important to insure that the numerical methods employed for the solution of the integral equations describing its scattering properties give the correct behavior of the currents and charges at wire junctions. A number of investigators have looked at the junction problem in the past. However, the majority of such research has been related to the Hallén form of the E-field integral equation, which requires that

specific boundary conditions be imposed on the wire currents in order to obtain a unique solution. It is well known that the Pocklington form of the E-field equation gives results which are almost identical to those of Hallén's equation for a single straight or curved wire. This is done, moreover, without making use of explicit boundary conditions for the current. As will be seen, the same is true for intersecting wires which are treated by the Pocklington equation. The computed values of current at wire end points and at the junctions can then be used to determine the accuracy of the overall solution since their behavior at these points is already known from Kirchhoff's law and charge conservation. There is more than just academic interest to warrant further studies of the junction problem. Since the ultimate goal is to obtain the frequency domain and corresponding time domain behavior of the induced charge and current on an actual object such as an aircraft, it is necessary to have a computer code which is efficient and rapidly converging. This is true not only if conventional FFT methods are used to compute the transient response, but also if SEM is used. Because the vector potential $\bar{A}$ is not oriented in a single direction for a general collection of intersecting wires, the Hallén form of the E-field equation becomes tedious to program and time consuming to run on the computer. In this paper a brief study of the application of Pocklington's equation to intersecting thin-wire structures is outlined. It is found that remarkable convergence is obtained, but that a certain degree of consistency must be maintained in numerically performing the integrations and differentiations required in the process of obtaining a solution.

2-7 A NEW SOLUTION FOR THE CURRENTS ON A WIRE SCATTERER: C. W. Prettie and D. G. Dudley, University of Arizona, Tucson, Arizona.

The potential integral equation formulation for the currents on a wire scatterer is re-examined. An integration by parts to produce a harmonic operator operating on the current, as suggested by Mayes, is found to be invalid because of singularities produced by the harmonic operation. The singularities, however, may be isolated and are shown to be removable. After removal, the integration by parts becomes valid and a new formulation results. A solution may then be obtained by the method of moments. Numerical results are compared with results compiled from various programs by Miller, et al. at Lawrence Livermore Laboratory.

2-8 DESIGN CONSIDERATIONS FOR PARASITIC SCREEN ANTENNAS: R. M. Bevensee, Lawrence Livermore Laboratory, Livermore, California.

This paper describes the results of a computer study of a model of a parasitic screen antenna. The antenna consists of an array of N parallel wires, driven by uniform current at a sinusoidal frequency in the exciting wire parallel to the others. All wires are infinitely long, but the significance for arrays of finite length wires is pointed out. Arrays considered are: planar, wedge or corner reflector, and paraboloid. Interactions among the wires and ohmic loss is accounted for in the computer code. For a given array the position of the exciting wire, spacing between parasitics, and their radius all are varied to maximize the forward-to-backward ratio F/B. This ratio can be orders of magnitude larger than for a comparable solid screen array. Radiation patterns are then obtained as a function of frequency about the reference frequency. The effects of small changes in parameters on the patterns is described. Conclusions are drawn about the choice of parameters for narrow-beam, high-F/B parasitic screen antennas.

2-9 ELECTROMAGNETIC SCATTERING BY PENETRABLE CYLINDERS OF ARBITRARY CROSS SECTION: R. Kittappa, Lincoln University, Oxford, Pennsylvania; R. E. Kleinman, University of Delaware, Newark, Delaware.

The problem of scattering of an electromagnetic wave by an infinitely long homogeneous isotropic cylinder of arbitrary cross section whose permittivity and permeability differ from that of the surrounding medium is considered. For both E and H polarizations, the unknown field component is the solution of a transition problem for the two-dimensional Helmholtz equation, that is, satisfies Helmholtz equations with different wave numbers inside and outside the boundary of the cylinder and prescribed jumps at the boundary. This problem is reduced to a system of coupled boundary integral equations for the unknown field component and its normal derivative. These equations are regularized in the sense that the unknown function occurs so as to cancel the singularity of the kernel. It is proven that the Neumann series obtained by straightforward iteration converges for sufficiently small frequencies and ratios of interior and exterior permittivities and permeabilities sufficiently close to one. The method appears simpler than the corresponding Born approximation since only line integrals along the boundary are involved rather than integrals over the entire interior medium.

## COMMISSION VI, Session 3

Tuesday, October 15 8:30 am - 12:00 noon
COMMUNICATION CHANNELS WITH EMPHASIS ON SATELLITE CHANNELS
CHAIRMAN: J. J. Bussgang, Signatron, Incorporated

3-1 OPTIMUM PULSE REFLECTION FROM THE IONOSPHERE: R. E. McIntosh, University of Massachusetts, Amherst, Massachusetts.

The reflection of RF pulses having linear-frequency variation off an inhomogeneous ionosphere is considered. Approximate analytical results are compared with results obtained from a computer study that shows how pulse compression varies with magnetic dip angle, solar zenith angle, transmitter-receiver separation distance and propagation direction with respect to a magnetic meridian. It is found that moderate pulse compression can be achieved by utilizing the intrinsic dispersive properties of the transmission channel. We have observed that compression ratio decreases with transmitter-receiver spacing at a given pulse center-carrier frequency. Further, there appears to be a maximum attainable compression ratio of approximately 22 dB for those distances studies. Finally, we have found ionospheric anisotropy to play a minor role compared to ionospheric inhomogeneities.

3-2 THE MEASUREMENT AND STATISTICAL CHARACTERIZATION OF TIME-VARIANT DISPERSIVE CHANNELS: Gordon F. Sargent, REL-REEVES, Incorporated, Boynton Beach, Florida.

Efficient usage of most communication channels requires one to adequately describe the statistics of the communication path. Channel characterization is most meaningful if one's mathematical description is closely related to the channel's physical and observable properties. Time-variant dispersive channel characteristics are described. The relationships between what one may measure and the statistics one desires are explained. A digital signal processor is described that will provide communication channel characteristics. The processor monitors the channel, processes the measured data, reduces it and displays channel statistics on a real time basis. The channel statistics displayed require no external processing and are available on a real time basis. The advantages of using modern digital processing techniques for deriving statistical information are shown. The usage of large scale integrated (LSI) circuitry, digital techniques, linear integrated circuits, and display devices is emphasized in an explanation of the circuit design. A currently designed processor yields the distribution function of the radio channel transmission loss and the various parameters associated with the distribution function. Possible applications for this

processor are explained. A future design is explained that would yield in addition, channel coherence bandwidth, and correlation between channels.

3-3 IONOSPHERIC CHANNEL MODELING: C. L. Rino, Stanford Research Institute, Menlo Park, California.

Mathematical models for the transionospheric channel provide a framework within which ionosphere-induced signal degradations can be analyzed. The kernel of such a model involves an analysis of the interaction of electromagnetic waves with a randomly irregular medium. Because the wave equation is linear in the vector field, it is sufficient to characterize the transmission properties of a monochromatic plane wave; in particular, the combined space-frequency correlation functions. Indeed, for a gaussian complex field these quantities are sufficient to completely determine the statistics of an observable, e.g., signal amplitude and phase.

We shall present analysis of ionospheric scintillation data that shows the transionospheric channel to be gaussian but highly non-rician. We have found that at UHF typically more than 90% of the scattered power is in phase quadrature with the coherent signal component. This structure holds at least to moderate scintillation levels, and it is only weakly dependent on wavelength.

We shall show that this latter fact is just one manifestation of the presence of a continuum of irregularity scale sizes characterized by a power-law spectral-density function. By postulating, after Kolmogorov, a locally homogeneous irregularity structure for the ionospheric electron density perturbations, we obtained good theoretical agreement with our data.

The consequences of locally homogeneous fields for channel modeling are important. Basically one has quasi-deterministic trends in the signals that alter the space or time stationarity that one almost always assumes. Thus, the concept of an angular spectrum of waves must be carefully reexamined. This greatly complicates the frequency dependence of the signal parameters. As an example, we show that the complex signal variance has a non-quadratic wavelength dependence.

As yet no data are available that will permit direct measurement of the complex moments for ionospheric signals. However, late this year (or early in 1975), an elaborate satellite experiment will be flown that will permit full multifrequency and spaced-receiver correlation measurements at UHF. Thus, we are approaching a time when accurate and detailed ionospheric diagnosis will be possible.

3-4 REVIEW OF A GLOBAL SCINTILLATION MODEL AND ITS MODIFICATIONS: J. H. Pope, National Oceanic and Atmospheric Administration, Boulder, Colorado.

A model of scintillation activity imposed on transionospheric signals by ionospheric irregularities was developed by Fremouw of Stanford Research Institute. This model uses a number of input parameters pertaining to solar activity, geographic location of the receiver and transmitter, temporal variations, and signal frequency to predict the average scintillation activity, as given by scintillation index, under the given set of parameters. This model was modified to better represent the recent scintillation boundary data presented by Aarons and to take into consideration the nonsymmetrical behavior of this region with respect to the northern and southern hemispheres. The resulting model is compared with several sets of scintillation and in situ irregularity data showing a considerable improvement in fit. An attempt to extend the range of validity to the GHz region is also included in this review.

3-5 DIVERSITY SCHEMES FOR UHF IONOSPHERIC SCINTILLATION: R. K. Crane, Massachusetts Institute of Technology, Lexington, Massachusetts.

Morphological studies of ionospheric scintillation at UHF have shown that scintillation is a fact of life for communication systems operating through either the equatorial ionosphere or the high latitude (auroral and polar) ionosphere. To mitigate the deleterious effect of scintillation the use of one or more possible diversity schemes are often proposed; frequency, space, time and polarization. The effectiveness of each of these schemes was studied using simultaneous UHF (400 MHz) and VHF (150 MHz) measurements between the low orbiting Navy Navigation satellites and the Millstone Hill Radar Facility. Simultaneous observations using orthogonal circular polarization channels at UHF show that the fluctuations in the received signal amplitude for each channel were highly correlated and polarization diversity will not work. This result was obtained both for weak and strong amplitude scintillations. The correlation coefficient for simultaneous UHF and VHF amplitude measurements ranged from 0.0 to 0.6 depending upon the elevation angle. At high elevation angles values near 0.6 were obtained indicating that frequency diversity is of limited usefulness. The data show that either time or space diversity will be useful. The spatial diversity distance is the order of the first Fresnel zone radius and, knowing the path geometry and effective drift rate of the irregularities across the line of sight, the diversity distance or time may be computed.

## COMMISSION VI, Session 3

3-6 EMPIRICAL DESCRIPTORS OF IONOSPHERIC SCINTILLATIONS AND THEIR USES FOR SYSTEM DESIGN: Herbert E. Whitney, Air Force Cambridge Research Laboratories, Bedford, Massachusetts.

Ionospheric scintillations can be a serious problem for many systems that transmit through the ionosphere, particularly the VHF and UHF range. The fading induced on the signal by the ionospheric irregularities can exceed the link margin for some satellite communication systems even at mid-latitudes. The situation can be worse for equatorial and auroral transmissions because of the greater occurrence of deep scintillations. A large data base of scintillation index (SI) measurements was available for scintillation morphology but not directly applicable to systems design. Based on experimentally derived relationships SI was converted to cumulative amplitude distributions (cdf). Good agreement was found between the experimental data and the Nakagami distribution. Frequency dependence was measured from the 137 MHz and 412 MHz transmissions at ATS-5 thus allowing interpolation of a cdf to other frequencies. The distribution of fade durations was measured for selected periods of strong scintillations at 137 MHz and 254 MHz. Estimates of message reliability were obtained for cases of strong scintillation for a specified margin and message length.

3-7 PANEL DISCUSSION

Ionospheric Scintillation on Satellite Links
Chairman: D. Leichtman, MITRE Corporation

## COMMISSION I, Session 2

Tuesday, October 15 1:30 pm - 5:00 pm
LASER PARAMETER MEASUREMENTS
CHAIRMAN: H. S. Boyne, National Bureau of Standards

2-1 FREQUENCY MEASUREMENTS IN THE OPTICAL REGION AND THE SPEED OF LIGHT: K. M. Evenson, National Bureau of Standards, Boulder, Colorado.

Since the advent of the laser and saturated absorption locking of the laser, the extension of radio frequency technology into the optical region has produced exciting new results, such as a 10,000 fold increase in the resolution of spectroscopy in this region and a new value of the speed of light, 100 times more accurate than the previously accepted value. This talk will describe the techniques and results achieved.

2-2 PROVISIONAL EXTENSION OF THE FREQUENCY SCALE INTO THE VISIBLE: Howard P. Layer, National Bureau of Standards, Washington, D. C.

The frequency scale has been extended upwards from the cesium frequency standard to the near infrared by use of an infrared-frequency synthesis chain. Although attempts to provide a similar direct frequency scale extension from cesium to the visible have not yet been successful, a provisional extension into the visible has been made from infrared lines of known frequency by means of a very high resolution resonant cavity interferometry. This extension has been accomplished by measuring the frequency ratio between the laser-saturated absorption line of $^{129}I_2{}^{(K)}$ at 633 nm and the laser-saturated absorption line of methane at 3.39μ but is generally applicable to arbitrary frequency comparisons between 33 and 750 THz with a precision of several parts in $10^{10}$. The accuracy of the measurement is limited by variations in the curvature of the test cavities mirrors and by instabilities in the mirror coatings. The measured ratio of 5.359,049,260,6 (0.0002 ppm) agrees with the ratio calculated from two independent measurements relative to $Kr^{86}$ and provides a frequency value of 473.612,310,803 THz (0.00074 ppm) for the iodine line based on the published value of the methane line.

2-3 STANDARDS FOR LASER SAFETY: H. S. Boyne, National Bureau of Standards, Boulder, Colorado.

Voluntary and regulatory performance standards for laser products have been established. The standards and the measurements necessary to implement the standards will be discussed.

2-4 RESULTS OF PRELIMINARY TESTING OF COMMERCIAL LASER POWER AND ENERGY INSTRUMENTS: R. W. Peterson, Bureau of Radiological Health, Rockville, Maryland.

The Food and Drug Administration, Bureau of Radiological Health, is developing a laser product performance standard applicable to the manufacturers of laser products. In the process of preparing for the technical enforcement of such a standard, testing of commercially available laser power and energy measurement instrumentation was undertaken. The testing was designed to determine the long term stabilities as compared to a National Bureau C-series calorimeter system, and to determine instrument performance under various ambient environment conditions. Preliminary results concerning the performance of vacuum photodiode detectors and of pin diode detectors employed in moderate cost measurement systems will be presented.

2-5 PERFORMANCE MEASUREMENTS OF A MODELOCKED LASER RANGE-FINDER OVER 18 KM PATH: K. E. Golden, E. E. Reber and E. O. Ozaki, Aerospace Corporation, El Segundo, California.

The pulsed ruby modelocked laser ranging system being tested has the potential performance characteristics needed to advance global geodetic, earth and ocean physics technology. In these applications, the precision laser rangefinder is a tool used to obtain high accuracy (± 3 cm or better) quasi-simultaneous range measurements between a satellite and four or more ground sites. A satellite system is desirable because of the obvious global coverage, and intercontinental base line potential. A pulsed system is required to minimize satellite velocity aberration effects. Specific applications may involve altitude, surface distance reconstruction, surface strain rate, and refined satellite ephemeris measurements. This rangefinder consists of a ruby modelocked laser transmitter, a pulse selector which allows only one of the central sub-pulses to be transmitted, a course range receiver with ±30 cm range resolution, and an image converter vernier range receiver with ±6 mm range resolution. The transmit reference and return pulses are focused on the image tube photocathode. The resulting photoelectrons are sinusoidally swept across the image converter output screen. The linear separation of the reference and return images are related to the elapsed time. The vernier receiver alone produces multiple range ambiguities since the device does not count the number of sweep cycles separating the transmit reference and return pulses. The coarse range receiver is used to remove these ambiguities. Extensive laser measurements are presented for 7, 12, and 18 km ranges. The group index of refraction corrections were calculated from end

point meteorological data and applied to the time of flight measurements. The total range uncertainty was about ± 1.2 cm at the 18 km range.

## COMMISSION II, Session 4

Tuesday, October 15 1:30 pm - 5:00 pm
RADIO OCEANOGRAPHY II
CHAIRMAN: Dennis B. Trizna, Naval Research Laboratory

4-1 IMAGING SURFACE CURRENTS WITH A SYNTHETIC APERTURE RADAR: T. R. Larson, J. W. Wright, Naval Research Laboratory, Washington, D.C.

The optical image density produced by a synthetic aperture radar looking at the ocean surface is derived in standard fashion keeping a term in scatterer velocity, $u(x)$, along the line of sight. For the range resolution cell about R, the result is $S(x) \propto \rho(x)/[1 - (R/V)(\partial u(x)/\partial x)]$. Here x is parallel to the scanning direction, $S(x)$ is optical image density, V is platform velocity, and $\rho(x)$ is surface scattering strength. By choosing a resolution cell size containing several dominant wavelengths, short scale variations in $\partial u/\partial x$ and $\rho(x)$ can be averaged out, leaving only images of large scale (0.5 kilometers, say) variations in $\rho(x)$ and $\partial u/\partial x$. The effect of the latter, which are surface current gradients, can be enhanced by making R/V large, which is consistent with large resolution cells. Numerical estimates and approximations made will be discussed.

4-2 DEPOLARIZATION OF THE SECOND ORDER DOPPLER SPECTRUM OF RADAR SEA ECHO: G. R. Valenzuela, Naval Research Laboratory, Washington, D.C.

The second order contribution to the doppler spectrum of radar sea echo for the polarized return was obtained by Hasselmann (1971), Barrick (1972) and Valenzuela (1973) in various degrees of approximation. The main contribution to the polarized return (vertical and horizontal polarization) of the "mean" second order doppler spectrum comes from water wave components along the radar line-of-sight and furthermore the transfer coefficient (i.e. the weighting factor to the partial contributions) has a hydrodynamic and an electromagnetic contribution.

However, the depolarized contribution to the second order doppler spectrum is predominantly from water wave components which travel at an angle from the line of sight of the radar and the transfer coefficient is purely of electromagnetic origin since in first order depolarization is zero from a slightly rough surface. Therefore, in many applications the depolarized doppler spectrum might be a more interesting signature of the water surface, which by the way, is not contaminated by the large first order Bragg peak as in the case of the polarized return.

An important application of the second order doppler spectrum might be in finding out once and for all if depolarization from a water surface is due to surface scattering or volume scattering as some may believe.

Numerical results will be presented for the depolarized second order doppler spectrum from our generalized theory, Valenzuela (1973).

4-3 DETERMINATION OF SIGNIFICANT WAVEHEIGHT FROM THE SECOND-ORDER HF SEA-ECHO DOPPLER SPECTRUM: Donald E. Barrick, National Oceanic and Atmospheric Administration, Boulder, Colorado.

In the remote measurement of sea state with HF over-the-horizon radars, the extraction of significant waveheight from the sea echo represents perhaps the single most important sea-state descriptor, and yet it is also the most elusive. The first-order echo amplitude at typical long-range skywave frequencies samples the ocean waveheight spectrum at one point, usually in the saturation region; hence it does not yield the ocean waveheight. The second-order sea-echo Doppler spectrum is related to a convolution of the waveheight directional spectrum with itself (i.e., a nonlinear relationship), and hence it is not generally possible to uniquely determine the ocean waveheight directional spectrum from the echo spectrum. If it were, the significant waveheight would be obtainable as the square root of the integral of the waveheight spectrum.

A technique is demonstrated whereby the significant waveheight can be extracted from the second-order Doppler spectrum without deconvolving the waveheight spectrum from itself. One merely integrates the second-order Doppler spectrum--divided by the average of the known Doppler integral kernel--over the Doppler domain of significance. This number is then divided by the first-order echo amplitude to obtain a number proportional to the mean-squared sea waveheight. This final division process also has the effect of removing any unknown signal path losses from the result, eliminating the need for an accurate radar system sensitivity calibration.

4-4 THE STATISTICS OF HF SEA-ECHO DOPPLER SPECTRA: Donald E. Barrick and Jack B. Snider, National Oceanic and Atmospheric Administration, Boulder, Colorado.

The statistics of sea-echo Doppler spectra have been measured with an HF surface-wave backscatter radar at many frequencies and for several resolution-cell sizes. In particular, the normalized standard deviation, $\sigma_f$, and the correlation coefficient (vs time), $\rho_f(\tau)$ were obtained for both the first-order and second-order portions of the Doppler spectrum. These statistics are important in specifying the optimum processing parameters of HF radars used for remote sea-state sensing.

It was found that $\sigma_f$ is 0.92-0.95 for fixed Doppler frequencies at or near the first-and second-order peaks; this compares with 1.0 expected for a Gaussian process, indicating that the HF sea

echo is very close to Gaussian. If one tracks the absolute Doppler peaks from spectrum to spectrum and calculates $\sigma_f$ for this quantity, he arrives at 0.5-0.7; this agrees with expectations that it be less than the previous $\sigma_f$. Calculation of $\rho_f(\tau)$ from the data at the peaks of consecutive spectra indicates that the echo is essentially decorrelated for a lag time greater than ~200 seconds. This is for a resolution cell size ~7.5 km x 7.5 km. Hence one is obtaining independent spectrum samples every 200 seconds. This does not agree with the currently accepted Rayleigh model relating decorrelation time to the velocity of the scattering wavetrains; this model predicts considerably longer decorrelation times. Neither $\sigma_f$ nor $\rho_f(\tau)$ appear sensitive to either the radar operating frequency or the scattering patch size, again not conforming to predictions from the conventional models.

4-5 INTERPRETATION AND EVALUATION OF A SECOND-ORDER EXPRESSION FOR HIGH-FREQUENCY RADAR CROSS SECTIONS OF OCEAN SURFACES: D. L. Johnstone, G. L. Tyler, Stanford University, Stanford, California.

Techniques for evaluating a second-order integral expression relating the per unit area ocean-surface radar backscatter cross section at HF to first-order waveheight directional spectra are presented. The integral is interpreted in terms of multiple Bragg scattering and the regions of integration are identified with evanescent or freely propagating radio waves. A coordinate transformation provides paths of integration which clearly show the relationship between ocean-wave frequency and propagation direction and the scattered signal doppler shift. Singular points are identified as the paths of integration traverse the boundaries between regions of integration. Results of numerical evaluation are presented for several first-order ocean waveheight directional spectra models.

4-6 BACKSCATTER FROM ANISOTROPICALLY ROUGH SEA SURFACE: A. F. Fung and H. L. Chan, University of Kansas, Lawrence, Kansas.

A theory for radar sea scatter is developed using a two-scale roughness model which integrates the effects of frequency, look angle, polarization, wind speed and anisotropic roughness characteristics of the sea surface. Measured sea surface slope density and sea spectrum reported by oceanographers are incorporated into the theory to examine the variation of the scattering coefficient as a function of the above stated parameters. The difference between the upwind and downwind observations is shown to be due to the combination of the non-zero mean slope in the slope density function along the up/down wind direction and the interaction between the two scales of roughness. The difference between crosswind and upwind observations is a result of both the anisotropic character of the sea spectrum and the interaction

The useful signal coverage from an OMEGA transmitter is conceptually bounded by a contour beyond which the signal is too weak for use in position determination. OMEGA signal computations are based on the VLF (earth-ionosphere) waveguide model with varying earth conductivity and geomagnetic field. The ionosphere, on the other hand, is characterized by a simple day or night electron density profile which varies only with altitude (and not latitude). A number of profiles have been reported in the literature to provide a good match between theory and experiment. The differences in the profile description would result in variations in predicted OMEGA signal coverage contours. A sensitivity study of the signal computations for all OMEGA transmitters, if repeated for several selected profiles encompassing the known variations, would consume an inordinate amount of computer time. In this paper, a simple methodology is developed wherein the sensitivity of the signal to each of the various waveguide parameters including electron profile is determined. These parameters are chosen so as to include all realistic variations of these parameters. These computations are then used to assess the sensitivity of the signal coverage of OMEGA transmitters to waveguide parameters. This methodology requires significantly fewer computations without adversely affecting the accuracy of the results. An example of coverage variation with change in electron density profile is presented for an OMEGA transmitter.

3-4 VARIATIONS IN EXTREMELY LOW FREQUENCY PROPAGATION PARAMETERS: Peter R. Bannister, Naval Underwater Systems Center, New London, Connecticut.

For the past four years, the U.S. Navy ELF Wisconsin Test Facility has been employed as the source for 1.6-11.2 Mm range ELF propagation measurements. At each receiving site, the horizontal magnetic field strengths were measured at a band of frequencies centered at 45 and 75 Hz in order to determine the average attenuation rate ($\alpha$) and relative excitation factors (E) for daytime and nighttime propagation conditions. These measurements have shown that there is a definite seasonal (or temporal) variation in both $\alpha$ and E. The variation in $\alpha$ is approximately 0.4 dB/Mm for both daytime and nighttime propagation conditions. The variation in E is approximately 1.5 dB during the day and 3-4 dB at night (i.e., nighttime propagation is much more variable). At both frequencies, $\alpha$ is proportional to E. At 75 Hz, $\alpha$ is approximately 1.4E dB/Mm, while at 45 Hz, $\alpha$ is approximately 0.9 to 1.0E dB/Mm. For nighttime propagation, an isotropic ionospheric model (ionospheric conductivity = $6 \times 10^{-6}$ mhos/m) with a variable reflection height provides a good fit to the measured values of $\alpha$ and E (at least for reflecting heights from 50 to 90 km). However, for daytime propagation, an exponential ionospheric model provides better agreement with the measured values of attenuation rate and phase

velocity. Since $\alpha$ is directly proportional to E, field strength measurements could be taken at just one site in order to determine average values of both $\alpha$ and E for a particular measurement period.

3-5 RAY TRACING INTERPRETATION OF SATELLITE DOPPLER-SHIFT SIGNALS FROM GROUND BASED VLF TRANSMITTERS: Bruce C. Edgar, The Aerospace Corporation, El Segundo, California.

VLF data from ISIS 2 of signals received over New Zealand between 45 and 60 degrees invariant latitude from a VLF transmission experiment in Alaska on September 3 and 6, 1973 shows a continuum of negative and positive doppler shifts from a fixed transmission frequency of 13.275 kHz. Most of the gross features of the doppler shift signatures have been reproduced using a two dimensional, whistler mode ray tracing program and a magnetospheric electron density model which features a smoothly descending density gradient which drops the equatorial density level by three orders of magnitude between L~2.4 and L~4. The density gradient is believed to be a part of the erosion of the plasmasphere caused by the severe magnetic storm of 27-28 August. Observed temporal changes in the doppler signatures from 3 to 6 September can be reproduced in the ray tracing calculations by reducing the severity of the density gradient between L~2.4 and L~3 and thus correspond to the gradual recovery of the plasmasphere after a magnetic storm.

3-6 NEW ELF PROPAGATION CALCULATIONS USING THE ZONAL HARMONIC SERIES: Richard L. Lewis, University of Colorado and the National Bureau of Standards, Boulder, Colorado.

Computational agreement of the computer program developed to implement field strength propagation calculations in a stratified earth-ionosphere waveguide using the zonal-harmonic series has been obtained with generally accepted results for the ground wave calculation, the sharply-bounded ionosphere model, and the nominal daytime stratified ionosphere profile. In the latter case, excellent agreement using stratified ionosphere profile variations was obtained with Pappert's results at 100 Hz (Radio Science 3, 219-233, 1968). Using the newly proven computational routine, some interesting attenuation curve values were obtained for hypothetical two-layer ionosphere models. Similar high attenuation results conceivably could be predicted for periods following nuclear detonations, say. Also presented are reformulated equations showing new, compact expressions for the mathematical model used by the computer program.

COMMISSION IV - JOINT WITH COMMISSION III (See Page 66 )

Tuesday, October 15 1:30 pm - 5:00 pm

VLF and ELF

CHAIRMAN: T. P. Quinn, Naval Research Laboratory, Arlington, Virginia

COMMISSION V, Session 2

Tuesday, October 15 1:30 pm - 5:00 pm
OBSERVATIONAL RESULTS
CHAIRMAN: F. J. Kerr, University of Maryland

2-1 THE TEXAS RADIO SURVEY--A PROGRESS REPORT: F. N. Bash, The University of Texas, Austin, Texas.

The University of Texas Radio Astronomy Observatory (UTRAO) Sky Survey is well underway. The survey will cover the sky north of $\delta = -35^{\circ}$ down to a flux density of 0.2 Janskys at 365 MHz. Positions of the radio sources will be determined to ±1 arcsecond and the optical identifications and radio brightness distributions will be determined for each object detected. The Survey is now 25% complete. Although the analysis of the data has concentrated so far on the brighter radio sources, positions and brightness distributions have been determined for about 3000 discrete radio sources, and 1000 of them have been located on Palomar Sky Survey glass plates, resulting in about 400 clear-cut position-coincident identifications. Examples of the kind of radio and optical data which will be available and measures of the position accuracy will be shown.

2-2 EXTRA-SOLAR-SYSTEM SOURCES FOR VLF AND ELF NOISES: B. Z. Kaplan, Ben Gurion University of the Negev, Beer Sheva, Israel.

The aim of the paper is to show that radio noise at VLF and even at ELF is not entirely due to sources of the near environment, but it can also be attributed to astronomical sources far outside our planetary system. The paper proceeds with an example provided by the electromagnetic field of pulsars. This example shows that low frequency radiation of pulsars may reach the neighborhood of earth. Under certain circumstances propagation of such noises through the ionosphere is also possible. An experimental proof of our expectations should provide astronomers with an utterly new tool for the probing of deep space. The related experimental methods are also discussed.

2-3 LOW FREQUENCY OBSERVATIONS OF VARIABLE RADIO SOURCES: J. R. Fisher, National Radio Astronomy Observatory, Green Bank, West Virginia; W. C. Erickson, University of Maryland, College Park, Maryland.

About fifty radio sources are being monitored periodically with the NRAO 91 m telescope, at eight frequencies between 250 and 1000 MHz. The purpose of this program is to confirm and broaden Humstead's (Astro. Lett. 1972, 12, 193) observations of source variability at 408 MHz. Our program has now been running for approximately one year. We have observed definite variations in 3C454.3 and BL Lac which amount to 20-30%. Under ideal

conditions, our data on non-varying sources are reproducible to 1-2%. However, interference due to the sun or terrestrial sources often cause 10-15% errors. CTA102 and 1504-16.7 show 10% changes, but due to possible interference we are not yet certain of their reality. Other possibly varying sources are 3C138, 273 and 279. We find no variations in the other forty sources that we monitor. The variations appear to be well correlated at the different frequencies, and the strongest variations are in the well-known centimeter wavelength variables. These facts suggest that the same physical mechanisms are responsible for the centimeter and meter wavelength variations.

2-4 A MEASUREMENT OF THE GRAVITATIONAL BENDING OF RADIO WAVES NEAR THE SUN USING THE NRAO 35-KM INTERFEROMETER BASELINE: E. B. Fomalont and R. A. Sramek, National Radio Astronomy Observatory, Green Bank, West Virginia.

On April 11, 1974, the radio source 0116+08 was occulted by the sun. In order to measure the relativistic bending of the radio waves, the source, along with two nearby companions (0111+02 and 0119+11), were observed for fifteen days during April 1974 at wavelengths 11.1 and 3.7 cm with the NRAO four-element interferometer. Two frequencies are necessary to separate the coronal and relativistic bending. By using two comparison sources positioned in nearly opposite directions from the occulted source, long term (>1 hour) phase drifts (atmosphere and ionospheric refraction, baseline changes, polar motions, clock errors, differential telescope heating, etc.) could be calibrated. The value of the relativistic bending obtained from this experiment is $\gamma$ = N.NN±0.NN (to be filled in soon!) where $\gamma$ = 1.00 corresponds to an 'Einstein' deflection at the solar limb of 1.75. The error was determined by (1) analyzing the frequency spectrum of the residual phases from the best solution; (2) generating many sets of data with residuals having the same frequency spectrums; (3) analyzing these data to determine the error distribution. This type of error analysis includes the effects of long term phase errors which usually dominate the error of the experiment.

2-5 HIGH RESOLUTION OBSERVATIONS OF RADIO SOURCES AT 5.0 AND 10.7 GHz: David B. Shaffer, Yale University, New Haven, Connecticut.

Long baseline interferometry, using antennas in California, Texas, West Virginia, Ontario, Germany and Sweden, has been used to study the time variation of the 5.0 and 10.7 GHz milli-arcsecond structure of several radio sources over a two-year period. The visibility functions of some sources vary rapidly, while other sources are relatively stable. Most of the sources look similar at the two frequencies.

2-6 THE MILLIARCSECOND STRUCTURE OF EXTRAGALACTIC OBJECTS AT 2 CM: A. E. Niell, Jet Propulsion Laboratory, Pasadena, California; K. I. Kellermann, National Radio Astronomy Observatory, Green Bank, West Virginia; B. G. Clark, National Radio Astronomy Observatory, Charlottesville, Virginia; D. B. Shaffer, Yale University, New Haven, Connecticut.

The visibility amplitudes and some models will be presented for 3C273, 3C279, 3C84 and other sources for observation between 1973 February and 1974 July. For some epochs the visibilities of 3C273 and 3C279 cannot be fit with any model having fewer than three components. Furthermore, the 1973 February and April data for 3C273 cannot be fit by an collinear model.

2-7 HIGH VELOCITY CLOUDS: THEIR MASSES AND LOCATION IN THE GALAXY: G. L. Verschuur, University of Colorado, Boulder, Colorado.

One-hundred and three intermediate-velocity and 67 high-velocity cloud concentrations are found to have characteristically different masses ($2 \times 10^{-3}$ and $0.2 \times 10^{-3}$ $M_{\odot}pc^{-2}$) while intermediate and high-velocity cloud complexes have typically different masses as well ($31 \times 10^{-3}$ and $2.5 \times 10^{-3}$ $M_{\odot}pc^{-2}$ respectively). These differences, combined with a knowledge of the distribution of the clouds on the sky, support the models in which the clouds are in distant spiral arms with the highest velocity clouds in the most distant arms. The highest latitude intermediate-velocity clouds have masses that are differently distributed than those of the lower latitude intermediate-velocity clouds. The former are probably located in the solar neighborhood.

2-8 A COMPARATIVE STUDY OF $H_2CO$, OH, AND HI IN THE DARK TAURUS DUST CLOUD: Carl Heiles, University of California, Berkeley, California.

High sensitivity spectra of $H_2CO$, OH, and HI, all taken with the same angular resolution, were obtained in the dark dust cloud in Taurus. At some positions there exist three velocity components, instead of the two revealed by previous investigations. The relative abundance of $N_{OH}/N_{H_2CO}$ appears to be nearly constant within the cloud, equal to about 20 or perhaps somewhat more (this refers only to $H_2CO$ in the $1_{11}$ and $1_{10}$ ortho states), so that the molecules are coexistent. The excitation temperature of OH and $H_2CO$ appear to be highly correlated and we conclude that the excitation for each is determined by collisional processes. Variation in relative line intensity appear to be caused by variations in excitation temperature, with components showing a weak OH line and a strong $H_2CO$ line having a low excitation temperature for $H_2CO$,

relatively small molecular column densities, and relatively high ($5^{o}K$) kinetic temperatures as compared to usual (3.5 to $4^{o}K$). HI correlates rather well but not perfectly with the molecules, suggesting that much of it resides outside the region containing the molecules. We have carefully examined the OH principal line data in this cloud for the presence of anomolies. None are found except for one position which has a strong anomoly. Various considerations suggest that the OH at this position is atypical of that usually found in dust clouds, or that the observational data are in error.

2-9 ON NEBULAR NON-EQUILIBRIUM THERMODYNAMICS: Eric J. Chaisson, Smithsonian Astrophysical Observatory, Cambridge, Massachusetts.

Revised interpretation of nebular radio recombination lines of low and intermediate frequencies, coupled with recent high-frequency observations, displays an overall frequency dependence of the Orion A hydrogen line radiation that agrees poorly with current non-LTE models but surprisingly well with simple LTE theory. Contrary to popular belief, the LTE-derived electron temperature is not very much lower than that deduced from the relative intensities of forbidden optical lines. It is suggested that $H n\alpha (n>80)$ recombination lines might arise predominantly from regions of low-to-moderate electron density (30 - 1000 $/cm^{3}$, typical of those values derived from single-dish continuum observations), for which the effect of stimulated emission on the line intensity may be negligible, and for which there would be little conflict with the theory of impact broadening.

2-10 VLBI STUDIES OF OH/IR STARS: Robert L. Mutel, University of Colorado, Boulder, Colorado.

VLBI observations of the 18 cm OH emission from the infrared stars NML Cygnus, VX Sagittarii, R Aquila, VY Canis Majoris and W43a were made with a resolution of 0.08 arcsecond. A comparison of the auto-correlation and cross-correlation spectra shows that the strongest, most narrow line features are least resolved. Variations in fringe amplitude and phase are analyzed as scintillation effects. Source sizes for NML Cygnus and VY Canus Majoris are in general agreement with observations of Davies, et al. (1971) and Moran, et al. (1974).

COMMISSION VI, Session 4

Tuesday, October 15 1:30 pm - 5:00 pm
NUMERICAL METHODS II
CHAIRMAN: R. Mittra, University of Illinois

4-1 RADIATION FROM A FINITE SINUSOIDALLY MODULATED REACTANCE SURFACE (SMRS): S. H. Cho and R. J. King, University of Wisconsin, Madison, Wisconsin.

An integral equation is used to study the surface field and radiation from a planar structure which has a sinusoidally modulated reactance. The surface reactance is assumed to be piecewisely uniform near a magnetic line source and modulated sinusoidally in the propagation direction beyond the uniform segment. The surface reactance of the uniform segment is chosen as the average value of the modulated reactance. We have solved the problem accurately by using numerical solution of the integral equation, taking full account of the feed and termination. On the modulated section, the magnetic field on the surface is essentially that for an infinitely long SMRS, provided that most of the energy is radiated through the fast waves before they reach the termination. By taking account of only the radiation through the fast waves, the approximate radiation pattern is also obtained, and this compares well with the radiation pattern found numerically which includes all of the extraneous radiation due to the source, the transition between uniform and modulated reactance, and the termination insofar as the main beam and largest side lobe are concerned. Also the effects of parameters such as modulation amplitude, period, length of modulated section, and average surface reactance on the radiation pattern are discussed.

4-2 THE CHOICE OF EXPANSION AND TESTING FUNCTIONS AND HOW THEY CAN AFFECT THE RESULTS IN THE MOMENT METHOD OF SOLUTION: S. Klein and R. Mittra, University of Illinois, Urbana, Illinois.

In this paper we report the results of some numerical experiments which shed considerable light on the effects of choosing the testing and expansion functions in the moment method of solution for thin-wire antenna problems. For this investigation we used piece-wise sinusoidal basis functions and rectangular testing functions. These testing functions have computational advantages over sinusoidal ones. The width of the rectangles was varied from extremely narrow to the full width of the basis function. In particular, for this latter width, wildly erroneous results occur even though the matrix is well conditioned. Thus, it is possible that even though the matrix is generated according to the prescription of the moment method, results may be erroneous and the integral equation may, in fact,

not be satisfied. To understand what has actually happened, it is necessary to look at the near field values which show how the solution does not satisfy the intended boundary conditions. However, accurate results and satisfactory near field behavior are obtained with the same testing functions when the width is chosen optimally. The paper presents guidelines on methods to improve the convergence of the solution. Also discussed will be the relative computation times required by the two different computer algorithms.

4-3 ANALYSIS OF A WIRE EXCITED THROUGH AN APERTURE-PERFORATED CONDUCTING SCREEN: Chalmers M. Butler, University of Mississippi, University, Mississippi.

Integral equations are formulated for the problem of finite-length wire excited through an aperture-perforated conducting screen. The wire is assumed to be thin and is arbitrarily oriented behind the perfectly conducting screen which is treated as being infinite in extent. The aperture may be of any general shape and a known incident field illuminates the perforated screen. The integral equations presented fully account for the coupling between the wire and the aperture/screen. Due to the complexity of the general equations, they are specialized to the case of the wire parallel to the screen with the aperture a narrow slot of general length. These special equations are solved numerically, and data are presented for wire currents and aperture fields under varying conditions of illumination as well as of wire-slot lengths and orientation. Also, data indicative of the slot-wire coupling are presented.

4-4 DIFFRACTION BY APERTURES OF ARBITRARY SHAPE: D. R. Wilton, University of Mississippi, University, Mississippi; O. C. Dunaway, Naval Weapons Laboratory, Dahlgren, Virginia.

While a great deal of effort has been expended in the past to determine the diffraction properties of an aperture in a ground screen, still, for all but the simplest shapes, little accurate data are available. Recently, however, it has become feasible to obtain numerical solutions to these problems by moment methods. Furthermore, Mittra has developed a Hallén-like integral equation which partially decouples the expressions for the two orthogonal components of vector potential. The coupling is obtained through a pair of arbitrary functions which are, in turn, related by an auxiliary boundary condition. In this work, we use a similar equation, but which differs in the form of the homogeneous solutions of the partial differential equations for the vector potential components. The new form exhibits explicitly the role of the aperture edge in coupling the two orthogonal components of current through the auxiliary

condition. The decoupled form of the equations resulting when moment methods are applied, permits the use of an algorithm for the solution of the equations which makes efficient use of the machine storage available. This enables one to handle the large system of the simultaneous equations. Numerical results are presented for the aperture fields and, in the case of small apertures, equivalent dipole moments for apertures of various shapes are given.

4-5 FREQUENCY AND TIME DOMAIN SHIELDING BY FINITELY CONDUCTING CYLINDRICAL SHELLS: T. K. Wu and L. L. Tsai, University of Mississippi, University, Mississippi.

The shielding properties of general, two dimensional finitely conducting cylindrical shells is analyzed in the frequency domain by integral equation and separation of variables methods. For the analysis of a thin cylindrical shell, integral equations appropriate to the finite conductivity boundaries are first derived via the volume equivalency principle and then solved using the moment method. The solution yields the induced currents on the shield walls from which fields everywhere interior to the shield are readily calculated. Because the moment method is used, this analysis is applicable for treating cylinders of arbitrary cross-section as well, and even slotted cylinders. Toward this end shielding properties are computed as functions of frequency and slot width for both circular and square cylinders, with and without slots.

Secondly, a thick circular cylindrical shell is analyzed via the separation of variables method. The results show that significant attenuation of the incident fields is achieved for thick cylindrical shields thus demonstrating that the resonances which occurred in the thin shell case can be alleviated. Using the same techniques, a circular shell is also analyzed with an obliquely incident plane wave. The axial components of the inner fields at the cylinder axis show that the apparent radius of the cylinder is contracted as compared to the normal incidence case.

Transient shielding properties for EMP applications are obtained through numerical Fourier transforms of the frequency domain results. Periodic resonance effects noted earlier now convert to time domain oscillations which may have significances in vulnerability studies.

4-6 ELECTROMAGNETIC SCATTERING AND RADIATION FROM SPHEROIDS LOADED BY CONTINUOUS AND DISCONTINUOUS SURFACE IMPEDANCES: George Tadler, University of California, Los Angeles, California, and Hughes Aircraft Co., El Segundo, California; Nicolaos G. Alexopoulos, University of California, Los Angeles, California.

The problem of electromagnetic wave radiation by/or scattering from spheroidal shapes loaded with arbitrary surface impedance has not been treated heretofore. In general, it is well known that the classical method of separation of variables is aplicable, if the spheroid is perfectly conducting, or if it is loaded with a surface impedance of specific variation. For arbitrary cases of surface impedance, only numerical methods such as Galerkin's method yield results, in conjunction with the application of the Leontivich boundary condition. In this paper we apply the Leontovich boundary condition and we present error curves for its applicability. These curves give error estimates in using the Leontovich boundary condition, in terms of radii of curvature, electrical properties of the surface and surface impedance discontinuities. Our results are completely general in that we treat cases where sections of the spheroid consist of different materials, while sections of it are perfectly conducting. The effect of such arbitrary impedance loading on the radiation pattern and/or radar cross section is discussed in detail. The importance of this study can be evidenced in terms of simple examples of thin spheroids which are loaded with arbitrary impedance at arbitrary points along their length.

4-7 DYADIC MUTUAL IMPEDANCE FOR RADIATION AND SCATTERING PROBLEMS: T. L. Blakney, The Boeing Aerospace Company, Seattle, Washington; A. Ishimaru, University of Washington, Seattle, Washington.

For many radiation and scattering problems it is sometimes necessary, and often convenient, to use the mutual coupling or impedances between several current elements to determine the composite characteristics of the system. However, impedance is normally viewed as a scalar quantity and, hence, difficulties occur in defining the impedance between regions that have independent currents flowing in more than one direction. An example of this would be the problem of scattering from two conducting or dielectric spheres. Such a problem was encountered in attempting a moment method solution on a class of dielectric-covered antennas. A solution was finally obtained by defining an impedance dyad, $\bar{\bar{Z}}_{12}$, such that

$$\bar{I}_1 \cdot \bar{\bar{Z}}_{12} \cdot \bar{I}_2 = \int_{V_1} dv_1 \int_{V_2} dv_2 \, [\bar{J}_1 \cdot G_o \cdot \bar{J}_2]$$

where $\bar{I}_1$, $\bar{I}_2$ and $\bar{J}_1$, $\bar{J}_2$ are the current and current densities, respectively, in volumes $v_1$ and $v_2$. The various terms of $\bar{\bar{Z}}_{12}$ give the relation between the current components in the two regions: e.g., the effect of an $\hat{r}$-directed current in volume 1 upon a $\hat{z}$-directed current in volume 2. Thus, solutions to a wide variety of problems can be systematically studied. The above formulation has been used to find the radiation

characteristics of a cylindrical antenna covered by a thick layer of dielectric and numerical examples are shown to illustrate the effectiveness of this formulation.

4-8 HOLLOW CYLINDER: NEW EQUATIONS AND ASSOCIATED SOLUTIONS: William Davis, Air Force Institute of Technology, Dayton, Ohio.

It is well-known that the H-field integral equations (HFIE) are not useful for obtaining the total current on a thin surface. The E-field integral equations (EFIE) are generally used in lieu of the HFIEs for thin structures, but tend to be ill-conditioned. To alleviate this problem of conditioning, which arises primarily from the strong coupling of the current components in the EFIEs, one combines the EFIEs with the tangential gradient of normal H. The latter is directly related to the normal derivatives of the HFIEs. Obtaining the equations for the hollow cylinder and separating into structural harmonics, the equation for $J_{\phi n}$ is decoupled from the $J_{zn}$ current component: $J_{\phi n}$ is weakly coupled to the equation for $J_{zn}$ by integration with a bounded kernel. For the two EFIEs, strong coupling exists for both equations with the associated coupling kernels being signular. Results have been obtained and are in good agreement with Kao (Radio Science, 5, 1970).

4-9 RAPID ANTENNA NEAR FIELD COMPUTATION BY PLANE WAVE SPECTRUM INTEGRATION: Alexander C. Brown, Jr., Atlantic Research Corporation, Alexandria, Virginia.

Substantially all aperture type antenna near field computation methods have been based on the aperture field distribution. Recently antenna near fields have been computed by integrating the plane wave spectrum (PWS), which is essentially the far field pattern modified by certain form factors, of an antenna. Thus PWS theory allows one to compute antenna near fields from actual measured far field data, rather than having to make assumptions about the aperture field distribution.

Rigorously the field at any point is computed by integrating the PWS over all wavenumber space. Practically, for all but supergain antennas, integration need be performed only over wavenumbers corresponding to visible space, as the contribution to the field due to integrating PWS over wavenumbers corresponding to invisible space is negligibly small for distances greater than a wavelength from the antenna. Up to now, all near field analyses have been performed by integrating the PWS over all visible space regardless of the distance from the antenna. This paper presents a new principle which reduces significantly the computation times of the PWS integration method. The principle is that the significant wavenumber bandwidth decreases

monotonically from $2\pi$/wavelength to zero as the distance increases from one wavelength to infinity. Results for some typical aperture antennas are presented.

## COMMISSION VI, Session 5

Tuesday, October 15 1:30 pm - 5:00 pm
ADAPTIVE ARRAYS AND SIGNAL PROCESSING SYSTEMS
CHAIRMAN: A. A. Ksienski, Ohio State University

5-1 THE VALLEY FORGE RADIO CAMERA: Bernard D. Steinberg and Earl N. Powers, University of Pennsylvania, Philadelphia, Pennsylvania.

The radio camera is a large, thin, randomly distributed, self-cohering antenna array designed to provide high angular resolution microwave images. The term "large" means an array of such size that the element locations cannot be known a priori with adequate accuracy to form a conventional phased array. One objective is the development of means for obtaining high angular resolution of radar targets from randomly distributed antenna elements aboard a ship, among a number of ships, or on a nonrigid structure such as an aircraft. The purpose of utilizing self-cohering techniques is to achieve a coherent aperture much larger than could be provided by a linear or planar array on a confined surface. The experimental work is at L-band; however, the program is designed to permit the results to be applicable to OTH bistatic radar employing a single ship or multiple ships, a nonrigid, X-band array distributed throughout the frame of an aircraft, an air dropped sono-buoy array, and a tactical surveillance radar consisting of many modules which are nonrigidly connected. Described in this paper is the system concept, the problems of a fundamental nature and the initial operating system which will permit test of the principles. This system will have a scanning receiving aperture approximately 1000 feet across, will operate at L-band and will consist of 50 elements. A smaller prototype, consisting of 20 elements and 100 feet in length, will precede the 1000 ft. array. The companion paper describes this system and the experimental results to date.

5-2 FIRST EXPERIMENTAL RESULTS AT VALLEY FORGE: Earl N. Powers and Bernard D. Steinberg, University of Pennsylvania, Philadelphia, Pennsylvania.

The conversion of radiation fields to high resolution images has, with few exceptions, been performed only at optical frequencies because it has not been possible to construct the large antennas required to obtain the resolution needed to image the long wavelength signals used in radar, sonar, seismology and other applications. This paper describes an experimental implementation of a large, thin, random, conformal and adaptive array. Such an array provides economical means for the construction of the huge antennas required for radio imaging. Arrays of this type do not demand precise specification of the antennas's mechanical structure, can function in a nonhomogeneous

propagation medium and their cost does not increase in proportion to the area as in conventionally designed arrays. A very frugal hardware implementation of the array module system has been developed. This array module was used to implement a 100 ft. random array at Valley Forge Research Center. A single module receiver was time-shared between the twenty elements of the array. Field measurements were processed off-line to generate beam patterns and to evaluate scanning performance. The 10 milliradian beam generated by the experimental array could be scanned $3^{o}$ from the beamforming point with little degradation. Performance has been analyzed in terms of recently developed tolerance theory of self-cohering arrays.

5-3 ADAPTIVE ARRAY PERFORMANCE WITH SPATIALLY DISPERSED INTERFERENCE: David M. DiCarlo, Ohio State University, Columbus, Ohio.

The performance of adaptive arrays based on the LMS algorithm is presented when interference is incident upon the array from an angular sector of finite width. A mathematical model of a two-element array is developed when an arbitrary number of discrete signals are incident upon the array. From this model the array weights are derived. It is then shown how the model is readily extended to the case of a continuous radiation sector. By representing the radiation sector by a large number of discrete signals, (many more than degrees of freedom of the array) numerical results of the array performance are given. The effects of the interference sector size and desired signal location on the array pattern and output signal-to-noise are displayed. It is shown that the array performance is not always degraded as the size of the interference sector increases.

5-4 ADAPTIVE BEAMFORMING USING A LARGE APERTURE HF ARRAY: Lloyd J. Griffiths, University of Colorado, Boulder, Colorado.

Adaptive beamforming techniques have been applied to digital samples obtained from the Wide Aperture HF Radio Research Facility which is located in the central valley of California and is operated by the Stanford Research Institute. This facility consists of a linear array of 256 vertical monopole elements with an interelement spacing of ten meters. Data for the present study were recorded at eight subarray outputs of the array with each subarray composed of 32 adjacent monopoles. Signals were recorded using one-hop forward scatter and backscatter transmissions. Array output signals generated by adaptively

combining the subarray signals were compared with those generated from a conventional Tchebychev taper and sum beamformer. Observations in the presence of high interference levels of unknown origin demonstrated output signal-to-noise ratio improvements of 25-30 dB using adaptive techniques. Total time for adaptation was shown to be less than 40 msec. The conclusion drawn from this study is that simple adaptive beamforming methods can be used to significantly reduce the effect of ionospherically reflected interference.

5-5 TAPPED DELAY-LINE PROCESSING IN ADAPTIVE ARRAYS: W. E. Rodgers and R. T. Compton, Jr. The Ohio State University, Columbus, Ohio.

This paper will discuss LMS adaptive arrays which use tapped delay-line processing behind each element. Such processing is useful for increasing the bandwidth of an adaptive array over that obtainable with quadrature hybrid processing. The paper will compare the performance of 4 processors--quadrature hybrid, 2-tap quarter wavelength delay-line, 3-tap half wavelength delay-line, and 5-tap half wavelength delay line--in each case for a 2-element array with half wavelength spacing. Signal-to-noise ratio (SNR) performance of the processors will be compared for signal bandwidths of 4%, 10%, 20%, and 40%, and for various angles-of-arrival of the desired and interference signals. The results show that at 4% BW the 3-tap processor produces only a small SNR improvement over the quadrature hybrid and 2-tap processors, but at 10% and wider bandwidths, the 3-tap processor is clearly superior. The 5-tap processor, however, showed only minor improvement over the 3-tap processor.

5-6 MULTIPLE SIGNAL ARRIVAL ANGLE ESTIMATION: Albert J. Berni, Ohio State University, Columbus, Ohio.

A direction finding technique is presented that is capable of simultaneously estimating the arrival angles of multiple signals. Pulsed, as well as continuous signals can be handled with the signal characteristics specified only in center frequency and bandwidth. Two approaches will be described. In the first an adaptive antenna array is used. The feedback is designed so that nulling of all incident signals occurs rapidly. The bearings of the nulls in the adapted pattern are the arrival angle estimates. The effects of input signal and feedback loop parameters upon estimate bias, loss of resolution and spurious estimates are discussed. The second approach involved a direct estimation of the signal correlation matrix and subsequent processing to obtain the arrival angle estimates. This approach is shown to have theoretical advantages over the first method and it has been implemented. Simulation and pattern range measurements with a three element prototype system will be presented.

5-7 OPTIMAL PERFORMANCE OF A MTI FILTER IN A MULTIPLE-CLUTTER ENVIRONMENT: J. K. Hsiao and B. L. J. Rao, Naval Research Laboratory, Washington, D. C.

A radar return echo usually contains unwanted clutter reflected from ground, sea, rain, clouds or chaff. For target detection these clutters must be filtered. A conventional MTI filter usually considers only a single type of clutter with a fixed mean doppler and spectral distribution. However, in reality the radar return may contain several different types of clutters. Each of these clutters may have a different mean doppler and a different spectral distribution. In this paper an optimal filtering of such clutters is considered. Since different types of clutters can be considered as statistically independent, the covariance matrix of such clutter returns is Hermitian and positive definite. It is shown that the optimal MTI filter weights are equal to the eigenvector associated with the minimum eigenvalue of the covariance matrix. It is assumed that the clutter spectral density function is a bell-shape function (Gaussian distribution). The improvement factors of such filters are a function of the relative strength, mean doppler frequency and the variance of the different types of clutters. Finally, numerical examples of performance of such filters will be presented.

## COMMISSION VIII, Session 2

Tuesday, October 15 1:30 pm - 5:00 pm
ATMOSPHERIC RADIO NOISE
CHAIRMAN: A. G. Hubbard, U. S. Army Electronics Command

2-1 RADIO EMISSION FROM LIGHTNING: John B. Smyth, Smyth Research Associates, San Diego, California.

Equations representing the electromagnetic field associated with lightning, based upon the dipole moment of the thundercloud and its time derivatives, have been extensively used. It is shown that these equations do not represent the radio fields emitted from the lightning discharge. A little known, simple and exact solution of Maxwell's equations discovered by Manneback (1923) appears to adequately represent the radio fields associated with lightning. Many interesting and previously puzzling characteristics of lightning are clearly in evidence through this solution: such as, the zig zagging and pausing of the stepped leader.

2-2 CORRELATION OF SFERIC DF DATA AND POTENTIALLY SEVERE THUNDERSTORM CELLS: R. L. Johnson, Southwest Research Institute, San Antonio, Texas.

Directional sferic data were gathered using a crossed baseline interferometer as a formal thunderstorm system moved through the San Antonio, Texas area on 9 May 1974. The data were collected during 3 to 5 minute intervals with 600-700 bearings per interval over a 5-hour period. Individual thunderstorm cell discrimination was maintained through the generation of histograms showing sferic count versus bearing. Radar weather maps and the station log of direction/range to max cloud tops and meteorological intensity were obtained from the Weather Bureau radar site at Hondo, Texas. This data provided a more precise description of cloud profile and meteorological content than had been cross-correlated with sferic directional information in earlier experiments at this facility. The directional sferic data show a high degree of correlation with the max cloud top recordings. The relative sferic counts shown by histogram peaks are closely correlated with the cells identified by Weather Bureau guidelines as potentially (or active) severe thunderstorm cells.

2-3 VARIATIONS IN THE BURST NATURE OF ATMOSPHERICS RELATIVE TO THUNDERSTORM SEVERITY: William L. Taylor, National Oceanic and Atmospheric Administration, Boulder, Colorado.

Variations in the characteristics of electromagnetic impulses were observed during various weather conditions at 15 locations during the thunderstorm seasons of 1972 and 1973. Results

indicate the severity of thunderstorms can be estimated by measuring the burst rate of radiation at an observing frequency of about 3 MHz. For example, during 1973 it was found that when the number of bursts comprised of large amplitude impulses exceeded 20 per minute, there was one chance in three that a tornado existed within the observational range of the recording equipment.

2-4 FURTHER ANALYSIS OF A VLF ATMOSPHERIC NOISE MODEL: James P. Hauser, Naval Research Laboratory, Washington, D. C.

At the 1973 URSI Meeting it was shown that a VLF atmospheric noise prediction model developed by E. L. Maxwell and based on mathematical expressions relating thunderstorm day data to received noise energy agrees better with the available noise data than does the empirical model presented in CCIR Report No. 322. It was also shown that minor empirical modifications to Maxwell's model further improve its agreement with data. Additional attempts have been made to improve Maxwell's model by altering the mathematical expressions themselves. Equations developed by E. T. Pierce relating thunderstorm days/month to number of lightning discharges and the proportion of discharges to ground give no better results than similar expressions developed by Maxwell. On the other hand, modifications to the algorithm for predicting upper decile noise have improved the agreement with $D_u$ data. Furthermore, the modifications to the algorithm make it possible to predict $\sigma F_{am}$ as well. The analysis presented in 1973 did not consider the numerically mapped version of the CCIR model developed by Zacharisen and Jones. The numerically mapped model is continuous at 1 MHz; however, at VLF frequencies this model contains discontinuities similar to those inherent in CCIR Report 322. Analysis shows that at VLF frequencies the numerically mapped model is no better than the CCIR model as presented in Report 322 and certainly not better than Maxwell's model. Also, the geographic areas of greatest difference between Maxwell's model and the CCIR Report 322 model are identified.

2-5 PREDICTION OF HF NOISE DIRECTIVITY FROM THUNDERSTORM PROBABILITIES: Leigh N. Ortenburger and Dean A. Schaefer, GTE-Sylvania, Mountain View, California.

A technique for predicting the azimuthal directionality of thunderstorm-generated noise is discussed and evaluated. A model relating the noise generated in a subdivided surface area of the earth to the probability of having thunderstorm activity in that area is derived using linear regression to relate the diurnal variation of received noise at a point to the diurnal variation of thunderstorm activity over the world. Once a model is derived the thunderstorm probabilities are used

to predict the directionality of the noise received at a point.

Inputs to the regression analysis included the atmospheric noise curves published in CCIR Report 322, and maps of the hourly probability of world-wide thunderstorm occurrence derived from World Meteorological Organization documentation. An implication of the model results is that there is an approximate quadratic relationship between number of thunderstorms in an area and transmitted noise power ($T_p$) of the form $T_p = S(f)\ [CN^2(t)]$ where S(f) is a typical power spectrum for lightning discharges, C is a constant derived from the regression analysis procedure, and N(t) is the expected number of thunderstorms in an area at time t.

Utilizing this thunderstorm-probability vs. power-transmitted relationship, the received noise power at a point was calculated as a function of the power transmitted from each area, the propagation mode losses between the receiving point and each area, and the gain pattern of the receiving antenna. The results indicate that differences of 20 dB can be expected for particular azimuthal directions, times-of-day, and frequencies.

2-6 RECENT STUDIES OF HIGH FREQUENCY ATMOSPHERIC NOISE IN CANADA: W. R. Lauber and F. D. Green, Communications Research Centre, Ottawa, Canada.

No radio noise data were contributed from Canada during the data collection period for CCIR Report 322. During the past two years, measurements of H.F. atmospheric noise levels have been made for four seasons on the East Coast, three seasons in the Ottawa area and two seasons on the West Coast. The results of the measurements, taken during the period 2000 to 2400 hours LST when atmospheric noise is predominant over the man-made noise levels of the day, show good agreement with the CCIR predictions for these mid-latitude sites ($44^o$ - $49^o$ N.). In addition, two seasons of amplitude probability distribution (APD) and dB ratio of $V_{rms}$ to $V_{ave}$ ($V_d$) measurements have been made near Ottawa. The measured APD's were compared with those predicted by CCIR Report 322 for the measured $V_d$ values and were found also to show good agreement. Directional characteristics of noise from large north and south pointing arrays on the East Coast, sampled over four seasons in the 2000 to 2400 hour time period, are compared to similar characteristics noted from a rotatable array near Ottawa. The directional differences in received levels were found to be greatest at the lower H.F. frequencies and decrease with increasing frequency.

2-7 EARTH AS AN HF RADIO NOISE SOURCE VIEWED FROM THE MOON:
John R. Herman, Radio Science Company, Lowell, Massachusetts; Robert G. Stone, National Aeronautics and Space Administration, Greenbelt, Maryland.

A technique has been developed to quantitatively assess the time-varying effects of ionospheric shielding and terrestrial radio noise source distributions on non-thermal noise propagating from Earth's surface to the Moon. Predictions of the noise magnitude to be expected by an observer near the Moon over a 24-hr period for lunar positions corresponding to the lunar quarter phases indicate that the terrestrial noise temperature may be to 15 dB greater than cosmic noise background on frequencies near 10 MHz. NASA's Radio Astronomy Explorer 2 (RAE-2) satellite orbits around the Moon at an altitude of 1000 km with a period of 3 hr 45 min, and its directive Vee antenna sweeps past Earth when the geometry is favorable. RAE-2 HF radio noise temperature data selected from northern hemisphere summer and winter full Moon periods at times when Earth is in the antenna's main beam are compared with the predictions.

## COMMISSION I, Session 3

Wednesday, October 16 8:30 am - 12:00 noon
TIME AND FREQUENCY TECHNOLOGY AND NAVIGATION
CHAIRMAN: J. A. Barnes, National Bureau of Standards

3-1 FREQUENCY AND TIME STANDARDS PERFORMANCE AND AVAILABILITY: Helmut Hellwig, National Bureau of Standards, Boulder, Colorado.

The standards principally used in technical and scientific applications are rubidium gas cell devices, cesium beam tubes, hydrogen maser oscillators, and quartz crystal oscillators. A general characterization and comparison of these four classes of precision standards is given, including accuracy, stability, environmental sensitivy, size, weight, and cost. Areas for special concern in practical applications are identified and solutions recommended. Modern atomic frequency standards are identified and sources for their procurement are listed. An attempt is made to predict physical and performance characteristics potentially available in the future.

3-2 APPLICATIONS AND EXISTING SERVICES FOR PRECISE TIME AND FREQUENCY: Gernot M. R. Winkler, U. S. Naval Observatory, Washington, D. C.

Present applications of precise time and frequency (T/F) technology can be grouped in several classes: 1) communications systems which require T/F for time division multiplexing and for using spread spectrum techniques, 2) Navigation systems which need T/F for position fixing using a timed signal, 3) scientific-metrological applications use T/F as the most precisely reproducible standard of measurement, and 4) astronomical/space applications which cover a variety of the most demanding applications such as pulsar research, VLBI and laser/radar ranging. In particular, pulsar time of arrival measurements require submicrosecond precision over a period of one-half year referred to an extraterrestrial inertial system, and constitute the most stringent requirements for uniform timekeeping to date.

The standard T/F services which are available to satisfy such requirements are based on an international system of timekeeping coordinated by the Bureau International de I/Heure (BIH). The system utilizes the contributions from the major national services for standard frequency and time (USNO and NBS in the USA), and it is implemented through a variety of electronic systems (HF, T/F signals, VLF, Loran-C, etc.). The performance of these systems will be discussed. Several of the user systems (such as VLBI) can in turn be used as contributors to the global effort of T/F distribution.

3-3 SOME EFFECTS OF RELATIVITY ON TIME DISSEMINATION AND NAVIGATION: Leonard S. Cutler, Hewlett-Packard Company, Palo Alto, California.

The rates of standard clocks such as atomic clocks depend on the gravitational potentials at their locations as well as their relative motions. Some of these relativistic effects and their influence on time dissemination and navigation will be discussed. Some simple techniques for making the calculations will be presented.

3-4 NAVY NAVIGATION SATELLITE SYSTEM: R. J. Taylor, Johns Hopkins University, Silver Springs, Maryland.

This paper will discuss the origin and development of the operational Navy Navigation Satellite System. The error budget for the operational system and various receivers will also be presented. Besides the operational system, the Transit Improvement Program will be discussed.

The Transit Improvement Program is a series of experimental/operational satellites which contain the following systems, modes of operation and devices: 1) DISCOS (Disturbance Compensation System) is a device that compensates for the effects of aerodynamic drag forces and solar radiation pressure which act on the satellite in orbit, 2) PRN (Pseudo Random Noise) is a wide bandwidth phase modulation of the 150 and 400 MHz carriers which can be used for range navigation and the dissemination of time, 3) IPS (Incremental Phase Shifter) is a device capable of compensating for long term frequency drifts of the satellite reference oscillator.

Experiments using PRN for range navigation and the dissemination of time from the TRIAD satellite, first satellite launched in the Transit Improvement Program, will be discussed.

3-5 NAVIGATION TECHNOLOGY SATELLITES: Roger L. Easton, Naval Research Laboratory, Washington, D. C.

The satellite known internationally as 1974 54A is simultaneously the last of the TIMATION series and has been adopted as the first of the Navigation Technology Satellites (NTS-1) of the NAVSTAR Global Positioning System program.

This satellite was launched at 0455z of 14 July on an Atlas F with dual solid motors as upper stages into a near circular, $125^{\circ}$ inclination orbit having a period of 7 hours 48 minutes.

The paper will discuss the uses of this satellite for disseminating time and frequency information and the improvements expected from future satellites of the NTS series.

## COMMISSION II, Session 5

Wednesday, October 16 8:30 am - 12:00 noon
RADIO OCEANOGRAPHY III
CHAIRMAN: John R. Apel, National Oceanic and Atmospheric Administration

5-1 MODELING THE RADAR SEA BACKSCATTER SPECTRUM AT HF: Dennis B. Trizna, Naval Research Laboratories, Washington, D. C.

Results are presented for theoretical modeling of first and second order features in the Doppler radar sea backscatter spectrum at HF. The model is parametric in wind-radar angle, wind speed (or radar frequency), and constants of the spreading function describing the directional sea spectrum. Comparison is made with data collected line-of-sight at the NRL/NOAA/ITS San Clemente HF radar facility.

5-2 EVALUATION OF HF MEASUREMENTS OF OCEANIC WINDS: Robert H. Stewart, University of California, San Diego, California.

HF radio waves backscattered via an ionospheric path have been used to measure oceanic winds at distances of up to 3000 km. To evaluate the accuracy of the technique, we conducted an experiment whereby radio scatter was compared with oceanic winds measured in the scattering area. Wind speed, direction, and the ocean-wave directional spectrum were recorded for three weeks by instruments on the manned spar buoy FLIP at 35N-155W in the north central Pacific. Radio signals in the 15-25 MHz band were scattered from the sea in this area using the Stanford Research Institute's WARF radar situated in central California. Local radar scatter was observed with an HF radar on the R/V THOMAS WASHINGTON, and HF transponders were operated on FLIP and WASHINGTON. Because the winds were generally weak during this period, these data were augmented with wind data recorded by ships of opportunity during stormy conditions at the same time the WARF radar observed scatter from their area. Wind direction, as deduced from the radio scatter, was compared with the measured direction. The two sets of data agree within $\pm 30^{o}$, or about one octant. Radio measurements of wind speed were poor. Calculated winds differed by a factor of two from the observed winds. We are presently determining the cause of this scatter in the comparison with the goal of reducing it.

5-3 AN EXPERIMENTAL DETERMINATION OF THE VALUE OF $\sigma^{o}$ FOR 7-SECOND OCEAN WAVES: C. C. Teague, Stanford University, Stanford, California.

The directional wave-height spectrum measurements from an experiment on Wake Island in November, 1972, have been extended

to include a determination of the absolute value of $\sigma^o$, the relative radar cross-section. The experiment utilized LORAN-A transmissions at 1.95 MHz and was sensitive to 7-second period (77 meter wavelength) ocean waves. The receiver was in both a synthetic aperture and a stationary mode. In situ buoy measurements on two of the eight days of the experiment indicate that the 7-second waves were near saturation during this period. Local wind velocity measurements showed average wind speeds ranging from 5 to 13 m/s, with a 48-hour segment of nearly constant 13 m/s velocity. The value of $\sigma^o$ was obtained by a careful observation of the ratio of the echo energy to the energy received in the direct pulse from the LORAN transmitter about 5 km from the receiver. Observed values of $\sigma^o$, using the free-space form of the radar equation, range from -31 dB to -40 dB.

5-4 SPATIAL DISTRIBUTION OF HF SURFACE WAVE SEA CLUTTER: A. H. Katz, S. E. Press, and R. B. Marshall, Raytheon Company, Sudbury, Massachusetts.

Spatial distributions of surface-wave sea clutter at 7, 10 and 12 MHz for a bistatic surface wave configuration are described. The radar, a bistatic system which utilized the FM/CW waveform and 1/4 wave tuned monopoles, consisted of a 10 kW transmitter located on Amelia Island, Florida (30° 40'N, 81° 25'W) and a receiving system at Cape Canaveral, Florida (28°32' N, 80°33'W). The baseline separation was 252 km. Measurements were made with 20 μs time delay resolution and 0.0078 Hz Doppler resolution. Utilizing the relationship between radar and ocean wave parameters, contours of normalized power per unit area were mapped. Maps are available for a period of four (4) weeks in the Fall of 1973 for a range of sea states from 2 through 6. Comparisons with theoretical calculations by Barrick indicate a preference for the Pierson-Moskowitz wave height spectrum with a $\cos^4\phi$ pattern dependence.

5-5 MICROWAVE SCATTEROMETER MEASUREMENTS OF OCEAN WIND VECTOR: W. Linwood Jones, William L. Grantham and Lyle C. Schroeder, National Aeronautic and Space Administration, Hampton, Virginia; John L. Mitchell, LTV Aerospace Corporation, Hampton, Virginia.

Aircraft measurements of ocean radar backscatter have been obtained for a variety of wind speed conditions using a microwave scatterometer. During the experiments, the instrument was mounted at the end of the open tail ramp of a C-130 cargo-type aircraft and thereby achieved an unobstructed view of the ocean's surface without the use of a radome. The scatterometer operated at 13.9 GHz in the beam limited

(interrupted continuous wave) mode and utilized a dual linear polarized mechanically scanned, narrow beamwidth parabolic antenna. Vertical and horizontal radar cross sections were measured as a function of incidence angle from nadir to approximately 55° while the aircraft flew upwind, downwind, and crosswind tracks. Data are presented which show a power law response of cross section to wind speed for incidence angles of 25° to 55°. Significant differences are noted between the upwind, downwind, and crosswind observations. To better examine this phenomenon, flight lines were performed where the antenna was pointed to the nadir and the aircraft was placed in a steep bank turn. This produced a fixed incidence angle azimuth scan so that cross sections could be measured as a function of angle relative to wind heading. Results are presented for several wind speeds. They show maxima in the upwind and downwind directions and minima in the crosswind directions. These observations are in qualitative agreement with the directional capillary wave spectra of the ocean.

5-6 DUAL FREQUENCY SCATTEROMETER MEASUREMENT OF OCEAN WAVE HEIGHT: J. W. Johnson, W. L. Jones, C. T. Swift, W. L. Grantham, National Aeronautics and Space Administration, Hampton, Virginia; D. E. Weissman, Hofstra University, Hempstead, New York.

A technique for remotely measuring RMS wave height averaged over an area of the sea surface has been developed theoretically and verified with a series of aircraft flight experiments. The measurement concept involves the cross-correlation of the amplitude fluctuations of two monochromatic reflected signals with variable frequency separation. The signal reflected by the randomly distributed specular points on the surface is observed in the backscatter direction at nadir incidence angle. The measured correlation coefficient is equal to the square of the magnitude of the characteristic function of the specular point height from which RMS wave height can be determined. The flight scatterometer operates at 13.9 GHz and 13.9 + $\Delta f$ GHz with a maximum $\Delta f$ of 40 MHz. Measurements have been conducted over relatively smooth seas (RMS height $\tilde{}$ 0.3 m) at altitudes of 2, 5, and 10 thousand feet. The results show the predicted decorrelation with frequency separation and with off nadir incidence angle. The validity of the technique over a wide range of sea state conditions will be explored in future flights and these results should be available for presentation.

5-7 PROBLEMS IN OCEANOGRAPHIC USES OF BEAM-LIMITED TARGET-REFERENCED RADARS: E. J. Walsh, National Aeronautics and Space Administration, Wallops Island, Virginia.

Langley Research Center has been developing a two frequency radar interferometer system proposed by Weissman. Wallops Flight Center has under study a linear-FM Spatial Correlation Radar developed by Fairchild Industries. The two systems are quite different although they both operate in a beam-limited mode and are target-referenced. Their simplified processing schemes eliminate the range information in the signal and develop a measure of the range extent of the target. At first glance this appears to be a simple way to obtain SWH without having to bother with range tracking. However, severe limitations are imposed by the fact that the wavelength/SWH ratio has a minimum of about 20 in the gravity wave region. Geometry is developed to show the range extent of a flat sea, $r_o$, which acts as a bias on all SWH measurements. The sensitivity of the measurements to changes in SWH is determined as a function of SWH/$r_o$. Minimum acceptable and desirable SWH/$r_o$ ratios are established and used to show the limitations of these types of systems both at aircraft and satellite altitudes. Under some conditions it is impossible to view sufficient wavelengths to approximate an ensemble average without incurring too large a bias. Frequently, even if the criteria can be satisfied the observation altitude will have to be adjusted proportional to the SWH to maintain acceptable measurement conditions.

## COMMISSION III, Session 4

Wednesday, October 16 8:30 am - 12:00 noon
IONOSPHERIC HEATING I
CHAIRMAN: W. T. Utlaut, Institute for Telecommunication Sciences

4-1 A SURVEY OF VERTICAL INCIDENCE RADIO OBSERVATIONS OF IONOSPHERIC MODIFICATION: W. F. Utlaut, Institute for Telecommunication Sciences, Boulder, Colorado.

Within the past four years, experiments with high-power high-frequency radio waves have proved the feasibility of temporarily altering the ionosphere's properties. This paper provides a survey of some of the regularly, or frequently occurring effects observed with vertical incidence radio techniques when the U.S. Department of Commerce's Platteville facility, near Boulder, Colorado is used to illuminate the overhead ionosphere. We shall also illustrate that relatively low power transmissions, producing power flux densities in the F region of the order of $1\mu W/m^2$, produce significant modification in the ionosphere. Such low power illuminations also create field-aligned ionization irregularities that produce a significant scattering cross section in the ionosphere which permits transmission of VHF signals over selected long distance paths that could not be used by natural means.

4-2 ANGULAR DISTRIBUTION OF SCATTERING ASSOCIATED WITH ARTIFICIAL SPREAD-F AND WIDEBAND ATTENUATION: E. M. Allen, G. Meltz, P. B. Rao, and G. D. Thome, Raytheon Company, Sudbury, Massachusetts.

Ionospheric heating with powerful HF waves produces rapid and pronounced O-mode wideband attenuation (WBA) on all frequencies near and above the heating frequency. We report observations of the angular distribution of attenuation obtained using a large phased array 11 km east of Platteville, Colorado. Scattering is observed from altitudes near the heater reflection level with both O and X-mode diagnostic waves. The earliest arriving return comes from magnetic north while latter arriving signals map to the south. Weak echoes associated with the appearance of WBA on an ionogram onset within seconds after heater turn-on and decay promptly within seconds following turn-off. This is in contrast to strong, slowly developing reflections from large ducts that persist minutes after turn-off. These returns, thought to be due to focused reflections of rays from field-aligned structure, are strongest to the south. When WBA is observed, the backscattering seen at the phased array maps mostly to the north and is greatly attenuated compared to echoes from large scale ducts. We interpret our observations of prompt O-mode scattering in terms of the effect of short wavelength field-aligned stimulated diffusion modes on propagation. Up-going O-waves launched to the north are weakly backscattered near the heater reflection level

by the nonlinearly enhanced diffusion mode and then strongly scattered after reflection, giving rise to a small return but an overall reduction in amplitude.

4-3 RADIO SCATTERING FROM A HEATED REGION OF THE IONOSPHERE: P. A. Fialer, L. E. Sweeney, Jr., V. R. Frank, Stanford Research Institute, Menlo Park, California.

The Institute for Telecommunication Sciences' (ITS) ionospheric heating facility located at Platteville, Colorado, has been shown to generate at least three distinct, new types of structure capable of scattering radio waves in the HF through UHF spectrum. The strongest scattering mechanism produces highly field-aligned scattering (FAS) of frequencies in the HF, VHF and low UHF bands. The intensity vs scale size spectrum has been determined by measurements made using wideband soundings. The angular distribution of scattered energy has been measured as has the spatial extent of the scattering region and the Doppler spectrum of the scattered signals. This artificial FAS has been observed at both E- and F-region heights. The second scattering mechanism, which has been observed at F-region heights with VHF and UHF signals, also scatters incident energy in a field-aligned scatter geometry. The scattered energy is, however, frequency shifted, by an amount equal to the heater frequency, above and below the frequency of the incident energy. Unlike the plasma-line observations which have been carried out using the Arecibo Observatory (AO) heater and radar, the frequency shift is not offset from the heater frequency by the ion-acoustic frequency. The third scattering mechanism has been observed weakly at VHF and is consistent with scattering from plane waves of ionization propagating along the geomagnetic field lines in both directions at the ion-acoustic wave velocity. Such waves are predicted by the parametric decay instability theory whch has been applied to the plasma line observations made at AO. No completely satisfactory theory for the generation of artificial FAS is yet available.

4-4 VHF/UHF FIELD-ALIGNED AND PLASMA-WAVE SCATTERING FROM A HEATED IONOSPHERIC VOLUME: J. Minkoff, P. Kugelman, I. Weissman, Riverside Research Institute, New York, New York.

It is observed that an ionospheric volume in the F-layer subjected to high-power HF illumination becomes an effective scattering medium for radio signals in the VHF/UHF-frequency range. The experimental results are representative of a field-aligned scattering geometry for which the first such observations of VHF/UHF scattering from a heated ionospheric volume are presented. Two distinct and markedly dissimilar scattering modes are observed: center-line and plasma-line scattering. Center-line scattering is observed at the

transmitted radar frequency f; plasma-line scattering is observed as a pair of sidebands at $f \pm f_h$ where $f_h$ is the heater frequency. Center-line scattering is highly aspect sensitive with respect to the direction of the geomagnetic field, $\vec{B}$; plasma-line scattering is found to be much less aspect sensitive, if at all. The longitudinal coherence length, L, for center-line scattering is found to be greater than the maximum antenna diameter of 85'; no more exact estimate for L is possible. A striking reversal in frequency-dependence is found between the center-line and plasma-line modes. The per-unit-volume center-line backscatter cross section is found to be ~7dB greater at VHF than at UHF; the per-unit-volume plasma-line backscatter cross section is found to be at least 11 dB less at VHF than at UHF. For both modes the scattering cross section is found to be effectively turned on and off very rapidly in response to the heater excitation; the spectral width of the scattering for both modes is found to be quite narrow (~10 Hz). The spatial configuration of the heated volume is investigated; significant differences are observed depending on whether $f_h/f_oF_2$ is greater or less than unity.

4-5 BISTATIC MEASUREMENTS OF RADIO FREQUENCY SCATTERING FROM A HEATED IONOSPHERIC VOLUME: J. Minkoff, M. Laviola, S. Abrams, D. Porter, Riverside Research Institute, New York, New York.

A variety of bistatic experiments which were carried out for the purpose of determining the scattering properties of a heated ionospheric volume in the F-layer over Platteville, Colorado are described. Results are presented from which it was first determined that the center-line scattering takes place from elongated field-aligned scattering structures. Measurements are presented showing that, for the center-line mode, the scattering of the incident signal consists, effectively, of specular reflections off the geomagnetic field lines.

4-6 GEOSTATIONARY AND ORBITAL SATELLITE MEASUREMENTS OF ARTIFICIAL SPREAD F PRODUCED BY IONOSPHERIC HEATING: S. A. Bowhill, E. K. Walton, D. R. Ward, Aeronomy Corporation, Champaign, Illinois.

The characteristics of artificial spread F (ASF) produced by the ionospheric heater at Platteville, Colorado have been investigated by spaced-receiver studies of the scintillation of geostationary and orbital satellite signals. Field-aligned structures with horizontal correlation distance of about 100 m appear within one or two minutes of the onset of heating, and extend through the entire F layer. They extend horizontally with a 50-km radius of the heater transmitter and drift with the velocity of the ambient plasma. The electron-density fluctuation associated with them is a few tenths of one percent, sufficient to produce scintillations of up to 20 percent at

150 MHz. The incidence of smaller structures of about 10 m is also described.

4-7 A MODEL FOR RF SCATTERING FROM FIELD-ALIGNED HEATER INDUCED IRREGULARITIES: P. B. Rao and G. D. Thome, Raytheon Company, Sudbury, Massachusetts.

The paper presents a model for radiowave scattering from the ionoshperic irregularities generated by the intense radiowave transmissions from the Platteville heater. The model is based upon the HF - UHF radar backscatter observations for a physical description of the scattering medium and upon the theory of weak scattering (Born approximation) from anisotropic irregularities for mathematical development. According to the model, the electron density fluctuations responsible for radiowave scattering having an RMS value of 1 to 1.5% are aligned along the earth's magnetic field and are distributed in a diffuse pancake-shaped volume of 15 Km Gaussian thickness vertically and of the size of the heater beam which is 100 Km in Gaussian diameter horizontally. At radio frequencies the irregularities within the disturbed volume are highly aspect-sensitive and consequently only those scatterers which lie on the surface of specularity where a radar views transverse to the magnetic field count in contributing to the received signal. Model computations have been made of the scattering cross sections for monostatic as well as bistatic radar configurations and they are found to be in good agreement with the observations. The radar cross section at a given frequency for bistatic geometry is substantially greater than that for monostatic geometry, all else being equal. Finally, it is shown that the width of the scatter illuminated bands on the ground is set primarily by the finite dimensions of the scattering volume rather than by the finite aspect sensitivity of the individual scatterers.

4-8 HF-VHF COMMUNICATIONS EXPERIMENT USING MAN-MADE FIELD-ALIGNED IONOSPHERIC SCATTERERS: G. H. Barry, Barry Research Corporation, Palo Alto, California.

Scatter from man-made, field-aligned, F-layer irregularities offers a means of over-the-horizon communication at VHF frequencies. Data collected in 44 days of field operation in the autumn of 1972 and 1973 defines representative characteristics of signals transmitted over such an experimental scatter circuit. A cloud of field-aligned scatterers was created by the Platteville, Colorado ionospheric modification facility; test transmitting sites were established in Texas and receiving sites in California. The data describes mean and peak cloud radar cross-section, the dependence of cross-section on heater power, heater modulation, time of day, and signal frequency, the circuit coherent and incoherent bandwidths, the signal amplitude statistics and spatial correlation, and the signal spectral

spreading. The experiment also included the transmission of representative types of modulated signals including SSB voice, 100 word/min FSK teleprinter data, 2400 bit/sec data, 30 kHz FM voice, and 3 kHz FSK facsimile. Examples of received signals are presented.

COMMISSION V, Session 3

Wednesday, October 16 8:30 am - 12:00 noon
VLBI INSTRUMENTATION AND TECHNIQUES
CHAIRMAN: J. M. Moran, Smithsonian Astrophysical Observatory

3-1 ASTRONOMY, GEODESY, AND GLOBAL TIME/FREQUENCY SYNCHRONIZATION BY VLBI: T. A. Clark, Goddard Space Flight Center, Greenbelt, Maryland.

During 1972 through 1974, about twenty different very-long-baseline-interferometry (VLBI) experiments were performed by the GSFC/HO/MIT Group in collaboration with other organizations. Some of these experiments involved as many as four separate sites spanning two continents; the longest baseline involved was nearly 8000 km. These experiments have yielded positions of extragalactic sources with uncertainties of only a few hundredths of an arcsecond and baseline lengths with uncertainties in the decimeter range. Clock epochs and rates have been synchronized a posteriori with uncertainties at the sub-nsec and sub-psec/sec levels, respectively. Variations in UT.1 and polar motion have been determined with the equivalent of sub-meter uncertainties. Detailed results on these aspects of the experiments will be presented.

3-2 RELATIVE POSITIONS OF PAIRS OF EXTRAGALACTIC RADIO SOURCES: A. R. Whitney, Massachusetts Institute for Technology, Westford, Massachusetts.

A 2-antenna VLBI technique has been developed to determine relative positions of pairs of extragalactic radio sources whose angular separation is small. The antennas observe the two sources alternately with a single cycle taking about 8 minutes. Hydrogen maser frequency standards are used at each site to insure that the fringe phases from each source can be connected across the "gaps" without the introduction of "$2\pi$ ambiguities". The differences in the fringe phases from the two sources are then used to estimate the relative positions. The detailed methods used in the data analysis will be described along with results for the source pairs 3C345 - NRAO 512 and 3C273B - 3C279.

3-3 PULSAR CALIBRATION OF VLB DATA: J. Broderick, Virginia Polytechnic Institute and State University, Blacksburg, Virginia.

The calibration procedure of VLB data, is usually an a posteriori one based on the assumption that one of the sources was completely unresolved. This assumption can be checked by observing no change in the visibility function over a wide range of projected baselines, but this is not always possible due to limited telescope tracking or lack of common sky coverage for widely separated telescopes. However, over a goodly range of

wavelengths pulsars step in to save the day; being plenty small enough (below 1 meter wavelength) and strong enough (for a 10 $\sigma$ detection) for many telescope pairs even down to 6 cm. wavelength. Pulsars were used on a recent 70 cm VLB experiment performed by J. Condon and the author and a surprising result was obtained.

3-4 MAXIMUM ENTROPY METHOD FOR THE INVERSION OF UNEQUALLY SPACED TWO DIMENSIONAL VISIBILITY DATA AND NUMERICAL TESTS OF ITS EFFECTIVENESS: Alan E. E. Rogers, Haystack Observatory, Westford, Massachusetts.

An iterative algorithm for maximum entropy inversion of unequally spaced samples of the visibility function has been tested and compared with other methods of transforming from visibility to brightness. The maximum entropy method usually yields a brightness distribution which is a better approximation of the original brightness, from which visibility samples were obtained, than any other method. The other methods tested were the conventional Fourier transform, beam cleaning, least squares Fourier interpolation and an approximate maximum likelihood method.

3-5 ON CLOSURE PHASE ANALYSIS OF VLBI DATA: L. K. Hutton and A. E. E. Rogers; Massachusetts Institute for Technology, Westford, Massachusetts.

Techniques have been developed for extracting source structure information from multibaseline VLBI data, using fringe amplitude and closure phase information. A scheme presented previously for linear sources involves one-dimensional Fourier series fits to the amplitude and phase data, and subsequent transformation of the Fourier series. This technique has been generalized to two-dimensions, making it applicable to arbitrary source brightness distributions. Results of the application of this technique to artificially generated data and to actual data from 3.8 cm Quasar Patrol observations will be presented.

3-6 AN APPROACH TO A CONTINENTAL ARRAY: M. H. Cohen, California Institute of Technology, Pasadena, California; G. W. Swenson, Jr., University of Illinois, Urbana, Illinois; B. G. Clark and K. I. Kellermann, National Radio Astronomy Observatory, Green Bank, West Virginia.

We discuss potential VLBI arrays based on existing telescopes in the USA and Canada. At present the system lacks sensitivity and has appreciable holes in the (u,v) coverage, especially at short centimeter wavelengths. The sensitivity could be greatly increased by making improvements at the various telescopes.

COMMISSION V, Session 3

3-7 AN INTERCONTINENTAL RADIO TELESCOPE ARRAY: B. G. Clark and K. I. Kellermann, National Radio Astronomy Observatory, Green Bank, West Virginia; M. H. Cohen, California Institute of Technology, Pasadena, California; G. W. Swenson, University of Illinois, Urbana, Illinois.

An intercontinental network of 8 to 10 antennas is considered as an ultra high resolution array capable of sub milliarcsecond resolution. By using 25 meter antennas, low noise receivers, wide-band instrumentation recorders and hydrogen maser frequency standards, it appears that sufficient sensitivity and phase stability can be obtained to study in detail the compact radio emission associated with a wide range of astrophysical objects. These include the nuclei of galaxies, quasars, stars, pulsars and molecular masers. Such an array offers the opportunity not only for astronomical research with unprecedented angular resolution, but for a variety of geodetic and geophysical experiments as well.

3-8 VERY LONG BASELINE INTERFEROMETRY USING AN EARTH SATELLITE: G. W. Swenson, Jr., University of Illinois, Urbana, Illinois; J. L. Yen, University of Toronto, Toronto, Ontario; N. W. Broten and D. Fort, National Research Council, Ottawa, Ontario; K. I. Kellermann and B. Rayhrer, National Radio Astronomy Observatory, Green Bank, West Virginia; S. H. Knowles, Naval Research Laboratory, Washington D. C.

An experiment in long-baseline interferometry is planned, using the Communication Technology Satellite to transmit the base-band "signal" from one telescope to the other for real-time correlation. A 20 megabit data rate is planned, calling for a delay-line of 10 MHz bandwidth and controllable delay up to 275 milliseconds. A number of sources will be studied on baselines from Ontario to West Virginia and California.

3-9 THE CALTECH - JPL VLBI PROCESSOR: M. S. Ewing, California Institute of Technology, Pasadena, California.

We are developing a correlation and data-processing system for the Mark II VLBI technique. The design allows up to 5 tape records to run simultaneously, providing 32 correlator delay channels for each of up to 10 baselines. Correlator channels may be ganged to provide up to 320 channels on a single baseline. (Three tape recorders are planned initially.) Particular emphasis is placed on the phase accuracy of the lobe rotation process; the specification requires the maximum instantaneous phase error to be less than $10^{-3}$ lobe. The range of lobe rate from 0 to the 4 MHz bit rate is permitted. Delay compensation and time-base correction are provided through dedicated core

memories; delays may be instantly switched over their entire 0 - 16.3 msec range. All logic systems except the Mark II decoders are capable of operation at an 8 MHz bit rate. A DEC GT44 computer programmed with the FORTH system will permit on-line fringe searches as well as sollutions for amplitude, phase, and delay. A modular bus-organized hardware design permits thorough diagnostic checks. Correlations may also be performed on data provided from the computer memory; thus "Mark 0" (24 kHz) and Mark I VLBI computer tapes potentially may be processed at the 8 MHz rate.

3-10 THE MARK III, 100 MBIT/S VLBI SYSTEM: H. F. Hinteregger, Massachusetts Institute for Technology, Westford, Massachusetts.

To permit the use of relatively small (including transportable) antennas in high-precision geodesy, a versatile, wideband data acquisition, tape recording, and processing system is being designed at Haystack Observatory and the Goddard Space Flight Center. This system is being developed as part of the Pacific Plate Motion Experiment, the principal aim of which is to make direct measurements of continental drift using NASA tracking stations as the interferometer elements. The preliminary system design stresses (1) maximum recording and processing rates in excess of 100 Mbit/sec through the use of multitrack instrumentation recorders, and (2) highly flexible high-density digital data formatting. The stress on wide bandwidth is simply for increased sensitivity whereas that on flexible formatting is for several reasons among which are the desires (a) to make the system operate efficiently for a wide variety of advanced VLBI experiments requiring different bandwidths, numbers of frequencies, antennas per site, etc., and (b) to make the specific characteristics of the tape recorders used--the physical number of tracks for instance--as "transparent" to the system as possible, mainly to allow for anticipated large improvements in high-density tape-recording technology.

3-11 DATA REDUCTION TECHNIQUES FOR CYCLE-COUNTING VLBI SYSTEMS: Robert W. King, Air Force Cambridge Research Laboratories, Beford, Massachusetts; Charles C. Counselman, III, and Irwin I. Shapiro, Massachusetts Institute for Technology, Cambridge, Massachusetts.

The continuously-accumulated count of carrier-wave cycles received from a spacecraft at one ground station can simply be subtracted from the count at another station to obtain an interferometric phase observable. If the sampling of the counts is done simultaneously in the coordinate frame of the receiving stations, the sampling is then generally not simultaneous in the transmitter's frame, so that the observable is

sensitive to short-term (several msec) phase variations of the transmitter. However, even very large variations in the transmitted phase or frequency on longer time-scales will have negligible effect on the determination of the position of the transmitter from such observations, provided that the value of the received frequency given by the counting rate of one station is used with approximate a priori knowledge of the Doppler shift to determine the transmitter frequency as a function of time, which is needed to convert from interferometric phase to propagation delay difference. Results will be presented from cycle-counting VLBI observations of the free-running crystal-oscillator transmitters in the Apollo Lunar Surface Experiment Packages.

COMMISSION VI, Session 6

Wednesday, October 16 8:30 am - 12:00 noon
ANTENNAS AND ARRAYS
CHAIRMAN: D. K. Cheng, Syracuse University

6-1 A SIMPLIFIED TECHNIQUE FOR PHASE CONTROL OF CONFORMAL ARRAYS: J. B. L. Rao and J. K. Hsiao, Naval Research Laboratory, Washington, D. C.

One of the most important problems to be overcome in the implementation of conformal arrays is the control of the element phases for beam steering. In this paper, an approximate technique is described which will simplify the hardware and/or software necessary to control the steering phases of conformal arrays on a general surface. The technique is to divide the conformal array into several sub-arrays. Within each sub-array the conventional row-column phase setting can be used by judiciously locating the element on the curved surface. Each sub-array requires an additional phase shift to compensate for the phase difference caused by its position on the curved surface. However, this correction is much simpler than that required for a conventional conformal array in which each element requires this compensation. Due to the nature of the approximate method, there will be some errors introduced into the required steering phases. However, for a given array size, the shape of the conformal surface and the required scanning range, the number of sub-arrays can be chosen such that the phase errors are within a specified limit. Analytical and computed results (phase errors, relative gain and radiation patterns) are obtained for the arrays on circular parabolic curves and on a circular cylinder using the approximate and the exact methods. The results show that in many practical cases the approximate technique described here can be implemented with negligible degradation in array performance.

6-2 EXACT ELEMENT PATTERNS FOR SLOTS ON CONICAL SURFACES: P. C. Bargeliotes, A. T. Villeneuve and W. H. Kummer, Hughes Aircraft Company, Culver City, California.

Exact element patterns of radiating slots on conical surfaces are calculated using general expressions for two potential functions representing the modal fields of apertures on a conducting cone. Pattern calculations have been made by means of appropriate high-speed computer programs written for both components of the fields radiated by half-wavelength circumferential and radial slots on a sharply tipped cone. The analysis and the computer programs are general; complete pattern calculations have been performed for a $10^{o}$ half-angle cone with slots located 6.22 wavelengths from the tip. It has been shown that relatively few modes are required for convergence of the modal series for such slot locations, the number of modes increasing with increasing distance from the tip. The lower order modes

reveal the significance of the tip diffraction, while the higher modes generally contribute to the broadside region of the radiating patterns. Measurements taken at 10.38 GHz for identical slot locations of circumferential and radial slots are in excellent agreement with the calculated patterns. The modal series analysis may also be used in mutual coupling calculations and to verify a pattern synthesis technique that used the equivalence principle.

6-3 INVESTIGATION OF CROSS POLARIZATION LOSSES IN PERIODIC ARRAYS OF LOADED SLOTS: R. J. Luebbers and B. A. Munk, The Ohio State University, Columbus, Ohio.

A periodic array of apertures in a conducting plane can act as a bandpass filter. With proper design the structure will be transparent at its resonant frequency but will have a transmission coefficient below unity at all other frequencies. These periodic surfaces are useful as radomes and in dual frequency antenna feeds. The resonant frequency of such an array may vary with incidence angle. This variation is undersirable for most applications, and can be greatly reduced by reactively loading the slots with the Babinet equivalent of a short circuited two wire transmission line. It has been found, however, that singly loaded slot arrays have transmission loss due to cross polarized radiation when scanned in the H-plane (perpendicular polarization). It is shown that this cross polarized radiation may be eliminated by using symmetrical loaded slots, which have the further advantage of transmitting waves of arbitrary polarization. In conjunction with this investigation, the modal matching method, previously applied only to arrays of rectangular and circular slots, has been extended to the more complicated loaded slot shapes. Both the single loaded and 4-legged symmetrically loaded slots are treated, and good agreement with measured data is obtained.

6-4 REFLECTION PROPERTIES OF TWO LAYER DIPOLE ARRAYS: B. A. Munk and R. J. Luebbers, The Ohio State University, Columbus, Ohio.

The mutual impedance method for determining the reflection from a loaded dipole array is extended to the case of two parallel, planar dipole arrays. The dipole arrays are illuminated by a plane wave with arbitrary incidence angle in either the E- or H-plane. The specular reflection coefficient obtained is shown, with proper design, to have a more narrow stop band with steeper skirts and a flatter top than that for a single array. The near field coupling is included in the analysis, and the criteria for the validity of a simple transmission line solution are given. For close spacing the near fields may cause the reflection coefficient curve to: 1) not reach unity

reflection, 2) attain unity reflection at one frequency, or 3) attain unity reflection at two frequencies, with a shallow dip between. The type of resonance curve obtained depends on the spatial arrangement of the two arrays. The evaluation of the mutual impedance sums is greatly simplified by certain impedance relationships which are presented. Calculated and measured reflection curves for various array separations are included.

6-5 YAGI ANTENNAS FOR BROADBAND OPERATION: Darko Kajfez, University of Mississippi, University, Mississippi.

The nonlinear optimization techniques have been recently applied to Yagi antennas with the objective of improving the directivity, or simultaneously improving both the directivity and reducing the sidelobes at a single frequency. In the work described here, a cost function was found for optimization of an antenna array by simultaneously achieving the flat behavior over the wide range of frequencies. The optimization of a 6-element Yagi antenna resulted in a virtually flat directivity over the bandwidths up to 33%. The lengths of all five passive elements were used as the variables of optimization, while the spacings and radii were kept constant. The sensitivity of the resulting antenna was also investigated showing that the required tolerances on element lengths are of the order of 0.25%.

6-6 ANALYSIS AND DESIGN OF THE LOG-PERIODIC FED YAGI: W. A. Imbriale and G. G. Wong, TRW Systems Group, Redondo Beach, California.

The Yagi functions as a directional antenna having power gain by proper phasing of the director elements as well as proper excitation of these elements by the driven-reflector element interaction. However, its use is limited because of its narrow bandwidth of operation. The Yagi can be broadbanded by utilizing the Log-Periodic Dipole (LPD) antenna to feed the parasitic elements instead of a single dipole. This arrangement gives greater gain than the LPD alone and provides greater bandwidth than the Yagi alone. The method-of-moments is used to analyze this LPD Yagi combination. Sinusoidal basis functions and Galerkin's method are used to provide a fast, efficient program for studying this structure. Design data is presented and comparisons are made between experimental and theoretical data. Examples are shown where the LPD Yagi combination provides greater gain than the LPD antenna alone for an octave bandwidth. In addition, the E- and H-plane beamwidths for the LPD antenna which are generally unequal can be equalized by use of the Log-Periodic-Fed Yagi.

6-7 A VARIABLE-BEAMWIDTH LONG WIRE ANTENNA: G. G. Wong, TRW Systems Group, Redondo Beach, California.

A novel design for obtaining variable-beamwidth performance from a long wire structure is presented. The design may be very useful as a communication antenna for various missions involving variable-beamwidth requirement. Variations from relatively wide beams to narrow beams can be achieved. For a single structure, a beamwidth of $113^{o}$ to $18^{o}$ was obtained at L-band. To vary the beamwidth of the radiator, it is only necessary to vary the positions of the short-circuits so as to change the number of active elements in the radiator. This is accomplished by activating a pair of symmetrically located diode switches at some position between $\pm$Nth and $\pm$(N+1)th elements, where (2N+1) is the desired number of active elements in the long wire antenna. Experimental test results for demonstrating validity of the concept will be shown; matrix solutions for analyzing the long wire structure will be discussed.

6-8 PHYSICAL LIMITATIONS ON INTERFERENCE REDUCTION BY ANTENNA PATTERN SHAPING: J. T. Mayhan and L. J. Ricardi, Massachusetts Institute of Technology, Lexington, Massachusetts.

We address the problem of nulling out an interfering noise source by appropriately modifying the antenna radiation pattern. We consider two complementary, one-dimensional antenna structures, i.e., a circumferentially symmetric line source of length a, and an axially independent cylindrical antenna of antenna of radius $\rho_o$. We consider first the case of N discrete noise sources and compute the loss in antenna directivity (and subsequent loss in signal/noise ratio) when the radiation pattern is modified so as to place a null at each angular position of the interfering noise source. The results indicate that if all noise sources are outside the main beam, the loss in directivity is negligible. When one or more noise sources are in the main beam, the antenna directivity can be reduced appreciably. It is shown that when uniformly distributed noise is superimposed over the discrete noise, the same antenna pattern maximizes the signal/noise ratio for those practical cases when the discrete noise source power is significantly greater than the uniformly distributed noise source.

6-9 NUMERICAL SOLUTION FOR THE COUPLING BETWEEN TWO SECTORAL HORNS: M. F. Iskander and M. A. K. Hamid, University of Manitoba, Winnipeg, Canada.

The total field in a sectoral electromagnetic horn excited by another sectoral horn of arbitrary size and orientation is found from a numerical solution of an integral equation for the induced current in the receiving horn. The induced current due

to the initially incident wave from the transmitting horn is computed and corrected successively to take into account the effect of multiple scattered waves which are particularly relevant for near field interaction.

Since the sharp edges of the two horns create the singularities of the induced currents, we employ a transformation which maps the cross sectional contour of the horns onto circles on which the induced currents are finite. This leads to a non-singular integral equation for the induced currents which is solved by the method of moments with various testing functions. Graphical results for the induced current and electric field distribution in the receiving horn are presented to illustrate the gain variation with broadside separation distance as a result of near field coupling.

COMMISSION VI, Session 7

Wednesday, October 16 8:30 am - 12:00 noon
INTERACTION OF EM WAVES WITH BIOLOGICAL MATERIALS AND OTHER PENETRABLE STRUCTURES
CHAIRMAN: Curtis C. Johnson, University of Utah

7-1 LONG WAVELENGTH ANALYSIS OF PLANEWAVE ELECTROMAGNETIC POWER ABSORPTION BY A PROLATE SPHEROIDAL TISSUE BODY: Carl H. Durney, Curtis C. Johnson, Habib Massoudi, University of Utah, Salt Lake City, Utah.

In the investigation of possible health hazards resulting from the absorption of electromagnetic radiation by the human body, there is a pressing need for a theoretical analysis which would provide the details of internal power absorption and total power that are required in order to predict hazards to man on the basis of animal and tissue experiments. Analyses carried out by several researchers using a sphere as a model of the human body have provided valuable information and indications that the absorbed power in man will vary greatly with frequency. This paper describes an analysis using a better model, a prolate spheroid, to represent the human body, animals, or cells. Since a general field solution is very difficult, a perturbation theory that is valid when the wavelength is long compared to the length of the spheroid has been used. The method of analysis and the results are described. There are dramatic changes in total and peak power absorption in the spheroid as a function of frequency, size, and orientation in the incident planewave. A physical explanation for the strong dependence of absorbed power on orientation of the spheroid with respect to the incident planewave is given. The theoretical results have been compared with preliminary measurements made by others and good agreement was obtained.

7-2 ELECTROMAGNETIC FIELDS IN A HOMOGENEOUS MODEL OF MAN: Peter W. Barber, University of Utah, Salt Lake City, Utah.

The Extended Boundary Condition Method which previously has been used to solve a wide variety of electromagnetic scattering problems is applied here to the calculation of the internal fields in a prolate spheroid which has been illuminated by a plane electromagnetic wave. The electrical parameters of the spheroid have been chosen to approximate the physical characteristics of the human body. Specifically, the man model consists of a homogeneous distribution of muscle tissue. The problem is solved in a spherical basis, which results in a set of equations for the coefficients of expansion of the internal field in terms of the incident field coefficients. The solution of the system of equations requires evaluation of a set of integrals over the surface of the spheroid and subsequently a matrix inversion. Once the coefficients of the internal field

expansions are obtained, the fields are calculated throughout the interior volume. The internal power density is calculated for different characterisitics of the model and for various orientations of the incident field. This technique can also be used to calculate the power desposition in small animal models. This capability to make calculations for both man-sized bodies and small animals will make it possible to extrapolate data obtained from animal experiments to man's body configuration. This will be useful in the determination of an electromagnetic radiation safety level and should also have application to medical use in diagnostics and therapy. The technique developed here can also be used to compute internal power density levels for in vitro tissue preparations.

7-3 INTEGRAL EQUATION SOLUTION FOR FIELDS IN ARBITRARY CYLINDERS OF BIOLOGICAL TISSUE: L.L. Tsai and T. K. Wu, University of Mississippi, University, Mississippi.

Biological hazards of microwave radiation is an area of current concern. Analytical predictions of electromagnetic field penetration in biological tissues have so far been rather limited. For realistic models with arbitrary contours, the versatility of moment method solutions of integral equations should prove to be advantageous. The geometry of the problem consists of arbitrarily contoured cylinders of biological tissue illuminated by a TM plane wave. The method entails first the derivation of appropriate surface integral equations using the Helmholtz equation, Green's theorem and boundary conditions. The solution for the surface fields then employs pulse expansion and point matching. Once the surface fields are found the fields everywhere interior to the cylinder may readily be determined as well. It should be noted that because surface fields are the unknowns, rather than fields throughout the interior if the volume equivalence principle is used, a much smaller, and thus tractable, matrix size is needed. To test the validity of the method, homogeneous circular cylinders of the muscle or fatty tissue are first studied. The surface fields thus computed by integral equation methods show excellent agreement with exact eigenfunction expansion results. Surface fields on homogeneous elliptical cylinders are next obtained to illustrate the arbitrary geometry capabilities of the integral equation solution. For a more complex structure, i.e., a multi-layered composite cylinder of circular cross section, the comparison between the numerical solution and the exact solution again shows excellent agreement. The extension in this case next consists of a model for an arm of elliptical cross section with a circular bone in the center. Field plots throughout the interior for the above models are also obtained, and they hopefully may aid in diagnostics of hazards from so-called "hot spots".

7-4 A COMPARISON OF ELECTRICALLY SHORT, BARE AND INSULATED PROBES FOR MEASURING THE LOCAL RADIO FREQUENCY ELECTRIC FIELD IN BIOLOGICAL SYSTEMS: G. S. Smith, Harvard University, Cambridge, Massachusetts and Northeastern University, Boston, Massachusetts.

Current interest in the effects of monionizing electromagnetic radiation on biological systems has created a need for accurate methods of measuring the local electric field internal to biological specimens. Field strengths at interior points of a biological body in general cannot be accurately determined from a simple measurement of the field external to the body and, therefore, electric field probes must be inserted directly into the body. The biological specimens studied are usually spatially inhomogeneous in the sense that the electrical constitutive parameters ($\sigma_e$,$\varepsilon_e$) of the specimens are not uniform throughout. Ideally a probe is needed that will measure the electric field strength at different points in the specimen in a manner that is independent of the local constitutive parameters. The response from the probe, i.e., the voltage V, should be proportional to the magnitude of the electric field $|\bar{E}|$ and the proportionality constant $K_e$ should be independent of the constitutive parameters of the surrounding medium. A probe with this kind of response would eliminate the need for dissecting a specimen to determine the constitutive parameters at each point where the probe was inserted. The probe could be calibrated absolutely by measuring a known field in one medium. The electrically short antenna is attractive for this application since its small physical size allows high spatial resolution with a minimum field perturbation. In this paper the properties of the electrically short, bare, electric field probe in a dissipative medium are reviewed and a simple description is given of the operation of the same probe when enclosed in a concentric, insulating sheath. The conditions that must be satisfied to make each of the probes have an electric field response that is independent of the constitutive parameters of the surrounding tissue are described. Measured input admittances and received voltages for both types of probes are compared with those predicted by the respective theories. The measurements were made with the probes immersed in a succession of liquids with dielectric properties in a range similar to that of biological tissues at radio frequencies.

7-5 DECREASE IN FERTILITY OF CHICKENS CONTINUOUSLY EXPOSED TO LOW LEVEL ELECTROMAGNETIC FIELDS: A. J. Giarola, W. F. Krueger and A. Shrekenhamer, Texas A&M University, College Station, Texas.

A very large decrease in fertility was noted when cocks and hens, kept in metal cages, were continuously exposed to various electromagnetic fields. Six groups, each consisted of four hens

and one cock were used. One was the control group and the other five were exposed to the following fields: Group 1: f = 260 MHz, $E^2/\eta$ = 2.5 W/m$^2$; Group 2: f = 915 MHz, $E^2/\eta$ = 2.5 W/m$^2$; Group 3: f = 2.435 GHz, $E^2/\eta$ = 2.5 W/m$^2$; Group 4: f = 60 Hz, E = 95 V/m; Group 5: f = 60 Hz, B = 1.4 G. Cage design for the control was similar to that of the exposed groups. The control cage was carefully positioned with respect to the electromagnetic fields to obtain a zero field environment inside the cage. All environmental factors (light, feed, water, air movement, humidity and ambient room temperature) were as identical as possible. Eggs collected were set in an incubator and the results from four hatchings, expressed in eggs fertile/eggs set are as follows: Control = 196/196; Group 1 = 48/211; Group 2 = 161/212; Group 3 = 110/197; Group 4 = 186/209; Group 5 = 97/213. These results differ substantially from our previous two experiments in which no significant effect on fertility was noted. This difference can be attributed to the different line of cock used in this third experiment.

7-6 ELECTROMAGNETIC FIELD PENETRATION THROUGH IMPERFECTLY CONDUCTING GASKETS: Thomas H. Shumpert, Auburn University, Auburn, Alabama.

Electromagnetic shielding problems become more and more important with the ever increasing need to protect certain field-sensitive devices from damage or malfunction due to high-intensity electromagnetic pulses. Often shielding around equipment enclosure access ports such as doors, hatches, or joints is provided by means of conducting gaskets. It is the purpose of this paper to present an analysis for quantitatively predicting the electromagnetic fields which penetrate one of these gasketed ports. In particular an attempt is made to model an annular joint with appropriate gasket and to predict the field penetration through this gasket configuration. The regions interior and exterior to the gasket are modeled as good conductors, and the gasket itself is modeled as an imperfect dielectric with high conductivity. Direct diffusion through the good conductors and induced current in the gasket are considered as the primary field penetration mechanisms. Quantitative results are presented in the form of equations and graphs of the penetrated fields.

7-7 THE EFFECT OF A DIELECTRIC JACKET ON COAXIAL-CABLE SHIELDING: K. F. Casey, Kansas State University, Manhattan, Kansas.

When a coaxial cable with a braided-wire shield is immersed in an electromagnetic field, energy can couple from the exterior to the interior of the cable by diffusion through the shield conductors or penetration of the apertures in the shield. The

latter coupling mechanism is affected by the presence of a dielectric jacket around the shield. To study its effect on the cable shielding, a simple shield model, for which the dominant coupling mechanism is aperture penetration, is considered. The model comprises a pair of M-filar counterwound filamentary helices, which may be imperfectly conducting, surrounded by a possibly lossy dielectric layer. It is shown that the cable's shunt admittance per unit length and capacitive coupling coefficient per unit length are each dependent upon the thickness and permittivity of the layer, while the series impedance per unit length and the transfer impedance per unit length are independent of the layer parameters. Numerical data are presented to illustrate the dependence of the transmission-line parameters on the optical coverage and conductivity of the shield and the thickness and permittivity of the outer dielectric layer. It is found that if the dielectric layer is sufficiently lossy, the capacitive coupling coefficient vanishes; however, this does not necessarily minimize the induced current and voltage on the cable, when it is illuminated by an incident plane wave.

7-8 A CYLINDRICAL MODEL FOR SMALL-APERTURE COUPLING OF ELECTROMAGNETIC POWER INTO INTERIOR CIRCUITRY: S. Sandness and C. Johnk, University of Colorado, Boulder, Colorado.

Many missile or rocket configurations employ in their metallic skins unavoidable slits or apertures that may couple varying amounts of power from exterior electromagnetic sources into the interior circuitry. A model simulating one such configuration has been built to test electromagnetic couplings obtained for various apertures against existing theories, and to investigate detection methods for such leakage fields. Worst-case conditions are simulated by use of a tunable interior circuitry, consisting of a coaxial or eccentric wire terminated in a suitable detector. One detection scheme investigated involves a conversion to a light output which is brought out of the missile through optic fibers, in an effort to inhibit the additional electromagnetic coupling through the detected-output aperture. Experiments employed a high-power cw source at 200 MHz, with the radiation incident at various angles ranging from normal to grazing. The aperture configuration was made variable through the use of an interchangeable cylindrical section; and the results verified satisfactorily the dependence of the detected output on the aperture coupling and interior circuitry employed.

7-9 TRANSIENT ELECTROMAGNETIC PENETRATION OF A SPHERICAL SHELL:
D. G. Dudley and J. P. Quintenz, University of Arizona, Tucson, Arizona.

The transient penetration of an electromagnetic plane wave into a cavity formed by an imperfectly conducting spherical shell is considered. The transient response is obtained by numerical Fourier inversion of the vector multipole representations of the cavity fields. Previous transient results have been obtained only at the cavity center where the field representations degenerate to a single term. Numerical results for other more general locations indicate that the transient fields at the center are poor indicators of the shielding effectiveness of the shell.

COMMISSION VI - JOINT WITH COMMISSION VIII (See Page 116)

Wednesday, October 16 8:30 am - 12:00 noon

NOISE AND RADIO SYSTEM PERFORMANCE MODELS

CHAIRMAN: M. Nesenbergs, Institute for Telecommunication Sciences, Boulder, Colorado

COMMISSION VIII, Session 3; Joint With COMMISSION VI

Wednesday, October 16 8:30 am - 12:00 noon
NOISE AND RADIO SYSTEM PERFORMANCE MODELS
CHAIRMAN: Martin Nesenbergs, Institute for Telecommunication Sciences

3-1 AN ATMOSPHERIC NOISE MODEL WITH APPLICATION TO LOW FREQUENCY NAVIGATION SYSTEMS: D. A. Feldman, Department of Transportation, Wildwood, New Jersey.

A prerequisite for the design of low frequency radio receivers is a model for low frequency atmospheric radio noise that encompasses the non-Gaussian nature of the actual noise process and is sufficiently tractable to enable performance analysis and optimization of receiver designs. This work describes a new model for atmospheric noise waveforms observed at the output of the antenna bandlimiting filter. This model, which is based on statistical analysis of sample records of these waveforms, is used to analyze the performance of typical radio navigation receivers and to determine near optimum receiver performance. The analysis is verified by simulating the receiver structure and testing the receiver with the actual noise sample records.

3-2 APPLICATION OF THE HALL MODEL TO THE HIGH FREQUENCY ATMOSPHERIC RADIO NOISE CHANNEL: Gary Brown, Naval Electronics Laboratory Center, San Diego, California.

The problem investigated was the application of a model to describe the first and second order statistical characteristics of atmospheric radio frequency noise in the region around 10 MHz. The development started with a model that had been previously verified for the low and medium frequency region (around 100 kHz) as a good characterization for atmospheric noise. The analysis for this "Hall" model was updated by supplying a justification based upon the physical considerations of high frequency propagation. A multivariate Gaussian distribution was assumed to represent the spatial distribution of noise sources about the receiver, with a simple inverse square path loss. The analysis showed that the model could be extended to cover the high frequency region by correctly adjusting one parameter. The model predictions of the noise envelope cumulative amplitude distribution function and level crossing interval distributions were compared to five samples of data recorded at San Diego, California between October, 1972 and March, 1973. The analysis verified that the model provided a good representation of high frequency atmospheric noise characteristics.

3-3 STATISTICAL-PHYSICAL MODELS OF MAN-MADE RADIO NOISE: FIRST-ORDER PROBABILITY STRUCTURES: David Middleton, Institute for Telecommunication Sciences, Boulder, Colorado.

A general statistical-physical model of man-made radio noise (i. e., interference) processes appearing in the input stages of a typical receiver is developed analytically. The first-order statistics of these random processes are generated in detail for both narrow- and broad-band reception, including an additive mixture of a gauss background noise and impulsively emitting sources. Attention is given to the basic waveforms of the emissions, including such geometric factors as the beam patterns of source and receiver, mutual location, doppler, far-field conditions, the physical density of the sources, and the propagation law governing the emissions.

Two principal classes of interference are distinguished: Class A noise, where the bandwidth is comparable to or less than that of the receiver; Class B noise, where the bandwidth is (usually much) larger than that of the receiver. "Intelligent" communications are examples of Class A, often, while automotive emissions (non-"intelligent") are an important example of Class B, which includes also such natural phenomena as atmospheric noise.

For Class A noise, the first-order results are highly canonical: the form of the p.d.'s and p.D.'s is only weakly sensitive to source density and emission law. For Class B interference, however, the statistics are much more strongly influenced by the combined geometric factors of the propagation law and source density. Both classes remain canonical with respect to signal waveform, receiver response, beam patterns and doppler. Finally, excellent agreement of our model with experimental observations is found for both classes of interference.

3-4 OPTIMUM RECEPTION IN AN IMPULSIVE INTERFERENCE ENVIRONMENT: A. D. Spaulding, Institute for Telecommunication Sciences, Boulder, Colorado.

The statistical-physical model of impulsive interference recently devloped by D. Middleton is applied to a class of optimum signal detection problems. Optimum detection algorithms are given for coherent and incoherent binary detection. The three basic digital signaling waveforms are considered, i.e., antipodal, orthogonal, and ON-OFF keying. Performance bounds are obtained for these signaling situations. General performance results are given for coherent detection, while performance results for both the weak signal and strong signal cases are obtained for incoherent detection. Since it has been shown that

in order to gain significant improvement over current receivers, the number of independent samples of the received waveform must be large, the results are given parametrically in the number of samples, or equivalently, the time-bandwidth product. Performance of the current sub-optimum receivers is also shown for comparison. Also treated, is the optimum interference discrimination detection problem.

3-5 DEGRADATION OF BASE STATION RECEPTION AT VHF AND UHF: Jules Deitz, Federal Communications Commission, Washington, D. C.

Last summer a report (FCC No. R-7302) was made to URSI which described the combined degradation effects of man-made noise and multipath propagation on mobile reception. Currently we are investigating, in the natural environment, the degradation of base station reception due to automotive ignition systems and multipath propagation. We are attempting to separate the two effects quantitatively since each requires different treatment when relief is needed. Observations are being made at 37.5, 87.154, 450 and 950 MHz. Some attempt is being made to identify those types of vehicles that are observed to be potent radiators. A progress report will be given which describes observation methods and the results so far obtained.

3-6 COMMUNICABILITY/COMPATIBILITY ANALYSIS METHODOLOGY OF A MOBILE AUTOMATIC RADIO SYSTEM: James Mazur, Lockheed Electronics Company, Incorporated, Tucson, Arizona.

This paper describes the communicability/compatibility analysis methodology for a division-size deployment of a Mobile Automatic Radio Telephone System (MARTS). This system provides telephone-type dial-up service to army division-level subscribers via radio links. Furthermore, the radio is frequency and power adaptive. This means that at the initiation of the call, the system automatically selects a clear frequency and adjusts to the minimum power required to provide a threshold signal-to-noise ratio. In addition, there is an automatic relay capability to extend the range of a call. The Army-supplied test bed conforms with the latest DA approved doctrine for divisions and the echelons above division (EAD), and defines the tactical and C-E environment. The performance criteria used in the analysis is the ratio of the average number of simultaneous calls which the system is capable of handling to the required average number of calls as specified by the concept. This is limited by the intrasystem compatibility. The objective of the methodology is to calculate the former. The average number of simultaneous calls for any size MARTS is dependent on the frequency availability and the geographic deployment. The first variable is complicated by the fact that a MARTS operates in

three modes, each of which requires a different frequency resource. These modes are primarily link-range dependent so that some method of factoring in the deployment is necessary. Briefly, the probability density function of the link range is constructed from the deployment. Then the probability of a link being handled by modes 1, 2, and 3 is calculated. By combining the probability of a link range by the probability of its mode, the proportion of the total links handled by each mode is calculated. The frequency reuse for each mode is then calculated statistically. Given the frequency allocation, these latter quantities are sufficient to determine the average number of calls which can be handled by each mode of operation.

3-7 THE ROLE OF NOISE IN "SELF"-ORGANIZING SYSTEMS: John S. Nicolis, University of Patras, Patras, Greece.

This paper deals with information transfer from the environment and "self"-organization in open, nonlinear systems far from thermodynamic equilibrium--in the presence of either non-stationary phase jitter noise, or amplitude stationary noise. By "self"-organization we mean here the progressive formation within the system of sequential ordered (coherent) relationships between appropriate dynamical variables--like for example, the phase difference between the oscillation components of the system. We take up first the classical Laser as a specific example and examine in detail the influence of phase jitter noise in the mode (phase) locking process. We find--as expected--that phase fluctuations in the cavity cause degradation of the coherent behavior (i.e., increase the entropy) of the system--which, however, levels off,-or saturates with time.

Further we examine systems where the number of self-sustained oscillating components may vary with time in such a way that the maximum entropy of the system increases faster than the overall instantaneous entropy. We put forth the hypothesis that in such cases--because of the increase of the redundancy--the system gets organized not just in spite of, but merely because of the presence of Noise. Possible applications in biological systems (especially concerning a model of cerebral organization) are briefly discussed.

COMMISSION I, Session 4; Joint With COMMISSION VI

Wednesday, October 16 1:30 pm - 5:00 pm
ANTENNA MEASUREMENTS
CHAIRMAN: Paul E. Mayes, University of Illinois

4-1 TWO METHODS FOR THE MEASUREMENT OF ANTENNA EFFICIENCY: E. H. Newman, P. Bohley, C. H. Walter, The Ohio State University, Columbus, Ohio.

Two methods for measuring antenna efficiency are described. The principal advantage of both methods is that they can be quickly and easily applied. The first method, referred to as the Wheeler method, determines the antenna efficiency by comparing the input resistance of the antenna radiating in free space to its input resistance radiating in a cavity with highly conducting walls. The second method, referred to as the Q method, determines the antenna efficiency by comparing the bandwidth of the actual antenna to the bandwidth of an antenna which is identical except that it has zero losses. Both methods relate the antenna efficiency to the input impedance rather than a far-field pattern integration. Thus, the methods are applicable at VHF frequencies and below where the design of an antenna range or anechoic chamber becomes increasingly difficult and expensive. The two methods are used to find the efficiency of electrically small multiturn loop antennas.

4-2 EFFECTIVE HEIGHT CALIBRATION OF VLF ANTENNAS USING RECIPROCITY RELATIONS: J. E. Lindsay, Jr., University of Wyoming, Laramie, Wyoming; and D. E. Rugg, University of Denver, Denver, Colorado.

A measurement scheme is presented where effective height calibration of two identical VLF antennas can be made by measuring basic quantities such as open circuit voltage, antenna base current and antenna separation distance.

The measurement scheme is based upon the reciprocity theorem. In this paper this theorem is reviewed. Its application (with appropriate limitations) to the calibration of VLF E-field sensing antennas is discussed.

An experimental verification of the method with comparisons to other measurements is made. These measurements were made over a range of 5 to 21 kHz. Sources of noise and measurement errors are also discussed.

4-3 APPLICATION OF AN AUTOMATIC NETWORK ANALYZER SYSTEM TO THE MEASUREMENT OF INDUCED RESPONSES OF ANTENNAS OVER GROUND: Werner J. Stark, Harry Diamond Laboratories, Washington, D.C.

An automatic network analyzer system is used in conjunction with a CW transmitting facility to measure the response of several

linear antennas to incident electromagnetic waves in the frequency range of 1.5 MHz to 110 MHz. The response is measured to both vertical and horizontal polarization using four types of transmit antennas. The frequency points and type of transmit antenna are under program control and the measurements of phase and amplitude are recorded in digital form on cassette tapes for subsequent analysis using an on-line computer. The purpose of these measurements is to determine the response of the antennas to an incident electromagnetic pulse containing frequency components in the above frequency range. The degree of accuracy of this technique is determined by comparing the measured transient response with the computed transient response based on CW measurements and data for the transient incident field.

4-4 A WIDEBAND DIRECTIONAL INSTRUMENT ANTENNA: J. E. Lindsay, Jr., University of Wyoming, Laramie, Wyoming.

There are numerous instrumentation applications where wideband electromagnetic sensors are required. Many of the so-called wideband antenna arrays, such as the log-periodic array, are not true wideband transient antennas, since their effective length and phase characteristics are functions of frequency.

The term "wideband instrument antenna" in this paper is applied to a linear receiving antenna whose open circuit output voltage is a direct measure of electric field strength over a specified range of frequencies. More explicitly, the directional E-field sensor under discussion is a wideband frequency independent antenna in the following sense:

1) It will have a directional pattern with a well-defined major lobe. A signal received along the center line of the major lobe will produce an output voltage proportional to the strength of the incoming E-field and be independent of frequency.
2) Signals received at any direction other than along the center line of the main lobe will be attenuated (relative to the main lobe). The resultant output voltages due to these signals will obviously be frequency dependent.

The directive instrument array is formed from frequency independent elements which are placed in an end-fire configuration along a staggered transmission line. This paper will present the required variation in transmission line properties and means of obtaining the frequency independent operating properties, as defined above in (i). An example of an array usable over the frequency range of 2 to 20 MHz will be given.

4-5 ELECTROMAGNETIC PROBING WITH ANTENNAS IN RECTANGULAR WAVEGUIDE: C. E. Grove, M. Siegel, and D. Nyquist, Michigan State University, East Lansing, Michigan.

An experimental and theoretical investigation is made of the use of linear antennas to measure the constituitive electrical properties of a general, linear, homogeneous, isotropic medium filling a rectangular waveguide. The theoretical model considers N antennas in any size rectangular waveguide having arbitrary terminations. From the general theory, results are obtained which relate the antenna charge and current distribution and terminal impedance parameters to the macroscopic electrical parameters of the medium surrounding the antenna in the waveguide. For purposes of verifying the theory the emphasis is primarily placed on the special case of a rectangular cavity, for which an experimental system was developed. Experimental measurements of current distribution and input impedance for both single and coupled antennas over a wide range of frequencies in the L-band show excellent agreement with the numerical solution. The strong coupling between the antennas and the cavity is evidenced in the unusual behavior of the current distribution and impedance as a function of frequency. It is shown that the often used cosinusoidal distribution function for the current is incorrect for this system. It is also found that the presence of the waveguide boundaries enhances the sensitivity of the antennas to the properties of the medium, so that realistic application of such a system is possible as a continuous flow through monitor of pollution in streams, smokestacks or other effluent systems.

4-6 NEAR-FIELD MEASUREMENTS OF ANTENNAS AND ELECTROACOUSTIC TRANSDUCERS: A GENERAL TREATMENT: Paul F. Wacker, National Bureau of Standards, Boulder, Colorado.

A new formulation of near-field measurements with probe correction includes known treatments (planar, cylindrical, spherical) as special cases, applies to both electromagnetic and linearized acoustic problems, makes available the mathematics of group representations (symmetry) for efficient data reduction, makes analysis for new measurement surfaces straight-forward, and shows that major parts of existing treatments apply to inhomogeneous, anisotropic, lossy media. In a mathematically linear system, let $a_o$ and $b_o'$ be complex traveling wave amplitudes fed to the transmitting antenna (or electroacoustic transducer) and received by the receiving antenna respectively and let $T_M$ and $R_M'$ be the respective radiating and recieving patterns in terms of complex modal coefficients referred to coordinates fixed in the given antenna, where M and M' are modal indices. Then neglecting multiple reflections, $b_o'(R) = \Sigma_M \Sigma_{M'} R_{M'}' G_{M'M}(R) T_M a_o$

where R transforms the primed into the unprimed coordinates. If the transformations (R) form a group and M' and M belong to irreducible representations n' and n and to rows m' and m respectively, then $G_{M'M}(R) = D^{(n)}_{m'm}(R)\ \delta_{n'n}$, where $D^{(n)}_{m'm}(R)$ is the representation coefficient of the group and $\delta_{n'n}$ is the Kronecker delta. Ordinarily, the $b'_o(R)$'s and properties of the probe ($R'_{M'}$ or $T_M$) are known and thousands of simultaneous equations are solved for the properties of the test antenna ($T_M$ or $R'_{M'}$). Symmetry permits decoupling of the equations, namely $\int b'_o(R)\ D^{(n)}_{m'm}(R)^*\ \rho(R)\ dR = \Sigma_M \Sigma_{M'} T_M R'_M\ a_o$ where * indicates complex conjugate $\rho(R)$ is known, and the sums are now restricted to modes M and M' belonging to representation n and rows m and m' respectively. For the acoustics of fluids decoupling is complete but for antennas the equation yields sets of two equations in two unknowns (polarization). Further, this explains the use of the Fourier transform for planar scanning and the Fourier transform-Fourier series decomposition for the cylindrical case and forms the basis for the author's new efficient data-reduction technique for spherical scanning. In each case processing is fast due to the use of the Fast Fourier Transform, coupled with matrix multiplication in the spherical case.

COMMISSION II, Session 6

Wednesday, October 16 1:30 pm - 5:00 pm

OPEN FORUM - FUTURE OF RADIO OCEANOGRAPHY

CHAIRMAN: Bradford R. Bean, National Oceanic and Atmospheric Administration, Boulder, Colorado

COMMISSION II - JOINT WITH COMMISSION VI (See Page 135)

Wednesday, October 16 1:30 pm - 5:00 pm

PROPAGATION IN RANDOM AND STRATIFIED MEDIA

CHAIRMAN: A. Ishimaru, University of Washington, Seattle, Washington

## COMMISSION III, Session 5

Wednesday, October 16 1:30 pm - 5:00 pm
IONOSPHERIC HEATING: II
CHAIRMAN: G. Meltz, Raytheon Co., Sudbury, Massachusetts

5-1 A SIMPLE MODEL FOR MONOSTATIC AND BISTATIC FIELD-ALIGNED SCATTER FROM AN ARTIFICIALLY HEATED F LAYER: S. A. Bowhill and E. K. Walton, Aeronomy Corporation, Champaign, Illinois.

A simple model is described for field-aligned scatter (FAS) at VHF and UHF produced by artificial heating of the F-layer. It is used to demonstrate: (1) The variation of scatter range with heater reflection height. (2) The effects of heater beam steering on scatter cross sections and (3) The choice of bistatic geometry to maximize the scattering cross sections.

5-2 CROSS SECTION CALCULATIONS FOR ASPECT-SENSITIVE RADIO-FREQUENCY SCATTERING FROM A HEATED IONOSPHERIC VOLUME: J. Minkoff, Riverside Research Institute, New York, New York.

Measurement of per-unit-volume properties of aspect-sensitive scattering media requires knowledge of the size of the effective scattering volume. This however is in general an unknown quantity since it requires quantitative information concerning the degree of the aspect sensitivity, or, equivalently, of the length of the field-aligned scattering structures, which may not be possible to obtain; the identical problem exists in radar-auroral measurements. This problem is considered, for which it is shown that, under certain assumptions regarding the parameters of the measurement system, a generalized radar equation can be derived in which the per-unit-volume quantities of interest are expressed in terms of the received power independently of the aspect sensitivity. The results are applied to calculating from experimental data the per-unit-volume scattering properties of a heated ionospheric volume as a function of frequency, from which a transverse scale size for the scattering medium of 3 m is estimated. For these experiments, under maximum heating conditions, a representative value of 1% for the rms fractional electron-density deviation is calculated; an upper bound is also established showing that values as large as 4 or 5 percent were probably never achieved. It is shown that, for an electron-density distribution axially symmetric with respect to the geomagnetic field, $\vec{B}$, the cross section for backscatter within a plane containing $\vec{B}$ uniquely determines the cross section for bistatic scattering axially around $\vec{B}$. Experimental results for small axial-bistatic angles are presented showing good agreement between calculated and measured values.

5-3 OBSERVATIONS OF INDUCED FIELD-ALIGNED IRREGULARITIES IN THE E-REGION: V. R. Frank, Stanford Research Institute, Menlo Park, California.

VHF scattering was observed from field-aligned irregularities in the E-region. The irregularities were produced by and over the ITS ionospheric modification facility at Platteville, Colorado. The echoes were observed during the daytime when the modifier transmitter operated at frequencies between 2.85 and 3.15 MHz; ordinary-ray reflection heights were between 100 and 160 km. The observations indicated a maximum scattering-region diameter of 100 km at E-region heights, and a thickness under 10 km. Radar cross sections as high as 65 dBsm were observed at frequencies between 25 and 100 MHz, and some echoes were observed between 14 and 200 MHz.

5-4 MODIFICATION OF THE LOWER IONOSPHERE BY HIGH POWER HF TRANSMISSIONS: L. Holway, Raytheon Research Division, Waltham, Massachusetts; G. Meltz, Raytheon Equipment Division, Sudbury, Massachusetts.

Numerical solutions, based on model ionospheres irradiated by HF energies comparable to those transmitted by the Platteville Ionospheric Modification Facility have been calculated for the three coupled differential equations describing the Poynting flux S, the electron temperature $T_e$, and the electron density, $N_e$. The results verify that $T_e$ increases rapidly (by a factor on the order of 4 when S varies by ± 25%) as soon as S exceeds the critical flux $S_c \approx .25 f_e^2$, where $f_e$ is the effective frequency in MHz and $S_c$ is in $\mu w/m^2$. The absorption for a 5 MHz ordinary wave passing through the lower ionosphere is only increased by 2.3 dB for 100 Mw ERP but this goes up to 8.1 dB for 800 Mw ERP. Many results are sensitive to the electron profile: for example, an X mode heater at 3.15 MHz does considerable heating at altitudes where $\omega < \nu$ for a 2.667 MHz X-diagnostic. As a result, absorption decreases for a noontime profile, although, with a 3 p.m. profile, the heater energy reaches higher altitudes and the absorption increases. If the heater is turned off after about ten minutes operation, an increased absorption is observed which requires another ten minutes to decay. This is consistent with published recombination rates for water-cluster ions, and our calculated increases in $T_e$ near 70 km. The frequencies and radiated powers for these calculations have been chosen to facilitate comparison with experiment.

5-5 SELF-HEATING OF THE PARTIAL REFLECTION EXPERIMENT: William A. Kissick, Illinois Institute of Technology Research Institute, Annapolis, Maryland.

Recent improvements in the D-region partial reflection experiment include higher power transmitters and higher gain antennas, both

of which contribute to an increased effective radiated power. It is well-known from artificial ionospheric heating experiments that high radiated powers can modify the ionosphere in the form of an increase in electron collision frequency; hence, the partial reflection experiment is susceptible to self-perturbation. This paper presents; first, a theoretical examination of this self-heating effect based on a volume model of partial reflections and, second, actual observations of the effects of power on the data of the partial reflection experiment.

5-6 SUGGESTIONS FOR FUTURE RESEARCH IN HF IONOSPHERIC MODIFICATION: L. E. Sweeney, Jr., Stanford Research Institute, Menlo Park, California.

This paper summarizes suggestions for future research in the modification of the ionosphere by high-powered HF radio waves. The research areas discussed include both theoretical and experimental work to: (1) better define and explain known phenomena, (2) verify the existence and establish the properties of effects that have been tentatively observed, (3) discover new effects, and (4) develop applications of known phenomena to science and engineering.

## COMMISSION V, Session 4

Wednesday, October 16 1:30 pm - 5:00 pm
TECHNIQUES, RECEIVERS, ANTENNAS
CHAIRMAN: K. I. Kellermann, National Radio Astronomy Observatory

4-1 SUPERCONDUCTING LOW NOISE RECEIVERS FOR RADIO ASTRONOMY: Arnold H. Silver, the Aerospace Corporation, El Segundo, California.

A new class of cooled low-noise receivers is being developed which apply to Josephson and other electron tunneling phenomena occurring in superconducting materials. This development promises centimeter- and millimeter-wave receivers for radio astronomy which have noise temperatures as low as $20^{o}$ K, up to a 2 GHz bandwidth, and are easily tunable over the entire waveguide band. This will be a major advance in receiver sensitivity--especially at the millimeter wavelengths. The first stage of the receiver will be a superconducting/Schottky mixer which will down-convert the signal to a 1 GHz IF frequency. Preliminary measurements have shown that this conversion adds very little noise and will only require $\sim 10^{-8}$ watts of local oscillator power. This small L.O. power requirement is especially important for wavelengths shorter than 3 millimeters since it will be possible to use a Josephson junction phase-locked multiplier local oscillator in the system. The second, third and fourth stages of the receiver are essentially very low noise ($\leq 4^{o}$ K) amplifiers at 1 GHz with a bandwidth of ~1 GHz and a gain of ~12 dB per stage. These amplifiers use a Josephson junction up-converting parametric amplifier coupled with a superconducting/Schottky down-coverting mixer. The components, system design and experimental results will be discussed.

4-2 THE AEROSPACE CORPORATION'S MILLIMETER-WAVE SPECTRAL LINE RECEIVER: W. J. Wilson, T. T. Mori, J. W. Montgomery and H. E. King, The Aerospace Corporation, El Segundo, California.

A spectral line receiver is now in operation with the Aerospace 4.6 m millimeter-wave antenna at El Segundo, California, to study interstellar molecular emission in the 70-120 GHz frequency range. The system noise temperature is $\leq 2200\ ^{o}$K at 115 GHz and the receiver has an IF bandwidth of 100 MHz. The local oscillator klystron is phase-locked to a 100-MHz frequency synthesizer and it can be frequency switched over a 100-MHz frequency range at a 10-Hz rate. All receiver tuning adjustments are servo controlled. Both a 64-channel 1-MHz and a 64-channel 250-kHz filter bank are available. The outputs of the filter banks are sent to a 128-channel multiplexer and then to a 13-bit A/D converter. This digital data is read by NOVA 800 minicomputer which has 16,384 words of memory. The computer system has 2 LINC magnetic tapes, a 7-track magnetic

tape, and a display terminal with hard copy output. The computer controls the receiver operations, the antenna positioning, and the data acquisition processing and display. The computer is programmed with the FORTH language, which provides a flexible and easy-to-use system. Three observing modes are available: frequencies, load and position switching.

4-3 A NEW MERIT MEASURE FOR SUPERSYNTHESIS ANTENNA CONFIGURATIONS: Y. L. Chow, National Research Council, Ottawa, Ontario.

The merit of an array configuration is usually measured by its transfer functions in terms of the number of u-v components (or its conjugate, the percentage of holes) counted in a square grid of cells within a circular boundary. The choices on the cell size and the boundary radius are arbitrary and effect the number of u-v components counted. This makes the above merit measure difficult, especially in comparing arrays of very different configurations.

A new merit measure is propsed here through converting the u-v components into equivalent numbers of completely orderly and completely randomly distributed baselines. These two equivalent numbers are fairly independent of the choices on cell size and the boundary radius since the actual number of baselines is completely independent of them.

It is shown that when the actual number of baselines lies somewhere between these two equivalent numbers, the array can be called "nearly optimum". A poorly designed array configuration will have many redundant baselines so that the actual number is much higher than both equivalent numbers. This paper ends with merit studies on various array configurations, including a study on the NRAO and the power-law Y arrays.

4-4 A MILLIMETER-WAVELENGTH INTERFEROMETER AT TABLE MOUNTAIN: M. Janssen, B. Gary, S. Gulkis, C. Ivie and F. Soltis, Jet Propulsion Laboratory, Pasadena, California.

A new millimeter-wavelength radio interferometer is now in operation at the Jet Propulsion Laboratory's Table Mountain Observatory in the San Gabriel Mountains. The frequency is fixed at 36 GHz ($\lambda$8.3 mm), the highest frequency of operation of any existing radio interferometer. A fixed 5.5-meter antenna and a moveable 3-meter antenna are employed. Two locations have been prepared for the latter, giving east-west baselines of 60 and 120 meters. The elevation is approximately 2300 meters, which is of advantage in minimizing signal phase fluctuations caused by inhomogeneities in the distribution of atmospheric water vapor and are of special concern at short

wavelengths. With equipment modifications now in progress we expect to be operating in the near future with an intermediate-frequency bandwidth of 400 MHz and a system temperature of 700°K, thus giving us the sensitivity to investigate a variety of astronomical problems. Initial astronomical tests were successfully carried out in May of this year at a reduced performance level. On completion of the present modifications, and following a further period of testing and calibration, we plan to begin a series of high resolution measurements of the planets Venus, Jupiter and Saturn.

4-5 INTERFEROMETRIC "SEEING": THE DECORRELATION OF MILLIMETER WAVES BY THE ATMOSPHERE: Leslie M. Golden, William J. Welch, University of California, Berkeley, California.

Extended studies of several sources at frequencies near the water line at 1.35 cm have been made employing the Hat Creek fixed baseline interferometer. Phase fluctuations and degradation of the amplitude of the correlated signal are found to vary with meteorological conditions and season. Such effects may be amenable to calibration, and the necessary procedures are outlined.

4-6 ATMOSPHERIC ELECTRICAL PHASE MEASUREMENT BY MICROWAVE RADIOMETRY: J. W. Waters, Jet Propulsion Laboratory, Pasadena, California.

Fluctuations in atmospheric parameters produce variations in the delay of a radio signal passing through the atmosphere. These variations, over a time period of 12 hours, are typically 1 to 2 cm due to dry air and 5 to 10 cm due to water vapor. As the instrumentation for Very Long Baseline Interferometry becomes capable of measuring baselines to centimeter accuracy, the atmospheric effects may be the limiting factor in the accuracy of such systems. One way of correcting for the water vapor phase delay is by inferring its value from measurements of microwave thermal emission by the water vapor. The expected accuracy of this technique is 1 to 2 cm rms. Experiments to test the technique have been performed with the Green Bank Interferometer of the National Radio Astronomy Observatory, and are planned for the Astronomical Radio Interferometric Earth Surveying (ARIES) system of the Jet Propulsion Laboratory. Results of these and related experiments will be described.

4-7 USE OF ATMOSPHERIC EMISSION MEASUREMENTS FOR LOW-ELEVATION ANGLE REFRACTIVE ERROR CORRECTION IN A HORIZONTALLY VARIABLE TROPOSPHERE: Marshall A. Gallop and Larry E. Telford Air Force Cambridge Research Laboratories, Bedford, Massachusetts.

Radar range and elevation angle errors due to refraction are often corrected by estimates based on surface refractivity or by computations made from periodic radiosonde soundings. Although these methods may be adequate where the radar is not required to operate at low elevation angles, systems which must operate below $5^{o}$ require more accurate procedures. Radio waves transmitted at low angles have a relatively higher proportion of their total path in the dense lower troposphere. This results in a substantial increase in refractive errors in addition to permitting the atmosphere at a great distance from the transmitter to have a significant effect on bending and range error. Where the troposphere is horizontally variable, conventional error correcting techniques give little information about down-range atmospheric conditions. The approach of this research is to rely on the similar dependence of refraction and atmospheric emission on the down-range atmospheric characteristics of the path. Non-horizontally stratified atmospheres determined from simultaneous radiosonde soundings at Portland, ME and Chatham, MA were used to calculate refractive bending and radio range concurrently with the output of passive microwave radiometers. By relating refraction to emission statistically, it was possible to reduce the errors in determining refractive effects well below performance attainable by use of surface refractivity alone and even below that attainable by radiosondes, without a need for troublesome radiosonde launches.

4-8 ANTENNA CALIBRATION WITH ATS-6: W. C. Erickson, University of Maryland, College Park, Maryland.

This is a minority report by one radio astronomer who is highly pleased with ATS-6. The 40.016 MHz beacon on the satellite forms an excellent calibration source for the Clark Lake telescope. Using our normal receiver configuration, the beacon can be observed with a good signal-to-noise ratio using two banks of elements as an interferometer. We do this regularly to determine the relative phase and amplitude of each bank. A simple and extremely inexpensive phase-lock system will be presented. This provides an excellent signal-to-noise ratio on each of the 720 individual elements of the array. Individual calibration of every element in the system is being undertaken. This program inevitably produces a wealth of data concerning ionospheric diffraction patterns since there are some 115,200 independent interferometer spacing and orientations available covering 3 km x 3.6 km area in the (u,v)-plane. Some of these data will be shown.

4-9 BANDEDGE PROBLEMS FOR RADIO ASTRONOMY DUE TO THE SATELLITES ATS-6 AND SMS-1: F. J. Kerr, University of Maryland, College Park, Maryland; W. E. Howard, III, National Radio Astronomy Observatory, Green Bank, West Virginia.

Radio astronomers have been very concerned about the possibility of interference from satellite transmitters operating close to radio astronomy bands. An extensive series of observations has been carried out on the 2667.5 ± 15 MHz television transmissions from ATS-6. Ten radio observatories in the United States and Canada took part. Spectral studies show that the signal transmitted inside the 2690-2700 MHz radio astronomy band is well above the CCIR limit within the satellite antenna's "footprint". Interference to astronomical observations occurs in some parts of the sky, but not others. Tests have also been carried out at Green Bank and Jodrell Bank on the signal levels at the 1667-MHz OH line frequency from the SMS-1 satellite, which radiates in a nominal 20-MHz band centered at 1681.6 MHz.

4-10 ANTENNA CHARACTERISTICS OF THE RADIO ASTRONOMY SATELLITES RAE-1 AND RAE-2: Edward P. Sayre, Avco Systems Division, Wilmington, Massachusetts.

The impedance and radiation characteristics of the Radio Astronomy Satellites, RAE-1 and RAE-2 are reported in this paper. The method of moments formulation was utilized to predict these characteristics using the actual in-orbit equilibrium shapes of the traveling wave V-antennas. The results of this investigation show (1) the results for the actual in-orbit shape for the V-antennas as drastically different from the results predicted from and idealized V-antenna used in earlier studies, (2) significant E-plane coupling between the 120 foot dipole and the V-antennas affects the impedance and radiation performance of the dipole, and (3) as expected little effect by the libration damper is observed.

The in-orbit shape of the V-antennas on RAE-1 and RAE-2 are different in that the lower V on the RAE-2 failed to erect properly resulting in different performance from either the normal in-orbit shape or the idealized V. It was found that the directivity of the in-orbit shape is lower and the pattern broader than what was expected due to the closure of the peripheral regions of the V's due to gravity gradient effects. Details of the RAE-2 results are included.

The coupling between the 120 foot dipole and the traveling wave V's was found to manifest itself in the real part of the dipole input impedance below 1 MHz. In the VLF and LF frequencies, the input resistance of the dipole in the presence of the

V-antennas differs from the free space dipole resistances. At 25 kHz the RAE dipole resistance is 3 orders of magnitude larger than free space conditions, and an order of magnitude at 200 kHz. These predictions have been verified by correlating temperature measurements made by IMP-6 with those made by the RAE satellites. Of significance is that the reactance results do not differ from the free space dipole over this frequency range. The capacitance probe on board the RAE thus can mislead one to believe that the RAE dipole has characterisitics similar to a free space dipole.

Extensive results were obtained for the radiation performance of the dipole and V-antennas on both RAE-1 and RAE-2 at 3.93, 6.55 and 9.18 MHz. These results obtained over the complete radiation sphere are reported using both power contours plotted over the usual radiation distribution pattern method as well as an equal area Mollweide projection of the contour data. The latter projection preserves spherical areas permitting rapid quantitative as well as qualitative visual evaluations of sidelobe and backlobe flux relative to the main beam.

4-11 A NEW METHOD FOR MEASURING SOLAR WIND DENSITY USING HALF THE RADIO EQUIPMENT PREVIOUSLY REQUIRED: Thomas A. Croft, Stanford University, Stanford, California.

For almost a decade we have measured the solar wind density with the "dual-frequency experiment". This requires the transmission of two coherent signals from Stanford's 46 meter dish to an interplanetary spacecraft where a special receiver compares their radio frequencies and the timing of their modulations. From these data, the interplanetary electron concentration has been calculated. This measurement capability is currently being incorporated into the S and X-band radios which are to transmit from spacecraft to Earth during a testing period while the NASA Deep Space Net (DSN) evaluates the X-band as a telecommunication frequency. The S-X approach is practical for current launches, but the frequencies are too high and in a few years the telecommunication requirement for both frequencies will vanish. To meet this coming challenge, we plan to exploit recent advances in cesium beam clocks which make it possible to perform the dual-frequency experiment by transmitting only a single radio science signal from our dish. The DSN's uplink communication will provide the timing signal usually derived from the second of the two science signals. I call this "VLBDF" for "Very Long Baseline Dual-Frequency"

since the concept is similar to VLBI. The method is inherently economical because the clock required for remote synchronization is much less expensive than a second transmitter, and also one less spacecraft receiver is needed. The interface with the DSN is simple; our cesium clock must be synchronized with the DSN maser, and aboard the spacecraft the telecommunications receiver must pass two tones to the science receiver.

COMMISSION VI, Session 8; Joint With COMMISSION II

Wednesday, October 16 1:30 pm - 5:00 pm
PROPAGATION IN RANDOM AND STRATIFIED MEDIA
CHAIRMAN: A. Ishimaru, University of Washington

8-1 PROPAGATION REGIMES FOR TURBULENT ATMOSPHERES: David A. de Wolf, RCA Laboratories, Princeton, New Jersey.

Although much progress has been made in the subject of propagation through random media recently, the average user of the results could be bewildered by the large number of governing parameters and conditions of validity of diverse scintillation statistics. Continuing from previous work summarizing a state of affairs of some years ago, we present some graphical representations of parameter regimes and discuss typical propagation links in non-ionized media at optical and at radiowave frequencies, as well as microwave links through ionized atmosphere. One useful graphical representation defines parameter regimes defined by a coordinate system that uses the number of mean free paths as one axis and the number of Fresnel radii as another. It is sketched for a medium defined by Kolmogorov turbulence laws in the inertial subrange.

8-2 THEORY OF PROPAGATION OF WAVES THROUGH STRONG TURBULENCE I: Marilyn Marians and V. H. Rumsey, University of California, San Diego, California.

Simple formulas for the complex covariance (and its transform, the angular spectrum) can be worked out for the case of an unmodified power law spectrum $q^{-\alpha}$ of refractive index fluctuations in three dimensional space $(q_x, q_y, q_z)$, for $2<\alpha<4$. The coherence length goes to zero and the angular spectrum becomes infinitely wide as $\alpha$ approaches 2 or 4. The spectrum of intensity fluctuations is well defined for $2<\alpha<6$ and becomes infinitely wide as $\alpha$ approaches 2 or 6. It conforms to the turbulence spectrum for spatial frequencies K above $UK_f/\pi$ where U is the Born approximation to $m^2$, the normalized mean square intensity fluctuation, and $K_f$ is the spatial frequency at the first null of the Fresnel filter. $m \approx 1$ if $U>3$ for $\alpha=3$. For an incoherent source of finite angular extent, m increases as $U^{0.5}$ for $U<1$ and decreases as $U^{-\frac{1}{\alpha-2}}$ for $U>10$. Observations at 4 meter wavelength on signals received from 3C 144 are in excellent agreement with this theory. The theory is based on nothing more than the wave equation specialized to the case of a narrow angular spectrum of plane waves, i.e., the parabolic wave equation.

8-3 THEORY OF PROPAGATION OF WAVES THROUGH STRONG TURBULENCE II: Marilyn Marians and V. H. Rumsey, University of California, San Diego, California.

Spectra of intensity fluctuations due to propagation through a thin, but arbitrarily strong, turbulent layer have been computed for the case of a power law turbulence spectrum using the theory of the companion paper. For $U < 1$ (see definitions in companion abstract) the calculations reproduce the Born or Rytov approximation. The effect of increasing U is to extend the intensity spectrum at high frequencies. At the low frequency end of the spectrum, the first Fresnel peak of the Born approximation becomes narrower and moves to lower frequencies. Calculations have been made describing the effect of the slope of the turbulence spectrum, the angular size of the source, and the bandwidth of the receiver. The scintillation index, m, for a point source has been found to saturate at unity as U is increased beyond 10. For an extended source, the index peaks and then decreases sharply as U increases, in agreement with the theoretical result in the companion paper. The calculations are in excellent agreement with interplanetary scintillation measurements.

8-4 A STUDY OF THE DEPENDENCE OF SCINTILLATION ON IONOSPHERIC PARAMETERS: K. C. Yeh, C. H. Liu, M. Y. Youakim, University of Illinois, Urbana, Illinois.

The problem of scintillation of transionospheric radio signals is studied using the parabolic equation method developed on the theory of wave propagation in random media. A power-law spectrum for the ionospheric irregularities is assumed. The range of validity of the spectrum is discussed from experimental data. The equation for the forth moment of the field is solved numerically. Scintillation index and intensity correlation function are computed. Their dependence on frequency and the ionospheric parameters will be presented. The effects of multiple scattering will be discussed in detail. The results are compared with those obtained for a Gaussian irregularity spectrum. Implications of the computed results to communication and geophysical problems will be indicated.

8-5 RADIATION FROM A LINE SOURCE CARRYING A TRAVELLING WAVE IN A MAGNETOPLASMA: D. C. Pridmore-Brown, The Aerospace Corporation, El Segundo, California.

One possible scheme that has been suggested for generating ULF and VLF waves in the upper ionosphere involves utilizing an antenna consisting of a modulated beam of charged particles launched from a satellite. To study the radiation from such an antenna one can model it as a line source carrying a traveling

wave of current moving out at the speed of the particles in the beam. This case is somewhat different from the one usually treated in that now not all portions of the wave number surface contribute to the radiation but only those which intersect the plane representing the prescribed wave number of the moving current pattern on the antenna. We derive formal expressions for the far field of such an antenna immersed in a uniform plasma and making an arbitrary angle with a uniform magnetic field. We also present plots of radiation patterns computed for typical parameter values of interest.

8-6 A NEW METHOD FOR REMOTELY PROBING STRATIFIED MEDIA: D. H. Schaubert, Harry Diamond Laboratories, Washington, D. C. R. Mittra, University of Illinois, Urbana, Illinois.

The problem of remotely probing a stratified, lossless, dielectric medium is studied. A spectral domain probing technique based on the Fourier analysis of the spatial variations of the field is used to formulate the problem. This technique is equivalent to illuminating the medium with plane waves at various angles of incidence and results in a Helmholtz wave equation. A new representation for the wave function (identified with the electric field) is used to solve the problem. This representation, which is actually an integral equation for the unknown wave function, provides an alternative to the Agranovich-Marchenko representation and is particularly well-suited to the spectral domain method of probing. Since the frequency of the probing wave appears as an independent parameter in the formulation, both dispersive and non-dispersive media can be treated. Furthermore, the new representation is a Fredholm equation of the second kind and is very amenable to numerical computations. Several examples of computed profile inversions are presented, including some cases which indicate that the procedure is stable in the presence of measurement noise. Some of the method's shortcomings are also discussed.

8-7 GROUNDWAVE PROPAGATION OVER PARALLEL STRATIFIED ANISOTROPIC MEDIA: R. J. King, Technical University of Denmark, Lyngby, Denmark, (on leave from University of Wisconsin).

Expressions for the surface impedance and admittance, and the corresponding Fresnel reflection coefficients are derived for uniform plane TM and TE waves which are obliquely incident upon plane layered anisotropic media. The permittivity and permeability tensors of each layer are assumed to be symmetric, and the propagation vector of the incident wave lies in one of the planes of anisotropy. The results can be used directly in well known formulas for groundwave propagation over isotropic media, and so there is no need to rederive these formulas for the various horizontal or vertical, electrical or magnetic

dipole sources. The effect of the anisotropy upon the wave tilt is also discussed. A particularly interesting model is an anisotropic conducting slab over a perfect conductor. If the slab's complex dielectric constant normal to the layer is sufficiently large, the surface impedance becomes independent of the angle of wave incidence. The wave in the slab is then TEM and only propagates in the normal direction. This leads to a surface impedance which is a local function and is primarily determined by the local slab thickness. Such a structure is very useful in the construction of nonuniform surface wave antennas because of the low losses and the fact that the surface impedance is only a function of the local structure. Corrugated periodic structures are of this class. But more generally such an anisotropic artificial dielectric can also be realized rather simply using normally oriented conductors of variable height randomly distributed over the perfect conductor.

8-8 TRANSIENT RESPONSE OF A PERIODICALLY STRATIFIED SLAB: C. Elachi and D. Jaggard, Jet Propulsion Laboratory, Pasadena, California; C. Yeh, University of California, Los Angeles, California.

The transient response of a periodically stratified slab to an incident rectangular and Gaussian pulse is studied. Both the reflected and transmitted pulses are illustrated and analyzed for a number of cases: different pulse width and different carrier frequency. The coupled wave theory is used to derive the reflection and transmission coefficients and the Fast Fourier Transform is used to derive the reflected and transmitted pulses.

COMMISSION VI - JOINT WITH COMMISSION I (See Page 120 )

Wednesday, October 16 1:30 pm - 5:00 pm

ANTENNA MEASUREMENTS

CHAIRMAN: P. E. Mayes, University of Illinois, Urbana, Illinois

## COMMISSION I, Session 5

Thursday, October 17 8:30 am - 12:00 noon

MICROWAVE TECHNIQUES IN BIOLOGICAL EFFECTS RESEARCH - A WORKSHOP

CHAIRMAN: S. W. Rosenthal, Polytechnic Institute of New York

5-1 ELECTROMAGNETIC FIELD MEASUREMENTS FOR BIOEFFECTS EXPERIMENTS AND THE CONTROL OF POTENTIAL HAZARDS: R. R. Bowman, National Bureau of Standards, Boulder, Colorado.

The measurement of potentially hazardous electromagnetic (EM) fields is very difficult because people are often exposed to fields with very complicated configurations. (These complications will be briefly discussed.) Though it has long been realized that instruments designed to measure simple plane-wave fields are not adequate, more suitable instruments have not been available until the last few years. Since the power density S of complicated fields often has little meaning as a hazard index, these new instruments measure the Hermitian magnitude $E \equiv (E_x^2 + E_y^2 + E_z^2)^{\frac{1}{2}}$, or some derived quantity such as the electric field energy density $U_E = \frac{1}{4} \varepsilon_o E^2$. The new instruments, as presently designed, respond to $E^2$ and the field sensors are essentially independent of their orientation in the field regardless of the complexity of the field. Further development of this type of instrument is expected to allow direct measurements of electric fields inside subjects and phantoms. The capability to measure internal fields is important for determining the internal exposure of subjects in bioeffects experiments and for developing phantom "dosimeters."

5-2 MEASUREMENT OF POWER ABSORBED IN THE TISSUES OF MAN AND ANIMALS EXPOSED TO ELECTROMAGNETIC FIELDS: A. W. Guy, University of Washington, Seattle, Washington.

In order to ascertain the mechanisms involved in the interaction of electromagnetic fields with biological tissues and to extrapolate the results from exposed laboratory specimens and animals to an exposed intact man it is necessary to quantify the absorbed power and fields within the tissues of the specimens, animals, and man.

The absorbed power may be quantified by 1) theoretical calculations based on the particular source and geometric shape of the exposed object, 2) measurement of the fields within the tissues by field sensing probes, 3) indirect point by point measurement of the absorbed power by rate of change of temperature increase in the tissue under exposure, and 4) indirect thermographic measurement of the absorbed power by rate of change of two dimensional temperature patterns in sectioned phantom models of the tissues or in the actual tissues of sacrificed animals.

The determination of the power absorption in laboratory specimens can generally be done by all four of the above methods and in laboratory animals, the latter three methods. Non-invasive measurements in humans can only be done by the latter method.

In the first method, the shape of the exposed specimen and the source is necessarily restricted to specific configurations. Specimens in vitro corresponding to cell cultures or biological solutions may be contained in cylindrical disk shaped or spherical containers and exposed to plane fields or waveguide fields in such a way that the total absorbed power or absorbed density distribution can be easily calculated from the incident fields, measured by standard means.

The fields may be directly measured in the tissue by appropriate field sensing probes. This is extremely difficult, however, and though such probes are under development, no satisfactory instruments are available at this time for accomplishing this.

The most straight forward method for determining the power absorption in the exposed tissues is simply measuring the rate of change of temperature rise at the site of interest and converting it to power absorption density and electric field strength from the known thermal and electrical properties of the tissues. This measurement must generally be done without the use of metallic probes or wires in order to avoid disturbance of the original field patterns in the tissues. The method requires sufficient applied power levels to provide the necessary rapid temperature rise in the synthetic or real tissues. Under certain conditions, the use of thermistors or thermocouples with small diameter high resistance lead wires may be satisfactory and have been used successfully. Other preparations require the use of dielectric guides to allow the metallic probes to be quickly withdrawn prior to irradiation and quickly reinserted after the fields are removed. New dielectric fiber optic temperature probes appear to be promising for continuous monitoring of temperature during irradiation.

All methods require information on the thermal and electrical properties of the tissues being probed.

The lack of internal field measurements in exposed tissues in both past and current biological effects research is a serious problem resulting from lack of standard instrumentation and the difficulties of developing such instrumentation by most groups carrying out such research.

## COMMISSION II, Session 7

Thursday, October 17 8:30 am - 12:00 noon
REMOTE SENSING OF LAND SURFACES
CHAIRMAN: Maurice W. Long, Georgia Institute of Technology

7-1 THE URSI SPECIALIST MEETING ON MICROWAVE SCATTERING AND EMISSION FROM THE EARTH: R.K. Moore, University of Kansas, Lawrence, Kansas.

The author, who served as Chairman of the Organizing Committee for this conference, will summarize the highlights of this international meeting on passive and active microwave studies of land and ocean surfaces, held in Berne, Switzerland, September 23-26, 1974.

7-2 EXPERIMENTAL VERIFICATION OF TWO SCALE SCATTERING THEORIES: R. M. Axline and A. K. Fung, University of Kansas, Lawrence, Kansas.

The scattering coefficients, $\sigma^o(\Theta)$, of two targets were determined experimentally at 25 GHz. One target was a lossy dielectric (plaster). The other target was a good conductor (aluminum). The target had identical roughness profiles. The roughness was two-scale composed of the sum of a small-scale (to which the small perturbation method is applicable), and a large scale (to which the Kirchhoff method is applicable) surface. Backscattering measurements were taken for the VV, HH, VH, and HV modes. The experimental $\sigma^o$ was obtained from the measurements. The statistical parameters of the target roughness were estimated by processing numerous profiles measured directly from the targets. These parameters served as input to two-scale theories. For the VV and HH modes, predictions of both a Coherent Theory (CT) and a Non-Coherent Theory (NCT) were compared to measurements. The CT showed excellent agreement with measurement. The NCT predictions, while in general agreement, were several dB below the measurement at large angles. For the VH and HV modes, the cross-polarized result for the small perturbation method was significantly higher than the measured $\sigma^o$ for the metal target, and lower than the measurement for plaster. The trend with incident angle, however was approximately correct.

7-3 STATISTICS OF Ku BAND MICROWAVE RESPONSE OF THE UNITED STATES WITH A SATELLITE-BORNE RADIOMETER/SCATTEROMETER: R. K. Moore, F. T. Ulaby, A. Sobti and T. Burton, University of Kansas, Lawrence, Kansas.

The S-193 Skylab Radiometer/Scatterometer was operated over the United States many times. The statistics of the data from

this gross-resolution ($2^{o}$ beam width) sensor are reported herein. Histograms are presented of distribution of the radiometric temperature and the differential backscattering coefficients for various data segments broken up by polarization and incidence angles; a similar composite histogram for the first and second occupancies; upper and lower quartile and decile points; a qualitative comparison between expected histograms of known targets and ones produced from the Skylab data. The S-193 Radiometer/Scatterometer is a composite microwave sensor operating at 13.9 GHz. The radiometer and scatterometer share the same antenna and rf section. The instruments also share the common hardware with an altimeter, but this report does not include any results from altimeter operation. The antenna is a mechanically scanned parabolic reflector with an effective one-way beam width of $2.02^{o}$ and an effective two-way beam width of $1.54^{o}$. The scattermometer, during noncontiguous mode of operation, records data for four polarization pairs: VV, HH, VH, HV. The radiometer also records data for both vertical and horizontal polarization. The target cell size varies from 95 sq. kms for nadir incidence (scattermometer) to over 500 sq. kms at oblique incidence (radiometer). For contiguous modes used more often over land, the polarization combinations available are more restricted.

7-4 VEGETATION PENETRATION WITH RADAR: F. T. Ulaby, T. F. Bush, and P. P. Batlivala, University of Kansas, Lawrence, Kansas.

Radar return from agricultural targets was investigated using a truck-mounted 8-18 GHz radar spectrometer system. Spectral data were measured at incidence angles between $0^{o}$ (nadir) and $70^{o}$ in $10^{o}$ steps for VV and HH polarizations. Several types of crops were considered under a variety of soil moisture conditions and growth stages. The data was analyzed to determine the radar response of each crop type to soil moisture as a function of incidence angle and frequency. In addition to defining quantitative design criteria for radar systems intended for water resource applications (low angle of incidence range) and crop type inventory (high angle of incidence range), the results of this study include some interesting new observations. Among these is the effect of plant wilting on the radar return. The wilting of the plants was caused by the presence of excessive water as a result of heavy precipitation (15 cm of rain). The radar return from a corn field was measured shortly after the rain and at three-day intervals thereafter over a period of two weeks. Soil samples indicated a change from 42% moisture by weight to 4.5% over the same period. The corresponding radar return dropped by as

much as 8 dB at normal incidence, but at angles above 30°, it increased slowly until it resumed the behavior observed before the rain. The wilting effect, which is both incidence angle and frequency dependent, can be explained well by a facet scattering model.

7-5 A RADAR POLARIZATION MODEL FOR TERRAIN: Maurice W. Long, Georgia Institute of Technology, Atlanta, Georgia.

In principle, it is possible to calculate radar cross section for any polarization if all information contained in the polarization matrix is known. The various elements of the matrix, in general, fluctuate with time. Therefore, a voluminous amount of relative amplitude and phase data would be necessary to calculate expected average values. There is a need to calculate averages for various polarizations when only a few data on averages exist. To this end, equations are developed by using a model consisting of (1) scatterers that reradiate coherently and do not depolarize and (2) scatterers that may or may not depolarize and reradiate incoherently. The model is applicable to angles near vertical incidence, i.e., angles that are often of interest for altimeters, satellite-borne radar, and radar astronomy. Let x and y represent directions of linear polarizations that are arbitrary except that x and y are perpendicular. Let 1 and 2 represent a circularity of one sense and of the opposite sense, respectively. Let $\sigma_{ij}$ represent average cross section if polarization i is transmitted and polarization j is received. The model permits calculating $\bar{\sigma}_{xx}/\bar{\sigma}_{xy}$ if $\bar{\sigma}_{12}/\bar{\sigma}_{11}$ is known or vice versa. By using previously published data, the model has been tested and found satisfactory for the moon. Under the assumptions used, the model will provide the ratio of average power scattered coherently to that scattered incoherently if either $\bar{\sigma}_{xx}/\bar{\sigma}_{xy}$ or $\bar{\sigma}_{12}/\bar{\sigma}_{11}$ are known. In the case of the sea, the limited data available indicate that at near vertical incidence the average power scattered coherently exceeds that scattered incoherently by a factor of at least 10.

7-6 CAN MICROWAVE SENSORS MEASURE SOIL MOISTURE FROM SPACE?: F. T. Ulaby, A. Sobti, J. Barr and R. K. Moore, University of Kansas, Lawrence, Kansas.

The microwave response to soil moisture is investigated using data collected by Skylab's 1.4 GHz microwave radiometer and 13.9 GHz radiometer/scatterometer systems over a test site in Texas. The test site covered an area of approximately 300 km x 200 km. The 13.9 GHz sensors operated in a cross-track contiguous mode at an incidence angle of 29.4°. The antenna

was vertically polarized during the entire pass. The recorded data was processed to produce scattering coefficient and antenna temperature contour maps for the test site. Using air temperature information reported by weather stations and cloud information from Skylab photography, an emissivity map was prepared from the antenna temperature map. A soil moisture map was also prepared based on composite rainfall history, soil permeability maps, Skylab infrared photography and soil samples gathered by ground crews of another Skylab project. Scattergrams were then constructed between each two of the following three maps: 1) scattering coefficient, 2) emissivity and 3) soil moisture. Considering all the extrapolation and positioning errors inherent in the contour map construction process, the results of this study look very promising as far as water resource mapping is concerned. The 1.4 GHz radiometer is a nadir-looking non-scanning system having a 110 km diameter circular footprint. For each footprint the recorded radiometer temperature was correlated with the average soil moisture within the footprint. Due to the large size of each resolution cell, the radiometer response indicated a very high degree of correlation with soil moisture.

## COMMISSION III, Session 6

Thursday, October 17 8:30 am - 12:00 noon
PROPAGATION AT HF AND HIGHER FREQUENCIES
CHAIRMAN: T. N. Gautier, National Oceanic & Atmospheric Admin.

6-1 EXPERIMENTAL OBSERVATIONS AND A PROPOSED EXPLANATION OF VERY LONG DELAYED RADIO ECHOES FROM THE IONOSPHERE: F. W. Crawford and D. M. Sears, Stanford University, Stanford, California.

For over 40 years, one of the unsolved problems of radioscience has been the sporadic observation of echoes of radio signals occurring with delays of the order of tens of seconds. Explanations have ranged from speculations that they are spurious observations, and that the effect does not exist, to the hypothesis that they are coded signals from an extraterrestrial civilization trying to communicate with our own. During the last seven years, an ionospheric sounding experiment has been in progress at Stanford, aiming to establish whether or not the phenomenon exists, and if so to determine its mechanism. After several thousand hours of experimentation, a number of records have been obtained which tend to confirm the occurrence of the very long delayed echo effect. (A tape-recording of some of the specimens will be played). Clues to its origin have been obtained by simultaneous measurements at Stanford of the ionospheric density profile by an ionosonde. We advance the explanation that the echoes are due to very low group velocity (1 km/s) propagation effects, near the peak of the F-layer. The strong collisional attenuation that such propagation would normally suffer is supposed to be offset by beam-plasma interaction due to fast electrons precipitated into the ionosphere. Calculations will be presented indicating that very weak fluxes of kilovolt energy electrons could readily cause delays of several seconds.

6-2 SPECTRAL BEHAVIOR OF IONOSPHERIC WAVES: Kurt Toman, Air Force Cambridge Research Laboratories, L.G. Hanscom Field Bedford, Massachusetts.

Techniques are described of measuring, processing, and analyzing characteristics that are associated with waves in the ionospheric F-region. Although a radio signal that is returned from the ionosphere usually consists of several (or many) signal components, only the signal of the dominant reflection mode is selected from HF Doppler records for further analysis. Amplitude and period of waves and their occurrence frequencies are deduced selectively from data gathered over four years. The undulating Doppler traces of ionospheric returns are spectrum analyzed and isometrically displayed with overlapping data windows to observe the dynamics of ionospheric waves in the frequency domain. Comparable data samples are derived from

random processes whose isometric spectral displays are compared with those obtained for the ionosphere. This display technique is also tested by using truncated sinusoids as input functions.

6-3 DIGITAL COMMUNICATION VIA IONOSONDES: Klaus Bibl and Bodo W. Reinisch, Lowell Technological Institute Research Foundation, Lowell, Massachusetts.

The existing network of Digisondes can be used to exchange scientific and operational data reliably between Digisonde stations. The data can be any message of language or results of measurements taken at one station and needed at another. For example, an inexpensive pulse transmitter can send keyed messages to a central station equipped with a Digisonde. Meteorological or radio measurements including the on-line analyzed information of the vertical ionogram can be comprised in the message.

Frequency stepping together with phase coherent pulse modulation provides an optimum means of data transmittal via the ionosphere even under disturbed conditions, as aurora and magnetic storm events. The modem of data transmittal is based on the phase sequence of 16 consecutive pulses. At maximum pulse rate of 400 Hz a coherence time of the ionosphere of only 40 msec is required. Sixty-four phase codes of 16 bits have been found which have not more than 50% cross-correlation with each other. Thus simultaneous 64 level digital filtering can be applied to extract the message on-line in real time.

6-4 A NEW TECHNIQUE FOR AUTOMATIC MULTIFREQUENCY HF ABSORPTION STUDIES: Bodo W. Reinisch and Sheryl Smith, Lowell Technological Institute Research Foundation, Lowell, Massachusetts.

Modern ionosondes measure and record digitally the field strength of the ionospheric echoes as functions of reflection height and frequency. Automatic trace identification of these digital ionograms together with adequate calibration provides for routine studies of radio absorption as functions of frequency and time. E and F reflections are treated separately. A small computer program corrects the measured field strength values such as to eliminate the frequency variation of the transmitter-antenna system and to compensate for the geometrical effects caused by different reflection heights. In the frequency range from 1.7 to 8.3 MHz median values are formed over 1 hour periods for each of seven 0.7 MHz wide frequency bands. For each day of observation 24 (hours) times 7 (frequencies) median field strength values in dB are presented as one line of optically weighed numbers showing the diurnal variation and its frequency dependence. Consecutive lines give the daily and season variations. Data for September 1973, the first data processed this way, are shown as an example.

6-5 A COMPARISON OF HF ANGLE-OF-ARRIVAL ERRORS AND THOMSON SCATTER PREDICTIONS: John M. Goodman, Naval Research Laboratory, Washington, D. C.

Thomson scatter radar measurements at high zenith angles are employed to monitor the electron concentration variations of the lower ionosphere. Simultaneously HF Group-path and angle-of-arrival measurements are made over a nearby path. It is found that traveling ionospheric disturbances give rise to a certain class of HF fluctuations which may be estimated through an analysis of Thomson scatter data. A Faraday rotation technique is employed in conjunction with Thomson scatter radar to deduce the ionospheric electron density profiles and movement of the F2 maximums. Traveling disturbances give rise to observable fluctuations in the Faraday rotational isopleths and exhibit layer height variations as a basic signature. It is shown that HF bearing angle errors are proportional to layer height variations and inversely proportional to the disturbance wavelength.

6-6 REFRACTION CORRECTIONS BY MOMENT EXPANSIONS: J. Berbert, H. Parker, A. Mallinckrodt, National Aeronautics and Space Administration, Greenbelt, Maryland.

The ionospheric refraction range errors, to a zero order approximation valid for plane earth, are directly proportional to the total columnar refractivity content or zeroth order moment of the electron density profile and a simple function, CSC E, of the elevation angle. For spherical earth, a first order correction is available which depends only on the effective height, or first order moment of the electron density profile. In a previous report the authors developed a second order correction for ionospheric range error, based on the second order moment of the profile distribution, which reduced this error by a factor of 10 for elevation angles below $10^{o}$. The second order moment expansion concept for refraction correction is extended to angle and range rate refraction errors through a generalized relationship between angle and range error developed in another report in this series. The moment series for range rate errors is shown to be identical to that for angle errors so that convergence and general utility properties of the series are the same for both types of errors. The range error to elevation angle error transformation produces a zeroth order angle correction good to within 8% of the reference ray trace results, but the second order angle and range rate correction does not appear to be justified.

6-7 UHF MEASUREMENTS OF IONOSPHERIC REFRACTION AT HIGH LATITUDES: J. V. Evans and A. Freed, Massachusetts Institute of Technology, Lexington, Massachusetts; R. J. Riley and D. E. Marr, Bell Telephone Laboratories, Inc., Whippany, New Jersey.

An 84-foot diameter steerable antenna has been employed to observe the apparent positions of the 400 MHz beacons carried by the Navy Navigation Satellites while simultaneously tracking the satellite at 1295 MHz by radar. These observations were conducted at Millstone Hill, Westford, Massachusetts during the period August 1972 through March 1973.

The radar observations of a number (10 or more) of successive passes of each satellite were employed to solve for the orbit and hence the true position with time. UHF data gathered at night was then utilized to establish a correction law for UHF beacon tracker angle errors that depended on the polarization of the received signals. Daytime results showed anomalous refraction to the north at some times, as well as the normal refraction produced by the ambient ionosphere. Using a differential-doppler experiment during the course of the tracking, it was established that this anomalous refraction was associated with ray paths intersecting the equatorial edge of the trough. This remained the case in one instance when the trough assumed an overhead position. No anomalous refraction effects appear to be associated with the onset of radar auroral returns along the line-of-sight to the satellite.

6-8 IONOSPHERIC SIGNAL PROPAGATION DELAY ESTIMATES FROM TWO CHANNEL DOPPLER MEASUREMENTS: R.J. Taylor, Johns Hopkins University, Silver Spring, Maryland.

Estimating the Ionospheric Signal Propagation Delay is necessary in using an Experimental Satellite Passive Submicrosecond Time Dissemination System developed by the Johns Hopkins University, Applied Physics Laboratory. An estimate of the ionospheric delay is the following:

$$\Delta\tau_{ion}\,(t_{TCA}) = \frac{\rho\,(t_{TCA})}{f_2}\;\frac{32\,f_1}{55}\;\frac{\dot{f}_R\,(t_{TCA})}{\ddot{\rho}\,(t_{TAC})} \qquad (1)$$

where

$\rho\,(t_{TCA})$ = Slant range between satellite and observer
$t_{TCA}$ = Time at closest approach of the satellite
$f_R\,(t_{TCA})$ = Refraction correction frequency from two channel doppler
$f_1$ = 150 MHz
$f^i$ = Frequency of signal for which the delay is being estimated.

400 MHz signal ionospheric delays, calculated using equation (1) for 17 passes of the TRIAD satellite over APL, Howard County, Maryland were compared with estimated delays using columnar electron densities measured between Sagamore Hill, Massachusetts and the ATS-3 satellite using Faraday Rotation. The average absolute difference between these two methods was 25 nanoseconds with an average delay of 133 nanoseconds (19% average

disagreement). Note, absolute agreement is not expected because the two different methods are not looking at the exact same section of the ionosphere.

## COMMISSION V, Session 5

Thursday, October 17 8:30 am - 12:00 noon
SOLAR SYSTEM
CHAIRMAN: J. W. Warwick, University of Colorado

5-1 INTERPLANETARY SCINTILLATION: J. W. Armstrong and W. A. Coles, University of California, San Diego, California.

Scintillation of the compact radio sources in the Crab nebula has been observed at 74 MHz. Earlier work (Armstrong et al., 1973) used these observations to derive the brightness distribution of the source, but did not give a satisfactory estimate of its strength. We have calculated the scintillation index using the known brightness distribution and the numerical results for strong scattering given by Marians and Rumsey (1973). A comparison with the data shows that the flux of the compact source must be 120 ± 20 f.u., which is in remarkable agreement with VLBI observations (Vandenberg, 1974). The standard methods of estimating the flux from the scintillation index lead to an error of about 80% when applied to this source. The indication is that all fluxes and source diameters derived from scintillation observations near 74 MHz should be revised. A procedure for this is given. The effect for most sources is that the interferometer fringe visibility for long baselines will be smaller than had been expected previously.

5-2 INTERPLANETARY SCINTILLATION OBSERVATIONS WITH THE NOAA/IOWA COCOA CROSS: W. M. Cronyn, National Oceanic and Atmospheric Administration, Boulder, Colorado; F. T. Erskine, III and S. D. Shawhan, University of Iowa, Iowa City, Iowa.

Results of synoptic observations of IPS (interplanetary scintillation) activity using the $7 \times 10^4 m^2$ , 34 MHz N.O.A.A./University of Iowa Cocoa Cross will be presented. The observations were taken on a grid of over 90 sources, of which over 60 have displayed measurable IPS. Solar elongation angles have ranged from $20^o$ to nearly $180^o$. Association between enhancements in IPS which we observed and other signatures of solar and interplanetary activity will also be discussed. Finally, the IPS observations have provided significant information about arcsecond source structure at a dekametric wavelength.

5-3 RECENT RADIO OCCULTATION FINDINGS ON VENUS, MERCURY AND JUPITER: Arvydas J. Kliore, Jet Propulsion Laboratory, Pasadena, California.

The Pioneer 10 and Mariner 10 fly-bys of Jupiter, Venus and Mercury provided much new radio occultation data on their atmospheres. In addition to discovering an atmospheric Io, manifested through the presence of both daytime and nighttime

ionospheres, the data from the S-band experiment on Pioneer 10 revealed temperatures in the neutral atmosphere of Jupiter far in excess of those based on infrared and microwave observations from the earth, as well as the Pioneer 10 infrared radiometer experiment. The Mariner 10 S- and X-band measurement at Venus revealed a nighttime ionosphere having two peaks, as well as four distinct temperature inversions in the neutral atmosphere. Mercury was found to have no measurable atmosphere and ionosphere, with a radius of about 2440 ± 2 km.

5-4 OBSERVATIONS OF TURBULENCE IN THE ATMOSPHERE OF VENUS BY MARINER 10: R. Woo, Jet Propulsion Laboratory, Pasadena, California.

In a recent study (Woo et al., J. of Atmos. Sci., Sept. 1974), we demonstrated that small-scale turbulence in the atmosphere of Venus can be sensed and probed using the frequency spectrum of the radio signal received from a fly-by spacecraft such as Mariner 5. As a result of this study, turbulence of appreciable intensity was discovered in the upper Venusian atmosphere for altitudes up to approximately 65 km. In the present work, we have carried out a similar study based on the Mariner 10 S-band signal. The results are remarkably similar to those of Mariner 5. Analysis of the entrance occultation data indicates that above 35 km turbulence is strongest in the vicinity of 45 km and 60 km. These turbulence results appear to be corroborated by the four distinct inversions observed in the temperature profile derived from the Mariner 10 S-band doppler data (Howard et al., Science, Vol. 183, March 1974). The top inversion occurs at approximately 63 km and probably marks the transition between the stable region above and the convective layers below.

5-5 BEAMING CONE EFFECTS INFERRED FROM THE REPEATABILITY OF JUPITER'S DECAMETER-WAVE DYNAMIC SPECTRA: J. K. Alexander, Goddard Space Flight Center, Greenbelt, Maryland.

Among the many remarkable aspects of Jupiter's decameter-wave radio emission is the pronounced repeatability of its dynamic spectra. Nine strong decametric events recorded in 1973 and 1974 with the University of Colorado spectrograph have been paired with events having the same dynamic spectra which were recorded very nearly 11.9 yr. (one Jovian year) earlier with the same instrument. Upon comparison of the members of a pair, we find that certain spectral features always occur at the same central meridian longitude to within ± 10°. The variation in the longitude of the spectral landmarks is attributable to variations in the orientation of the beaming

envelope into which the radiation escapes. That the variation of the azimuthal orientation of the beaming cone appears to vary by ± 10° is likely to be due to variations in the precise field geometry of plasma distribution at or near the source which control the emission pattern and the escape of the radiation from the source region. The comparison of the dynamic spectra of events separated by ~12 yr. also provides an estimate of the radio rotation period of the planet ($9^h\ 55^m\ 29\overset{s}{.}71 + 0\overset{s}{.}07$), but the precision of this determination is limited by the ± 10° beaming effect.

5-6 SPECTRAL CORRELATIONS BETWEEN SOLAR FLARE RADIO BURSTS AND ASSOCIATED PROTON FLUXES: Pradip Bakshi, Boston College, Chestnut Hill, Massachusetts; William R. Barron, Air Force Cambridge Research Laboratory, Bedford, Massachusetts.

According to the Castelli criterion, solar flare radio spectra of sufficient intensity and a U-shaped intensity-frequency profile are indicative of a significant proton event. Combining some characteristics of recent synchrotron radiation and particle acceleration models suggests an association between wider U-spectra and more energetic electrons and proton events. We have studied the spectral correlations for significant U-shaped radio events and the relative energy distributions of the associated proton spectra for 1967-72. Let $x = \log(\omega_3/\omega_2)$, $\omega_3$= frequency of maximum radio peak flux of the upper branch and $\omega_2$=cut-off frequency for the lower branch of U; $y=\log(I_1/I_2)$, $I_{1,2}$=peak intensity of proton flux for energies greater than $E_1, E_2$; $E_1$=10 Mev, $E_2$= 30 or 60 Mev. We find significant correlations for linear, exponential and power fits $y(x)$, for 10 Mev/30 Mev($r\approx0.80$) as well as 10Mev/60Mev ($r\approx0.75$). Relative merits of the various fits will be discussed. These results indicate a significant correlation between wider(narrower) U's and relatively higher (lower) abundance of higher energy protons. The best fit parameters obtained here can now be used to predict the relative intensities of the proton spectra on the basis of immediately observable radio burst spectral characteristics.

5-7 SOLAR ACTIVITY IN THE FREQUENCY BAND, 22 - 25.4 gc./sec, DURING THE PERIOD OF AUGUST 7 - SEPTEMBER 17, 1972: Mohamed El-Raey, University of Alexandria, Alexandria, Egypt; A. R. Cannon and Samuel Silver, University of California, Berkeley, California.

Maps of the distribution of the microwave temperature of the sun were obtained in connection with an experiment on spectral broadening conducted during the superior conjuction phase of

Mars and the Mariner 9 spacecraft in August - Sept., 1972. The maps, in the form of isophotes, show centers of activity (enhanced emission) which can be correlated with other features such as sun-spots, plage area, filaments, etc. The technique of generating these maps with a pencil beam radiotelescope is discussed and some general characteristics of the "microwave sun" are presented. It is shown that activity-centers move across the solar disc and exhibit rise and fall in strength with the rotation of the sun. The relation between the observed microwave features and the flare-events of the August - September, 1972 period is discussed.

5-8 HIGH RESOLUTION INTERFEROMETRY OF THE SUN AT 3.7 CM WAVELENGTH: Kenneth R. Lang, Tufts University, Medford, Massachusetts.

Interferometric observations of the Sun at a wavelength of 3.7 cm and effective angular resolutions of 3" to 30" are presented. When active regions are observed, circularly polarized radiation is found with an angular size of 15", an effective temperature of $5 \times 10^5$ $^{o}$K, and 20 to 30% circular polarization. This S-component of solar radio radiation is interpreted in terms of the theory of gyroradiation and gyroresonant absorption. Prior to the onset of a solar flare an additional S-component is observed with an angular size of less than 7", and effective temperature greater than $10^6$ $^{o}$K, and nearly 100% circular polarization. A small scale, quasi-periodic component of solar radio radiation is also observed to be coming from all over the solar disk; and this component is found to be less than 10% circularly or linearly polarized. The angular size of this quasi-periodic emission is of the order of 10", and the periods, P, of the emission lie between 200 and 400 seconds. The brightness temperature fluctuations of the periodic component lie between $10^3$ and $10^5$ $^{o}$K. This component of solar radio radiation is thought to be the free-free radiation (bremsstrahlung) of temperature fluctuations associated with velocity oscillations in the chromosphere-corona transition region. High resolution observations of impulsive microwave bursts are also presented, and some of this radiation is linearly or circularly polarized, has an angular size less than 7", and a peak brightness temperature greater than $10^6$ $^{o}$K. This component of solar radio flares is interpreted in terms of the theory of gyro-synchrotron radiation; and phase shifts observed in the burst interferometer pattern are interpreted in terms of high velocity (7000 km $sec^{-1}$) hydromagnetic waves.

5-9 POLARIZATION VARIATIONS IN ACTIVE REGIONS AT 3.8 CM: R. M. Straka, Air Force Cambridge Research Laboratories, Bedford, Massachusetts.

Observations of brightness temperature and circular polarization in active regions were made with the 120-foot NEROC Haystack radiotelescope during 1970-73. Various kinds of polarization changes were recorded. On 18 October, 1970, a disappearing filament caused a fifty percent change of the region polarization value and shifted the position of the emission center. The event was associated with a long duration gradual-rise fall burst which had a peak flux of only 2.0 solar flux units (Ottawa). Other cases show polarization variations in the active region prior to optical flare occurrences. Power spectra of the polarization fluctuations indicate a peaking in the 250 to 380 second period interval. Variations of the brightness temperatures sometimes had good correlation with polarization ($r=0.85$), and at other times had very poor correlation ($r=0.16$). A few regions had abrupt polarization changes without noticeable temperature changes that occurred when another region was flaring and suggest sympathetic stimulation may have taken place.

5-10 SPECTRAL BROADENING OF SIGNALS AS A PROBE FOR THE STUDY OF THE CORONA: R. Goldstein and C. T. Stelzreid, Jet Propulsion Laboratory, Pasadena, California; A. R. Cannon, M. El-Raey and S. Silver, University of California, Berkeley, California.

The investigation of the spectral broadening of signals traversing the corona and the interplanetary medium between Mariner-9 and Pioneer-10 and the ground station at Goldstone, California is reported and discussed from the standpoint of probing the corona and the interplanetary medium. The variation of the bandwidth of the signal with the offset of the ray-path from the solar disc is related to the structure of the medium and to solar activity. It is shown that the relation between two-way spectra (ground to spacecraft to ground) and one-way spectra (spacecraft to ground) is an index to the stability of the structure of the corona. The results given in this report indicate that the structure of the corona is time-stationary over at least 30 minutes which is the time required for a round trip of a signal from ground to Mariner-9 to ground. Various scattering processes that give rise to a change in frequency are discussed and the implications of the experimental results with respect to the dominant processes are delineated and explained.

5-11 LUNAR OCCULTATIONS OF A TYPE III SOLAR RADIO STORM AT LOW FREQUENCIES: J. Fainberg, Goddard Space Flight Center, Greenbelt, Maryland.

The RAE-2 satellite, launched 10 June 1973, makes low-frequency observations at 32 frequencies extending from 13.1 MHz down to 25 kHz. It is in circular lunar orbit with the lunar disc subtending 76° from the satellite. This experiment allows studies to be made of discrete and distributed radio sources over a large portion of the sky by lunar occultation techniques. Expressions have been derived for the expected intensity scans of occulted distributed sources using Fresnel theory for the Rae-2 geometry configuration. A solar radio storm of Type III bursts lasting for several days around 20 February 1974 was observed by RAE-2 during a period of nearly central occultations of the Sun by the Moon. Fortunately during this period the intense radio emissions from the Earth's magnetosphere were not present so that occultation observations of the solar storm were visible at frequencies extending from several MHz down to well below 200 kHz. The occultation modulation of the radio source clearly visible at high frequencies virtually disappeared at 155 kHz (and below) indicating that a large portion of the radiation, although present, was not occulted. For the particular RAE-2 and lunar geometry this implies that much of the radiation at 155 kHz is emitted or scattered outside a radial distance of 110 $R_\odot$ from the Sun. This result is consistent with results previously obtained in an analysis of limb Type III bursts with IMP-6. A detailed analysis of source structure and source evolution for this storm will be presented.

5-12 SIMULTANEOUS OBSERVATIONS FROM THE IMP-6 SATELLITE OF KM-WAVE TYPE III RADIO BURSTS, OF THE SOLAR WIND AND OF ENERGETIC SOLAR ELECTRONS: Hector Alvarez, University of Michigan, Ann Arbor, Michigan; Samuel J. Bame, Los Alamos Scientific Laboratory, Los Alamos, New Mexico; Robert P. Lin, University of California, Berkeley, California.

The University of Michigan radio astronomy experiment measures the time and direction of arrival of type-III burst radiation at eight discrete frequencies between 3500 and 50 kHz. The University of California experiment detects solar energetic electrons with energies in the range of 18-400 Kev. The Los Alamos experiment measures the solar wind density and velocity. We have analyzed 12 type-III radio events that were observed down to 50 kHz, and that were temporarily associated with electron events. In the analysis of the radio data we assume that the burst exciters travel along an Archimedean spiral trajectory. Its tightness and the electron density distribution

are determined by the solar wind observations. We then find the exciter stream velocity which best fit the observed radio onset times. Finally the deduced velocity and the predicted arrival time of the exciters at the earth are compared with those of the observed energetic electrons. For 6/12 events we found that the observations from the three experiments fit consistently the model. The other 6 events did not fit a spiral trajectory. We discuss the advantages and limitations of the analysis.

COMMISSION VI, Session 9

Thursday, October 17 8:30 am - 12:00 noon
TRANSIENT ELECTROMAGNETICS
CHAIRMAN: C. L. Bennett, Sperry Research Center

9-1 EFFECTS OF POLARIZATION ON ELECTROMAGNETIC IMPULSE RESPONSE: C. L. Bennett, Sperry Research Center, Sudbury, Massachusetts.

The impulse response is a useful characterization of a scattering target for three reasons. First, it contains in a simple waveform all the electromagnetic information about a particular target. Second, the response due to any arbitrary incident waveform can be obtained from it by a simple convolution operation. Finally, its close relationship with the actual target geometry provides a useful basis for target identification studies. Approximations for the exact impulse response have been based on the physical optics approximation for the leading edge region and on other approximations, such as Rayleigh, for later time regions of the response. The physical optics approximation yields a leading edge variation that is proportional to the second derivative of the projected area function and, therefore, contains no polarization dependence. However, the results of space-time integral equation computations have indicated a polarization dependence of the impulse response even in the leading edge region. This paper presents smoothed impulse response calculations for the prolate spheroid and for the sphere-capped cylinder with both the TE and TM polarizations at various aspect angles. The polarization effects in the regions of the creeping wave and of the leading edge are discussed and the polarization dependence of the leading edge region is related directly to the nonsymmetry of the target geometry in the neighborhood of the specular point.

9-2 SHORT PULSE ELECTROMAGNETICS: THE EXPERIMENT: R. A. Anderson, F. J. Deadrick, J. A. Landt, E. K. Miller, University of California, Livermore, California.

Recent advances in subnanosecond pulse generation and sampling technology have created new concepts in various antenna and scattering measurement systems which avoid the need for an anechoic chamber. The use of a digital minicomputer is a prime requirement in this measurement system. This paper describes the LLL transient electromagnetic measurement system, and discusses the functional requirements of the minicomputer, and associated peripheral equipment. Measurements are made of temporal current induced in a body by an electromagnetic field. This data can be Fourier transformed to the frequency domain to obtain broad band performance. In addition to determining the response of these structures, broad band terminal impedance can be determined with minor changes in the experimental arrangement. It is indicated how the on line computer can be

used to obtain much greater data accuracy over conventional data reduction systems, and various types of measurements that can be performed are discussed.

9-3 SHORT PULSE ELECTROMAGNETICS: COMPARISONS OF NUMERICAL AND EXPERIMENTAL RESULTS: J. A. Landt, F. J. Deadrick, R. A. Anderson, E. K. Miller, University of California, Livermore, California.

Recent advances in modern large-core computers have permitted implementation of a sophisticated numerical solution procedure for a thin-wire time-dependent integral equation. The numerical analysis of scattering structures using this procedure is analogous to the time-domain measurements described earlier by Bennet, et al. and by Anderson, et al. at this conference. This paper discusses the advantages of these schemes over more conventional frequency domain techniques and compares experimental results obtained by Anderson, et al. with calculations obtained by the numerical solution procedure. These comparisons verify the calibration of the experiment as well as confirm the accuracy of the numerical solutions. Additional data are presented which address the application of both schemes. For example, experimental data have been obtained to study the modeling error resulting from approximating complex structures such as aircraft by a collection of wires or cylinders. In turn, the effects of the non-planar wavefront produced by the transmitting antenna of the experimental arrangement are studied by exercising the numerical solution procedure. The numerical solution procedure will be outlined and representative data will be presented to compare the two techniques.

9-4 TIME DOMAIN RESPONSE OF APERTURES WITH BACK PLATES: Y. R. Samii and R. Mittra, University of Illinois, Urbana, Illinois.

Although much has been written on the problem of electromagnetic coupling through apertures in the frequency domain, little has appeared in the literature on the important problem of computing the temporal response of apertures, particularly when the opening is backed by a resonant structure that has considerable influence on its properties. In this paper we compute the transient response of a rectangular aperture backed by a parallel-plate region, and excited by a double-exponential pulse. The starting point is the computation of the field in the aperture, and at a number of points inside the parallel-plate region, as a function of frequency of the incoming wave. Next, the response curves are weighted by the frequency spectrum of the incident wave and Fourier transformed via the FFT algorithm to yield the desired time-domain results. The computed transient

response exhibits the resonance effects of the aperture as well as those of the parallel-plate region. It shows that rather high fields may be excited in the aperture and in the parallel-plate region if the rise-time of the incoming pulse is short.

9-5 TRANSIENT RADIATION FROM WIRE ANTENNAS: C. H. Tang and R. S. Kasevich, Raytheon Company, Wayland, Massachusetts.

The problem of transient radiation from wire antennas has, in recent years, been studied by many authors for various EMP related applications. Our emphasis is on the antenna near field breakdown phenomena. Classically, the detailed investigation of the problem involves two major steps: 1) the determination of antenna current distribution-distortion of the current waveform due to radiation and multiple reflections at tips and input terminals, and 2) the evaluation of the space-time waveform resulted from the antenna current. Thus various numerical approaches have been introduced for dealing with the problem. The present effort attempts to analyze the problem in a slightly different light. The objective is to emphasize the explicit relationship between the antenna source and its near field strength. This is important in that various breakdown processes are known to relate to the leading edges of waveforms of various field components. Basically, the antenna source can be shown to consist of three species: the charge (Q), the induction current (I) and the radiation current ($d_t I$). Each of these sources contributes to various $R^{-n}$ field strengths with various field patterns depending on the initial antenna current waveform and the given antenna configuration. This picture is useful in that it can be used to account for the local source-field interactions. Explicit formulation of the problem will be illustrated together with some computed results. Using a simple antenna geometry, analytical results for various field components will be displayed in matrix forms. It is observed that for the near field analysis, the moments of the above-mentioned sources become important. In addition, explicit space-time field data for a long wire, excited by a narrow modulated pulse, will be shown.

9-6 PULSE RADIATION FROM A RECTANGULAR LOOP ANTENNA WITH DISTRIBUTED IMPEDANCE LOADING: Ronald F. Blackburn, Air Force Weapons Laboratory, Kirtland Air Force Base, New Mexico; Clayborne D. Taylor, Mississippi State University, Mississippi State, Mississippi.

A thin wire rectangular loop antenna is considered with resistive loading at discrete points along the loop to make the frequency response broadband. An integral equation is solved numerically for the antenna current. The field about the antenna

is obtained by dividing the wire into short segments and using the electric dipole moment fields. Finally the pulse response is determined by using Fourier transform techniques.

Comparison with a low frequency approximation is made to check the computer program. Also comparisons are made with experimental data in both the time and frequency domains.

9-7 A NOVEL TECHNIQUE FOR EXTRACTING THE SEM POLES AND RESIDUES OF A SYSTEM DIRECTLY FROM ITS TRANSIENT RESPONSE: R. Mittra and M. VanBlaricum, University of Illinois, Urbana, Illinois.

The advent of the Singularity Expansion Method (SEM) for describing the transient characteristics of antennas and scatterers has generated considerable interest in the possibility of direct extraction of the SEM poles and residues from given time domain system response. It may be noted that the response may be available either from computer modeling or experimental measurements. The conventional approach for determining the singularities is based on a search procedure that seeks the zeros of the system determinant in the complex frequency plane and direct extraction of poles from the given time domain response is not possible using this method. In this paper we present a novel approach for systematically deriving, in a non-iterative manner, the complex poles and residues from a set of time-domain data. The method is based on Prony's algorithm and involves the inversion of two matrices of moderate size, and a solution of the zeros of a $n^{th}$ degree polynomial, n being the number of desired poles. Numerical studies have demonstrated that the method is both efficient and accurate and the results compare well with those derived independently using other approaches. Finally, there are several numerical advantages in applying the method for computing the frequency domain response and the input impedance behavior from given time domain data.

9-8 TRANSIENT CURRENTS INDUCED ON A THREE-DIMENSIONAL CONDUCTING RECTANGULAR BUILDING: L. L. Tsai, University of Mississippi, University, Mississippi; D. G. Dudley and D. B. Seidel, University of Arizona, Tucson, Arizona.

The vector scattering problem of a perfectly conducting rectangular building illuminated by an incident emp plane wave is analyzed using integral equation and Fourier transform techniques. The scatterer is three dimensional and possesses no rotational symmetry. The solution for the induced currents is first obtained in the frequency domain by applications of moment methods to the magnetic field integral equation. Through appropriate use of symmetry arguments, the matrix size needed

is reduced by a factor of eight, as has been presented earlier. The emphasis in this paper will be on presentation of time domain results which are obtained by numerical Fourier transform using Filon's method.

One difficulty of integral equation solution for solid scatterers is that interior resonance anomalies occur at eigenfrequencies of the adjoint problem. Fortunately these have been found to be highly localized, and for the rectangular box, resonance frequencies can be determined a priori. By extrapolation through these frequencies when transforming into the time domain, interior resonance problems are thus minimized.

The structure treated is a conducting rectangular box of 24' by 59' by 24', with a broadside incident emp plane wave whose rise time is 20 ns. Transient currents induced are calculated at points on the various sides of the box and compared to measurements. On the front and back sides one current component is dominant while they are comparable on the remaining sides. There also exists a significant increase in rise time for the current on the back side due to shadowing of high frequencies. Good qualitative agreement between measurement and theory is found.

Comparison of currents on the box is also made with those calculated on an infinite rectangular cylinder of the same cross section. Trends at the early times are similar, before end reflections take place, with significant differences occurring at later times.

## COMMISSION I, Session 6

Thursday, October 17 1:30 pm - 5:00 pm
"SELECTED TOPICS"
CHAIRMAN: Howard E. Bussey, National Bureau of Standards

6-1 EXTERNAL ELECTRODE GLOW DISCHARGE PLASMA DETECTION OF MILLIMETER WAVES: N. S. Kopeika, Ben-Gurion University of the Negev, Beer-Sheva, Israel.

Centimeter wave detection with glow discharge plasmas was probably first observed twenty-two years ago. However, the wide-scale use of such devices has been held back primarily because of the relatively high plasma noise levels. This particular disadvantage has been significant because the glow discharge does exhibit to advantage many other properties desirable in a detector. These advantages include low cost, wide dynamic range, electronic ruggedness, ability to operate at relatively higher temperatures and incident power levels, simplicity of use (no refrigeration or magnetic fields required, etc.), extended spectral range and the ability to play the role of receiving antenna and transducer simultaneously. Thus, it is only the internal plasma noise which has held back the wide-scale use of these devices. The purpose of this paper is to describe a method found at millimeter wavelengths for dramatically decreasing the internal noise of glow discharge detectors such that their sensitivity is within an order of magnitude of that of the much more expensive and electronically "delicate" crystal diode devices when used for video detection at 70 GHz. (Success in synchronous detection has been reported but with little detail.)

Very short reviews are presented of the two primary theories of 'enhancement diffusion current' and 'decreased ionization potential' used to explain the detection mechanism. A short discussion of the noise mechanisms reveals that thermal noise, often the dominant noise source, arises from fluctuations in electron arrival rate of the anode, resulting from collisions with other plasma particles, chiefly neutral molecules. This effect decreases with increasing discharge current. However, at higher discharge currents, the shot noise, caused by the randomness of electron emission from the cathode, can be significant since it increases with increasing current.

An experimental study of the effects of gas type and pressure showed that heavier noble gases, such as xenon, yield increased detector responsivity in agreement with both detection mechanism theories. However, they also resulted in increased noise, apparently as a result of sputtering. This noise increased with increasing mass faster than did the responsivity. In an experimental study of the influence of electrode geometry it was

revealed that when parallel-wire electrodes are used, the responsivity increases with decreasing electrode separation. This result is in disagreement with the 'decreased ionization potential' theory. However, the increased potential gradient resulting from decreased electrode separation does appear to support the 'enhanced diffusion current' theory of detection mechanism.

An experimental study of commercially-available neon and argon indicator lamps as video detectors of millimeter wave radiation resulted in a novel way of biasing to decrease the plasma noise level at least 20 dB. It was found that when a third electrode is added externally to an ordinary 2-electrode neon glow tube, to sense the detected signal, the two internal electrodes could be used to generate a relatively high discharge current to decrease the thermal noise and increase the potential gradient, while the external electrode could sense the enhanced diffusion current passing through the glass of the glow tube. Since this current is a displacement current, no direct current component is present and the shot noise is thus minimized. The NEP of the 5AH commercial glow tube (whose cost is less than \$1) was found to be less than $10^{-9}$ W $\cdot$ Hz$^{-\frac{1}{2}}$ for video detection of a 50 kHz sine wave at 70 GHz. The NEP reported here is about 2 orders of magnitude improvement over that of the ordinary 2-electrode mode of glow discharge detection with the same tube using only the internal electrodes, and is within an order of magnitude of that of the crystal diode at 70 GHz.

Thus, the low cost, speed of response, electronic ruggedness, spectral range, simplicity and sensitivity of these detectors will hopefully pave the way for their more widespread use in millimeter wave technology.

6-2 A PRESSURE-SCANNING REFRACTION SPECTROMETER FOR ATMOSPHERIC GAS STUDIES AT MILLIMETER WAVELENGTHS: H. J. Liebe, Institute for Telecommunication Sciences, Boulder, Colorado.

A differential refraction spectrometer was developed capable of measuring under simulated atmospheric conditions molecular EHF propagation factors, especially the intensity distribution of the oxygen microwave spectrum ($O_2$-MS). Dispersion and attenuation pressure profiles are measured between $10^{-3}$ and $10^{3}$ torr. The sensitivities are better than 1 part of $10^{9}$ and 0.01 dB/km. The multi-line (~43) structure of the $O_2$-MS around 60 GHz complicates the data analysis. Special diagnostics evolved from the data for deducing spectroscopic parameters. Experimental difficulties and their elimination are discussed. Examples of data taken for the $9^{+}$ line (61.15 GHz) and the $7^{+}/5^{-}$ doublet (60.4 GHz) are given.

6-3 THREE-DIMENSIONAL SIGNATURE MAPS FOR A NEW WIDE BANDWIDTH INDUCTION SYSTEM: W. H. Davenport and E. A. Quincy, University of Wyoming, Laramie, Wyoming.

Three-dimensional maps of sounding responses are demonstrated in both time and frequency domains. Horizontal profiling information is presented as a function of time and also as a function of frequency to facilitate interpretation of the signatures. Two laboratory model surveys were performed, one over a conducting dike and the other over a conducting horizontal sheet. These laboratory models were used simply as a vehicle to obtain typical data to demonstrate the informative aspects of these three-dimensional maps. The experimental wide-bandwidth system utilizes pseudo-noise, cross-correlation techniques to characterize subsurface conducting bodies. The time-domain signatures are obtained by cross-correlation (in the receiver) of the received signal with a replica of the wideband pseudo-noise sounding waveform. The signature maps obtained directly by the system show the band-limited (100 Hz - 50 kHz) impulse response of the geologic media as a function of time and system location. The time domain signatures were processed in the laboratory with the discrete Fourier transform to obtain frequency domain maps of magnitude, phase, real part and imaginary part as a function of system location. Each of these three-dimensional frequency domain maps was normalized to the primary field to enhance the secondary field anomaly created by the conducting body. The normalization also eliminates characteristics of the measurement system.

6-4 OPTIMAL CLASSIFICATION OF GEOPHYSICAL INDUCTION SIGNATURES WITH UNKNOWN PARAMETERS: D. F. Moore and E. A. Quincy, University of Wyoming, Laramie, Wyoming.

The Boyes' algorithm for classifying noisy electromagnetic induction signatures is derived and its performance is calculated. Two classes of noisy geophysical responses are considered. The first class corresponds to a conducting half-space with unknown conductivity and the second class corresponds to a horizontal thin sheet with unknown conductivity-thickness product. The responses were contaminated with additive, independent, Gaussian random noise and our ignorance of the unknown parameters was expressed by assuming them to be uniformly distributed. Current techniques available in the literature typically classify induction signatures qualitatively by comparing measured signatures with catalogs of measured responses for various known subsurface geophysical structures or laboratory models. None of the techniques currently available attempt to statistically classify noisy responses on a quantitative basis as has been done in seismic work. Bayes' procedure was applied to the problem of

classifying the noisy data with minimum average probability of error. The resulting algorithm shows that for the noise-free case, two disjoint classes will result if $\omega$ the probing frequency is sufficiently large. Thus for this case classification is error-free even though model parameters are unknown. Minimum average probability of error is calculated versus "signal-to-noise" ratio for noisy data.

## COMMISSION II, Session 8

Thursday, October 17 1:30 pm - 5:00 pm
PRECIPITATION
CHAIRMAN: Jerome Eckerman, Goddard Space Flight Center

8-1 ATTENUATION AND WIDEBAND COHERENCE MEASUREMENTS AT 20 AND 30 GHz WITH THE ATS-6 SATELLITE: Louis J. Ippolito, National Aeronautics and Space Administration, Greenbelt, Maryland.

The ATS-6 Millimeter Wave Propagation Experiment, launched in May 1974, is providing the first opportunity for attenuation and wideband coherence measurements from an orbiting synchronous satellite at frequencies of 20 and 30 GHz. Two sets of nine equally spaced coherent tones, with a total bandwidth of 1.44 GHz, are transmitted from ATS-6, centered at 20 and 30 GHz. The attenuation of each of the eighteen tones, and differential phase between sets of tones, are measured and recorded by a receiving terminal at Rosman, North Carolina. Measurements during precipitation periods are accomplished with an auto-tracking 4.5 meter (15 ft.) antenna system, parametric amplifiers, and phase lock loop receivers, capable of fade margins in excess of 45 dB. Channel characteristics are determined by direct measurement of the propagation channel transfer function for various meteorological conditions. Backscatter radars, radiometers, rain gauges and other support equipment are available to determine the channel conditions and meteorological parameters. The multitone received signals are processed to develop autocovariance and cross-covariance functions of the test tone envelopes, from which an estimation of the two-dimensional (time-frequency) channel covariance function is available. From this analysis an evaluation of coherence bandwidth, time spread, fading bandwidth, coherence time, differential sideband phase, attenuation statistics, and other channel propagation parameters are developed, as a function of precipitation rate, storm height, and other meteorological parameters. Data results of the first three months of satellite measurements will be presented, with emphasis on the impact of the results on wideband earth-space communications at the millimeter wavelengths.

8-2 A STATISTICAL MODEL OF RAIN SHOWERS DERIVED FROM RADAR OBSERVATIONS: T. G. Konrad, Johns Hopkins University, Silver Spring, Maryland; R. A. Kropfli, National Oceanic and Atmospheric Administration, Boulder, Colorado.

A pressing need has existed for propagation models for the purpose of estimating attenuation and interference levels due to rain in both earth-satellite and terrestrial communication links. Various experimental programs have been performed to

accumulate the statistics of attenuation and interference at specific locations, e.g., the ATS-6 program. In order to extrapolate these results to other areas, a statistical storm model is needed with parameters that can be determined for any locality of interest on the basis of available meteorological information. The physics of the attenuation and scattering processes themselves are adequately understood. However, there is an inadequate description of the spatial and temporal characteristics of the precipitation structures causing the attenuation or interference. Previous storm models used in the design of communication links have been quite simple, e.g., the cylindrical model used by CCIR. An experiment has been performed to study the fine scale temporal and spatial characteristics of intense rain storms using radar leading to a statistical description or model of these storms. This paper presents the results of the program. Storm cells are categorized according to the reflectivity factor at the ground, i.e., at the lowest elevation angle. Statistical descriptions of the peak reflectivity, area of the 10 dB contour, eccentricities, and orientations with altitude for each category of storm, including virga, are presented. Probabilities of occurrence for each storm category with altitude are also included.

8-3 MEASUREMENT AND FREQUENCY EXTRAPOLATION OF MICROWAVE ATTENUATION ON THE EARTH-SPACE PATH AT 13, 19 AND 30 GHz: Paul S. Henry, Bell Laboratories, Holmdel, New Jersey.

The program to use the Crawford Hill sun tracker at Holmdel, New Jersey for measurement of attenuation on the earth-space path at 13, 19 and 30 GHz is described. Cumulative attenuation statistics for the year August 1972-August 1973 are presented, along with a discussion of likely sources of error. The results of the data analysis can be briefly summarized: 1) the probability of fades $\gtrsim$10 dB at 30 GHz was typically a factor of 1.4 higher during 1972-3 than in 1967-8, when R. W. Wilson made similar measurements, 2) the extrapolation procedure proposed by D. C. Hogg, wherein attenuation measurements at two frequencies are used to predict attenuation at a third, yields results in good agreement with observations except at very high attenuation levels, 3) because of limits on the measuring range of the sun tracker, more accurate estimates of fading statistics for fades >30 dB at 30 GHz can probably be made by extrapolation than by direct measurement.

8-4 DETERMINATION OF RAIN ATTENUATION AND PATH DIVERSITY STATISTICS USING RADAR: J. Goldhirsh and F. Robison, Johns Hopkins University, Silver Spring, Maryland.

During the summer of 1973 the rain reflectivity environment in three dimensional space was routinely recorded on digital tape at Wallops Island, Virginia. A mode of operation consisted of sampling periodically $60^{o}$ azimuth intervals over regions in which the rain activities were most intense and widespread. A series of PPI sweeps over these intervals were implemented at a sequence of elevation angles starting from $0.5^{o}$ up to an angle above which the reflectivity values were below designated threshold level. Approximately 500 such raster scans were acquired in which each scan was obtained in less than four minutes and covered a range interval of 10 to 140 km. Using the above data base, reflectivity profiles along representative earth-satellite paths were determined from which attenuation and space diversity statistics were calculated at the frequencies of 13 and 18 GHz. Specifically, the form $k = aZ^{b}$ was used to deduce the total path attenuation, where k is the attenuation coefficient (dB/km), and Z is the reflectivity factor ($mm^{6}/m^{3}$). The constants, a and b were calculated using the raindrop distribution for thunderstorm activity as proposed by Joss. Probabilities that the attenuations exceed given fade depths, diversity gain as a function of fade depths, and diversity gain as a function of site separation distances are characterized and compared at the various frequencies.

8-5 POTENTIAL USE OF DIFFERENTIAL REFLECTIVITY MEASUREMENTS AT ORTHOGONAL POLARIZATIONS FOR MEASURING PRECIPITATION: Thomas A. Seliga, and V. N. Bringi, Ohio State University, Columbus, Ohio.

A new method of radar reflectivity measurements at a single wavelength is proposed to determine rain rate, R, without the need to use an empirical relationship between reflectivity, Z, and R. The technique uniquely establishes $N_{o}$ and $D_{o}$, which symbolize the magnitude and breadth of the Marshall-Palmer raindrop spectrum respectively, by combining differential and absolute reflectivity measurements of cross-polarized waves. The differential cross-polarized reflectivity, which should be precisely determinate, occurs as a result of drop distortion. It is independent of $N_{o}$ and the constants of the radar equation and, therefore, uniquely yields the median volume diameter $D_{o}$. Combining $D_{o}$ with the reflectivity of either of the cross-polarized components produces the remaining parameter of the spectrum $N_{o}$. Calculations indicate very good sensitivity of the measurements with the spectrum parameters. Attenuation effects may also be accounted for and incorporated in the analysis. Finally, several radar system schemes are suggested to implement the method for meteorological and hydrological purposes.

8-6 THE PERFORMANCE OF MONOPULSE RADAR IN A REALISTIC RAIN ENVIRONMENT USING CIRCULAR POLARIZATION: Peyton Z. Peebles, Jr., The University of Tennessee, Knoxville, Tennessee.

The usual way to reduce rain clutter in monopulse radar is to use circular polarization. The clutter is completely eliminated if the system generates perfectly circular polarization and if raindrops are perfectly spherical. Both conditions are usually not true in practice and cancellation is often limited to 10 to 25 dB. This paper analyzes system clutter cancellation possible when: 1) the rain is spherical and the system is imperfect and 2) rain is realistic and the system is ideal. The former gives performance bounds of a poor system operating in drizzle type rain. The latter is an attempt to determine the limitations on performance introduced by realistic rain. Included in the analysis are effects of raindrop shape, the distribution of drop size, the distribution of drop orientation (related to wind distributions), rain intensity, and the source of the rain (melting snow, hail, etc.). Clutter cancellation curves are given for various rain assumptions.

## COMMISSION III, Session 7

Thursday, October 17 1:30 pm - 5:00 pm
SCINTILLATIONS AND IRREGULARITIES
CHAIRMAN: G. H. Millman, General Electric Co., Syracuse, N.Y.

7-1 POSITION OF THE MID-LATITUDE TROUGH AND THE SCINTILLATION BOUNDARY: R. H. Wand, Massachusettes Institute for Technology, Lexington, Massachusetts.

The scintillation boundary and the electron density trough are two important regions which separate the mid-latitude and auroral zones. The locations of these boundaries were determined as functions of invariant latitude ($42^{o}$-$70^{o}$N), local time, geomagnetic activity and season, using over 2500 satellite beacon tracks made at Millstone Hill in the period January 1971 to March 1973. Scintillation indices were calculated from fluctuations in the amplitude of the UHF beacon signal and normalized to zenith based on an assumed power-law irregularity spectrum with a spectral index of four. The scintillation boundary was defined as the invariant latitude where the scintillation index averaged over a number of tracks exceeded a fixed level. The latitudinal variation of the electron density at the F2 peak ($N_{max}$) was determined for each track using UHF-VHF differential Doppler measurements combined with local vertical incidence ionosonde readings. Averaging $N_{Max}$ for many satellite tracks served to define the mean location of the electron density trough in the nighttime period.

7-2 HIGH FREQUENCY SCATTERING IN THE LOWER D-REGION AT FT. CHURCHILL DURING THE NOVEMBER 2, 1969 POLAR CAP ABSORPTION EVENT: Thomas A. Seliga, Ohio State University, Columbus, Ohio.

During the November 2, 1969 Polar Cap Absorption Event at Ft. Churchill very low-lying ionosonde echoes were observed in the D-region. These echoes were found to be consistent with electromagnetic scattering from turbulent irregularities in electron density and collision frequency. A radar-type equation, relating the scattering cross-section of the ionosphere, ionospheric absorption and ionosonde system parameters was developed. Calculations of a receiver detection parameter were made to construct analytical ionograms based upon assumed threshold detection levels and for comparison with the PCA ionograms. The results indicate a general agreement with the observed ionograms and a sensitivity to irregularity scale size, strength and spatial autocorrelation. An electron density and collision frequency variation of the order of one percent of their mean values, a turbulent scale size of around 6 m at 45 km, and a Gaussian autocorrelation were found to produce the general features of the observed echoes.

7-3 DIFFERENTIAL PHASE VOLUME MODEL: David B. Newman, Pennsylvania State University, University Park, Pennsylvania.

This paper presents a partial reflection differential phase model which accounts for scattering from a volume of irregularities. This model improves the reliability of the reduced electron number density profiles from experimental data since the theory more accurately models the experiment. The method used to derive the expected value of the phase difference angle between ordinary and extraordinary mode partially reflected radio waves is given and computer simulated data from several electron number density profiles are presented. The effect of the transmitter pulse length is clearly indicated and limitations of the theory in terms of probing frequency are discussed.

7-4 SIMULATION OF RANDOM MOVING SCREENS, AND ANALYSIS OF THEIR DIFFRACTION PATTERNS BY CORRELATION METHODS: J. W. Wright, National Oceanic and Atmospheric Administration, Boulder, Colorado; M. L. V. Pitteway, Brunel Univeristy, Uxbridge, England.

The inference of ionospheric drift velocities from spaced-antenna radio diffraction pattern observations is a statistical sampling and parameter estimation process. Even when the measurements overdetermine these parameters (as in the least-squares treatment of Fedor, 1967), it is unclear a priori what statistical meaning can be attributed, for example, to the random or "characteristic" velocity $V_c$. Computer simulation of some aspects of the experiment, with explicit statistical control over most spatial, temporal, and velocity parameters is reported here. Our analysis procedures are applied to the simulation to demonstrate that usefully accurate estimates of mean velocity, spatial and temporal correlation scales (hence, random velocity) are obtained with four fixed antennas and over a range of wavelengths about one-third to three times the antenna spacing. The analysis process also provides realistic error estimates on each parameter. It is shown that $V_c$ is equal to the velocity standard deviation of the model velocity distribution over a wide range of distributions. "Dispersive motions" can be described by correlation methods through digital bandpass filtering of the data; for simulated cases of markedly bimodal velocity distributions, this is an informative procedure, but cases of moderate dispersion more nearly resemble most natural data. For these, $V_c$ provides the more informative description.

7-5 COMPUTER SIMULATION OF REFRACTIVE DIFFRACTION IN A WEAKLY-SCATTERING IONOSPHERE: M.L.V. Pitteway, Brunel University, Uxbridge, England; J. W. Wright, National Oceanic and Atmospheric Administration, Boulder, Colorado.

Some effects of refraction and reflexion on the scattering processes which produce the echo fading observed in radio sounding of the ionosphere are studied by numerical simulation in a digital computer. A wave theory analysis is presented for a two dimensional case only, but reflection level enhancements of the scattering process, focussing of the scattered waves by subsequent refraction and spaced frequency measurements of vertical motions are all included in the simulations. The effect of weak irregularities in the electron density of the ionosphere is determined by using solutions of the wave equations without irregularities as a starting point. As in actual experiments, a randomly-moving diffraction pattern is produced by the scattering refraction and diffraction processes; it is sampled as 1000-point complex amplitude time-series at spaced antennas and at a pair of closely-spaced radio frequencies. Analysis of these simulations by the correlation methods for natural data is also presented. Horizontal mean and random velocities are correctly recovered from spaced-antenna correlations, and spaced frequency correlation recovers the vertical velocity components. The 'observed' spatial correlogram is, however, mainly controlled by refractive processes. Some special focussing features of the amplitude distributions observed in natural data may be partially simulated and explained.

7-6 INCOHERENT-SCATTER OBSERVATIONS OF IONOSPHERIC IRREGULARITY SPECTRA: R. C. Livingston and C. L. Rino, Stanford research Institute, Menlo Park, California.

The incoherent-scatter technique of remote ionospheric probing makes possible the direct measurement of ionospheric irregularities. Such measurements complement in-situ rocket and satellite measurements as well as "coherent" backscatter observations, since the dynamics of the continuum of spread-F irregularities can be observed as a function of altitude.

During February 1974, a series of experiments was conducted at Arecibo in which we utilized the high-resolution (~600 m) pulse-compression system for density measurements, together with long-pulse digital-correlator measurements to obtain nearly simultaneous plasma-velocity data. Spectral analysis of both the high-resolution spatial density variations along the radar beam and the temporal variations transverse to the radar beam show significant changes in the spectra during the development of spread-F observed on concurrently recorded ionograms.

During quiet conditions the spectra are nearly flat over the range of scale sizes from a few kilometers to some tens of kilometers. Just prior to spread-F onset a depletion of the largest-scale structures is observed, followed by a rapid transition of the spectra to a power-law form composed of two linear regimes with slopes of ~-0.8 and ~-2.5. With the disappearance of spread-F on the ionograms, the spectra above the F-layer peak show a rapid return to the nearly flat form, while below the F-layer peak recovery is more gradual.

Plasma drift measurements made every half hour during the observing period indicate a reversal from generally downward to generally upward, coincident with the periods of spread-F, in agreement with the published observations of Mathews and Harper (1972).

7-7 IONOSPHERIC DIFFRACTION BY SMALL SCALE IRREGULARITIES: George A. Bakalyar, Analytical Systems Engineering Corp., Burlington, Massachusetts.

Appropriate expansions are used to model small scale size irregularities in the ionosphere and the free space Green's function. The multipole organizations of small scale scatterers are then investigated. Applications to polar and equatorial weak scattering are then considered using data reported in the open literature and supplied by other investigators.

7-8 DAYTIME EQUATORIAL SCINTILLATIONS IN VHF TRANS-IONOSPHERIC RADIO WAVE PROPAGATION FROM ATS-3 AT HUANCAYO, PERU: Gerald S. Hawkins, Smithsonian Astrophysical Observatory, Boston, Massachusetts.

While workers in equatorial regions generally consider daytime scintillation at VHF to be far less significant in occurrence and magnitude than nocturnal, a preliminary analysis of fading records from ATS-3 at 136 MHz at Huancayo reveals a surprising number of days that show this phenomenon. Averaged over the period 1968-74, the mean scintillation index (SI) shows a daytime increase for all months except Nov. and Dec. The effect is symmetrical about local noon, and maximum values of SI (>20%) occur in May. The previously established nocturnal scintillation region is present for all months except June and July, with mean values of SI 70% in the summer months. It would therefore appear that at geomagnetic latitude $0^{o}$ there are two scintillation regions separated by the line of the earth's terminator, dusk and dawn. The time of onset of nocturnal scintillations is correlated strongly with local sunset, occurring on the average 25 minutes after ground sunset. The time of onset of daytime scintillations varies through the year by

4 hrs. and is not correlated with solar illumination, i.e., the time of sunrise. The variation of scintillation with magnetic index is examined and the dependence on the solar cycle is estimated.

$$\bar{E}(R) = -j\omega\mu \int \bar{\bar{G}}_e(R|R') \cdot \bar{J}(R')\, dv'$$

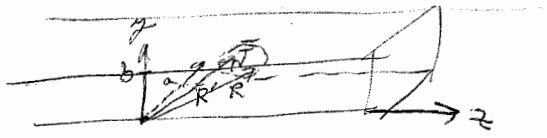


Completeness Thm:

$$(\nabla^2 + k^2)\begin{pmatrix}\bar{E}\\ \bar{H}\end{pmatrix} = 0 \leftarrow \left.\begin{matrix}\\ \\ \end{matrix}\right\} \text{no source}$$

$$\nabla \cdot \begin{pmatrix}\bar{E}\\ \bar{H}\end{pmatrix} = 0 \leftarrow$$

$$\hat{n} \times \begin{pmatrix}\bar{E}\\ \nabla\times\bar{H}\end{pmatrix} = 0 \quad \text{on walls}$$

eigenfcn. not complete set

" are complete if field is divergenceless

Dyadic Green's fcn.

$$\nabla\times\bar{H} = \bar{J} + j\omega\varepsilon\bar{E}$$
$$\nabla\times\bar{E} = -j\omega\mu\bar{H} \Rightarrow \nabla\cdot\bar{H} = 0$$
$$\hat{n}\times\bar{E} = 0$$

$$(\nabla\times\nabla\times - k^2)\begin{Bmatrix}\bar{E}\\ \bar{H}\end{Bmatrix} = \begin{Bmatrix}-j\omega\mu\bar{J}\\ \nabla\times\bar{J}\end{Bmatrix}$$

$$\rightarrow (\nabla\times\nabla\times - k^2)\,\bar{\bar{G}}_e = \bar{\bar{I}}\,\delta(R-R')$$
$$\hat{n}\times\bar{\bar{G}}_e = 0 \qquad \nabla\cdot\bar{\bar{G}}_e \neq 0$$

$$\rightarrow (\nabla\times\nabla\times - k^2)\,\bar{\bar{G}}_m = \nabla\times\bar{\bar{I}}\,\delta(R-R')$$
$$\nabla\cdot\bar{\bar{G}}_m = 0$$



Hormander - Lin. Part. diff. eqs - 1962

COMMISSION VI, Session 10

Thursday, October 17 1:30 pm - 5:00 pm
WAVE GUIDE AND TRANSMISSION SYSTEMS
CHAIRMAN: H. L. Bertoni, Polytechnic Institute of New York

10-1 ON THE APPLICATION OF THE THEORY OF GENERALIZED FUNCTIONS IN CONSTRUCTING THE DYADIC GREEN'S FUNCTION AT THE SOURCE REGION IN WAVEGUIDES, CAVITIES AND IN FREE SPACE: Y. Rahmat-Samii, University of Illinois, Urbana, Illinois

The difficulties arising in the computation of the dyadic Green's function in the source region have been discussed by a number of workers including Van Bladel, Tai and Collin. They have shown that the conventional expression used in the source free region is not complete when the field is computed in the source region, and an additional term must be added for completeness. In this paper, the structure of the dyadic Green's function in the source region is examined using an alternate approach based on the theory of generalized functions (distribution theory). This approach is used to construct the dyadic Green's function which includes the required singularity term $-\hat{z}\hat{z}\delta(\vec{r} - \vec{r}')/k^2$ in cylindrical waveguides. It is also found that the singular terms $-(\hat{x}\hat{x} + \hat{y}\hat{y} + \hat{z}\hat{z})\ \delta\ (\vec{r} - \vec{r}')/k^2$ and $-(\hat{x}\hat{x} + \hat{y}\hat{y} + \hat{z}\hat{z})\ \delta\ (\vec{r} - \vec{r}')/3k^2$ must be added to the source free solution in a rectangular cavity and in free space, respectively. The paper includes a comparative discussion of the results derived by the author and those published elsewhere.

10-2 INHOMOGENEOUS RESISTIVE LOADING OF TRANSMISSION MEDIA: H. E. Foster, Rockwell International, Anaheim, California; C. T. Tai, University of Michigan, Ann Arbor, Michigan.

Recent interest in resistively loaded transmission media prompted this report on the results of analyzing a variety of such loadings. By using numerical calculations where necessary, practically any distribution of resistance along the propagation direction of a TEM transmission medium can be analyzed. Among the resistance loading functions used as examples in this paper are linear, inverse, exponential, logarithmic, etc. functions. In addition to these continuous distributions, discrete quantized distributions are treated. The latter correspond to various progressions of lumped resistances spaced some distance apart along the medium. The cases described here are those which are analogous to inhomogeneous series resistance loaded on a TEM transmission line. The analysis shows the variation of current and impedance along the transmission medium. An optimum resistance distribution can be selected on the basis of criteria such as maximum current in the medium consistent with desired boundary conditions at the input and output ends of the medium. As an example,

several resistance distributions are rated quantitatively on their effectiveness in sustaining the largest net current in a medium with a well-matched input impedance and zero current at the output end. The paper concludes with a report on the transient response of these resistively loaded media.

10-3 PROPAGATION CHARACTERISTICS OF A DIELECTRIC COATED CYLINDRICAL CONDUCTOR WITH AN INTERVENING AIR GAP: T. C. K. Rao and M. A. K. Hamid, University of Manitoba, Winnipeg, Canada.

The characteristic equation for the propagation of electromagnetic surface waves of the fundamental TM mode over a cylindrical conductor of finite conductivity coated with a homogeneous lossy dielectric shell with an intervening air gap is derived by boundary value methods. Expressions for the propagation constant, phase velocity, characteristic impedance and line parameters are derived. The power carried by the surface wave is determined and the power profile over the cross-section is presented for various parameters of the structure. The special case of a completely lossless line is also treated where the critical air gap thickness is optimized for minimum attenuation leading to a modified Goubau line.

10-4 BEAM SCATTERING BY NON-UNIFORM LEAKY-WAVE STRUCTURES: A. Saad, H. L. Bertoni and T. Tamir, Polytechnic Institute of New York, Brooklyn, New York.

Current applications in integrated optics make extensive use of planar, thin-film structures in the form of multilayered media or (non-metallic) transmission gratings that can guide leaky waves. A beam incident at the radiation angle of the leaky wave can strongly excite this wave, which re-radiates its energy so that the resulting scattered beam (or beams) exhibit strong modifications in location and profile. By using a structure that is not uniform along the guiding direction, one can achieve desired changes in the profile of the scattered beam or strong excitation of a bound surface wave. In this work, we develop an operator having the form of a Green's function for determining the fields produced at such non-uniform structures when excited by a beam of bounded but large cross-section and having nearly parallel rays incident in the vicinity of the leaky-wave radiation angle. An operator that describes the specular reflection and the excitation and re-radiation of the leaky wave is first derived in terms of the electrical properties of a uniform structure. The operator is then generalized to the non-uniform case by introducing the local properties and by employing the reciprocity condition.

Specific examples of the effects of non-uniformity on the profile of scattered beams and on surface wave excitation are discussed.

10-5 ANALYSIS OF DIELECTRIC WAVEGUIDES; S. T. Peng and T. Tamir, Polytechnic Institute of New York, Brooklyn, New York.

Current applications in integrated optics have stimulated considerable interest into periodic thin-film dielectric waveguides, which serve as the principal structures in beam couplers, distributed-feedback lasers and other devices. Referred briefly as dielectric gratings, these structures have been analyzed either by rigorous techniques which usually need lengthy computer calculations, or by perturbation methods which lead to simpler but less accurate results. By combining the averaging concept implied in a modified Born approximation with a transmission-line analysis of the boundary-value problem, we have developed an improved perturbation procedure that provides two important advantages: 1) it approaches the accuracy obtainable from rigorous treatments while retaining the simplicity of perturbation methods, and 2) it yields a description of the electromagnetic fields in terms of a transverse transmission-line network, which brings considerable physical insight into the overall behavior of the dielectric grating. Whereas this approach can be applied to scattering of incident beams, we shall emphasize its utilization in waveguiding situations, which represent the more difficult problems. In particular, we shall discuss the evaluation of surface and leaky waves, the coupling of energy to outgoing radiation beams and the intensitites of the principal space-harmonic fields supported by dielectric gratings.

10-6 NON-DEGENERATE SURFACE-WAVES MODE COUPLING OF A SYSTEM OF DIELECTRIC WAVEGUIDES: Edward F. Kuester and David C. Chang, University of Colorado, Boulder, Colorado.

There are presently no fewer than five methods [Marcuse, 1971; Arnaud, 1974; Van Clooster and Phariseau, 1970; Matsuhara and Kumagai, 1972 and 1974; Bracey et al., 1959] in the literature dealing with the coupling between surface-wave modes on paralleloptical waveguides, with various extents of validity. The relationship between these methods is discussed, and it is shown that for degenerate modes these methods all give virtually identical results. A method is presented which permits a straightforward extension of the theory to arbitrary anisotropic guides. The most important differences between the theories occur for non-degenerate mode coupling. The character of these differences is discussed. Finally, the validity of all these methods is examined as the waveguides are brought close together.

10-7 RADIATION FROM A BEND IN A DIELECTRIC SLAB WAVEGUIDE: S. W. Maley, D. C. Chang, H. Haddad, University of Colorado, Boulder, Colorado.

Radiation from a bend in a dielectric slab waveguide has been analyzed theoretically as well as experimentally. The configuration studied consisted of two slab waveguides joined by a bend of constant radius of curvature. This study differs from most previous investigations because of the different configuration, that is, in the fact that the bend extends over only a limited angle and the effects of the straight slab waveguides joined by the bend are considered. The discontinuities at the junctions of the slab waveguides and the bend give the radiation a substantially different character than that obtained for structures without such discontinuities. The method of analysis used requires the assumption that the relative change in the structure of the guided wave within and near the waveguide caused by the bend is small. This, in turn, requires that the radius of curvature of the bend be many wavelengths. The results of the study are, therefore, valid only for bends having a radius of curvature of at least several hundred wavelengths. The results of the study indicate that the radiation pattern consists of a large number of closely spaced lobes, the number of lobes being proportional to the radius of curvature of the bend and also being a function of the angle of the bend. The total radiated power varies inversely as the square of the radius of curvature of the bend. Experimental measurements made at microwave frequencies have provided verification of some of the theoretical results.

10-8 ENERGY CONTAINMENT IN CURVED SECTIONS OF DIELECTRIC WAVEGUIDES: D. C. Chang, S. W. Maley, F. Barnes, H. Haddad, University of Colorado, Boulder, Colorado.

The radiation of energy at a bend in a dielectric waveguide is usually undersirable although, under certain circumstances, a bend could be used as a radiating element. A study has been conducted of methods of controlling radiation at bends, that is of minimizing it where it is undesired or of optimizing it where the bend is to be used as a radiating element. A theoretical investigation has shown that control of the profile of the refractive index near the waveguide on the outside of the bend provides substantial control over the radiation of energy at the bend. An experimental investigation was conducted using a slab type dielectric waveguide and microwave frequencies. The experimental equipment permitted the measurement of the amplitude and phase of the electric field as a function of position within and near the waveguide. Several profiles of the

refractive index outside but near the waveguide on the outside of the bend were investigated experimentally. The results verified that it is possible to control, to some extent, the radiation from bends.

10-9 RAYS, BEAMS AND MODES PERTAINING TO THE EXCITATION OF DIELECTRIC WAVEGUIDES: L. B. Felsen and S. Y Shim, Polytechnic Institute of New York, Farmingdale, New York.

The two-dimensional problem of excitation of an inhomogeneous dielectric layer by a Gaussian beam is considered, with emphasis on useful representations that treat the field either in terms of multiple reflections or in terms of guided modes. A recently developed method is employed whereby the beam fields are generated from line source fields by assigning a complex value to the source coordinates. When applied to the asymptotic solution for the line source field, this procedure furnishes a simple and quantitative relation between line-source-excited ray optics and paraxial beam optics. It also clarifies the role of lateral ray and beam shifts for reflection at a boundary with incidence-angle-dependent reflection coefficient, especially when multiply reflected fields are converted to modal form. Results are given for beams which are reflected at both boundaries, reflected at one boundary and refracted before reaching the other boundary, and trapped by refraction without reaching either boundary. In the first case, conversion to modal form is more convenient at large distances whereas in the latter case, paraxial beam tracking is preferable.

10-10 MICROWAVE PROPERTIES OF A SYMMETRICAL, SIX PORT H PLANE STAR WAVEGUIDE JUNCTION: Raymond S. Potter, Wright-Patterson Air Force Base, Ohio.

A perfectly symmetrical, six port, H plane star, lossless waveguide junction whose input waveguides propagate only $TE_{10}$ modes has been studied from the scattering matrix unitary restriction and normal modes of excitation. The input ports have been numbered counterclockwise from 1 to 6 so that port 4 is directly opposite port 1, ports 2 and 6 are 60 physical degrees away from port 1, and ports 3 and 5 are 120 physical degrees away from port 1. The device has been found to possess simultaneous impedance match at all input ports. When this impedance match is obtained it then follows that: 1) a unit of power incident upon port 1 divides equally into the other five ports, 2) the outputs at ports 2 and 6 are in phase, 3) the outputs at ports 3 and 5 are in phase, 4) the output at port 2 leads the output at port 3 by 90 electrical degrees, 5) the output at port 6

leads the output at port 5 by 90 electrical degrees, 6) the output at port 3 leads the output at port 4 by 90 electrical degrees, 7) the output at port 2 leads the output at port 4 by 180 electrical degrees.

# AUTHOR INDEX

FUTURE URSI MEETINGS

1975 USNC-URSI/IEEE-APS MEETING
June 2-5, 1975
University of Illinois
Urbana, Illinois

XVIII GENERAL ASSEMBLY OF URSI
August 11-19, 1975
Lima, Peru

1975 USNC-URSI MEETING
October 19-23, 1975
Boulder or Denver, Colorado

1976 USNC/URSI/IEEE-APS MEETING
October, 1976
University of Massachusetts
Amherst, Massachusetts

$$\rho = \langle f, h \rangle = \langle w, Lf \rangle$$

$h$: $I$, $L^{*}w$

$$\{jw \in E_z\} = \int I\,(k^2 + d_z^2)\, G\, dz'$$

$$= LI$$

$$\rho = \langle w, g \rangle = \boxed{w \otimes g}$$

$$\rho_f = \langle w, Lf \rangle = \boxed{w \otimes Lf}$$

$$(\quad\quad) = w(x - x_2)$$